

การสังเคราะห์อนุพันธ์ไตรเฟนิลแอมีน-พอร์ไฟรินเพื่อเป็นสารไวแสงในเซลล์สุริยะ

นางสาว รุณิสสา เก่งถนอมม้า

วิทยานิพนธ์นี้เป็นส่วนหนึ่งของการศึกษาตามหลักสูตรปริญญาวิทยาศาสตรมหาบัณฑิต

สาขาวิชาปิโตรเคมีและวิทยาศาสตร์พอลิเมอร์

คณะวิทยาศาสตร์ จุฬาลงกรณ์มหาวิทยาลัย

ปีการศึกษา 2553

ลิขสิทธิ์ของจุฬาลงกรณ์มหาวิทยาลัย

SYNTHESIS OF TRIPHENYLAMINE-PORPHYRIN DERIVATIVES AS
PHOTO-SENSITIZERS IN SOLAR CELLS

Miss Thanisa Kengthanomma

A Thesis Submitted in Partial Fulfillment of the Requirements
for the Degree of Master of Science Program in Petrochemistry and Polymer Science
Faculty of Science
Chulalongkorn University
Academic Year 2010
Copyright of Chulalongkorn University

Thesis Title SYNTHESIS OF TRIPHENYLAMINE-PORPHYRIN
DERIVATIVES AS PHOTO-SENSITIZERS IN SOLAR
CELLS

By Miss Thanisa Kengthanomma

Field of Study Petrochemistry and Polymer Science

Thesis Advisor Assistant Professor Patchanita Thamyongkit, Ph.D.

Thesis Co-advisor Assistant Professor Paitoon Rashatasakhon, Ph.D.

Accepted by the Faculty of Science, Chulalongkorn University in Partial
Fulfillment of the Requirements for the Master's Degree

..... Dean of the Faculty of Science
(Professor Supot Hannongbua, Dr.rer.nat.)

THESIS COMMITTEE

.....Chairman
(Assistant Professor Warinthorn Chavasiri, Ph.D.)

.....Thesis Advisor
(Assistant Professor Patchanita Thamyongkit, Ph.D.)

.....Thesis Co-Advisor
(Assistant Professor Paitoon Rashatasakhon, Ph.D.)

.....Examiner
(Associate Professor Nuanphun Chantarasiri, Ph.D.)

.....External Examiner
(Nantanit Wanichacheva, Ph.D.)

ฐนิสา เก่งถนอมมำ : การสังเคราะห์อนุพันธ์ไตรเฟนิลแอมีน-พอร์ไฟรินเพื่อเป็นสารไวแสงในเซลล์สุริยะ (SYNTHESIS OF TRIPHENYLAMINE-PORPHYRIN DERIVATIVES AS PHOTO-SENSITIZERS IN SOLAR CELLS) อ.ที่ปรึกษาวิทยานิพนธ์หลัก : ผศ. ดร.พัชณิตา ธรรมยงค์กิจ, อ.ที่ปรึกษาวิทยานิพนธ์ร่วม : ผศ. ดร.ไพฑูรย์ รัชตะสาคร, 91 หน้า.

ในงานวิจัยนี้ได้สังเคราะห์สารประกอบพอร์ไฟริน พร้อมทั้งทดสอบสมบัติทางเคมีไฟฟ้าและสมบัติทางแสง สารประกอบ พอร์ไฟรินที่ต้องการสังเคราะห์ได้จาก tris(4-iodophenyl)amine และ 5,10,15-triphenyl-20-(4-ethynylphenyl)porphyrin โดยใช้ปฏิกิริยา Sonogashira coupling ที่ไม่ใช้คอปเปอร์เป็นตัวเร่งปฏิกิริยา โดยผลิตภัณฑ์ที่ประกอบด้วยพอร์ไฟรินสามโมเลกุลจะนำมาใช้เป็นสารไวแสงในเซลล์แสงอาทิตย์ประเภท bulk heterojunction ส่วนผลิตภัณฑ์ที่ประกอบด้วยพอร์ไฟรินสองโมเลกุลจะถูกนำมาทำปฏิกิริยา Sonogashira coupling กับหมู่เกาะพื้นผิวสองหมู่ เพื่อนำไปใช้เป็นสารไวแสงในเซลล์สุริยะประเภทสีย้อมไวแสง การศึกษาด้วยเทคนิคไซคลิกโวลแทมเมตรีและเทคนิคโฟโตลูมิเนสเซนซ์ถูกใช้ในการพิจารณาความเป็นไปได้ของสารประกอบเหล่านี้ในการนำมาใช้ในเซลล์แสงอาทิตย์

สาขาวิชา...ปิโตรเคมีและวิทยาศาสตร์พอลิเมอร์ ลายมือชื่อนิสิต.....
ปีการศึกษา.....2553..... ลายมือชื่ออ.ที่ปรึกษาวิทยานิพนธ์หลัก.....
ลายมือชื่ออ.ที่ปรึกษาวิทยานิพนธ์ร่วม.....

5172271023 : PETROCHEMISTRY AND POLYMER SCIENCE
 KEYWORDS: PORPHYRIN / TRIPHENYLAMINE / PHOTOACTIVE
 COMPOUND / BULK HETEROJUNCTION SOLAR CELLS / DYE-
 SENSITIZED SOLAR CELLS

THANISA KENGTHANOMMA : SYNTHESIS OF TRIPHENYLAMINE-
 PORPHYRIN DERIVATIVES AS PHOTO-SENSITIZERS IN SOLAR
 CELLS ADVISOR : ASST. PROF. PATCHANITA THAMYONGKIT,
 Ph.D., CO-ADVISOR : ASST. PROF. PAITON RASHATASAKHON,
 Ph.D., 91 pp.

In this research, synthesis of porphyrinic compounds and investigation of their electrochemical and photophysical properties are described. Three novel porphyrinic compounds were synthesized by a copper-free Sonogashira coupling reaction between tris(4-iodophenyl)amine and 5,10,15-triphenyl-20-(4-ethynylphenyl)porphyrin. The completely coupled product having a triphenylamine core and three peripheral porphyrin moieties will be used as a photo-sensitizer in a bulk heterojunction solar cell. The di-substituted derivative was subjected to another Sonogashira coupling of the remaining terminal iodo group with two different surface anchoring units to obtain porphyrin products for dye-sensitized solar cells. Cyclic voltammetry and photoluminescence study of these compounds were performed to determine the potential of these compounds for being used in the solar cells.

Field of Study: Petrochemistry and Polymer science Student's signature:.....

Academic Year:2010.....

Advisor's signature:.....

Co-advisor's signature:.....

ACKNOWLEDGEMENTS

I would like to begin by thanking Assistant Professor Dr. Patchanita Thamyongkit, Assistant Professor Dr. Paitoon Rashatasakhon and Associate Professor Dr. Amorn Petsom for being the best advisors anyone could ever ask for. There no words that can express the depth of gratitude that I have toward them. They have supported me in everything that I set out to improve the synthetic skills, believe in me even at the moment of my life when I was down and help me to get back on my feet.

I also grateful to Assistant Professor Dr. Warinthorn Chavasiri, for serving as the chairman, Associate Professor Dr. Nuanphun Chantarasiri and Dr. Nantanit Wanichacheva for serving as the members of my thesis committee, respectively, for their valuable suggestion and comments.

I would like to thank Marie Curie international incoming fellowship (PIIF-GA-2008-220272), Thailand Research Fund-Master research grants-Window II (TRF-MAG-WII525S012), National Center of Excellence for Petroleum, Petrochemicals, and Advanced Materials (NCE-PPAM), and graduate school of Chulalongkorn university for partial financial support of this research.

I also thank Research Centre for Bioorganic Chemistry (RCBC) for warm welcome into their family, great experience and laboratory facilities. I feel blessed and very privileged to have joined a group with great members who supported me throughout this course. Moreover, I greatly appreciate the professional collaboration on solar cell fabrication and study provided by Linz Institute for Organic Solar Cells (LIOS) at Johannes-Kepler-University Linz, Austria.

Finally, I am grateful to my family and my friends, especially Aritat Leuchai and Salinthip Laokroekieat, for their love, understanding and great encouragement the entire course of my study.

CONTENTS

	Page
ABSTRACT (THAI)	iv
ABSTRACT (ENGLISH)	v
ACKNOWLEDGEMENTS	vi
CONTENTS	vii
LIST OF CHARTS	ix
LIST OF FIGURES	x
LIST OF SCHEMES	xiii
LIST OF ABBREVIATIONS	xiv
CHAPTER I INTRODUCTION	1
1.1 Objectives of Research.....	1
1.2 Scope of Research.....	2
CHAPTER II THEORY AND LITERATURE REVIEWS	4
THEORY	4
2.1 Solar Cells.....	4
2.1.1 Measurements for Solar Cell Performance.....	4
2.1.2 Generation of Solar Cells.....	6
2.1.3 Bulk-heterojunction Solar Cells (BHJ-SCs).....	7
2.1.4 Dye-sensitized Solar Cells (DSSCs).....	8
2.2 Porphyrin.....	10
2.2.1 Porphyrin Synthesis.....	13
2.2.2 Uses and Applications of Porphyrin Derivatives.....	15
2.3 Triphenylamine.....	15
LITERATURE REVIEWS	16
CHAPTER III EXPERIMENTAL	20
3.1 Chemicals.....	20
3.2 Analytical Instruments.....	21
3.3 Experimental Procedure.....	22
Part 1: Synthesis of Triphenylamine-porphyrin Compound for	
BHJ-SCs	22

	Page
3.3.1 5,10,15-Triphenyl-20-{4-[2-(trimethylsilyl)ethynyl]phenyl} porphyrin (4).....	22
3.3.2 5,10,15-Triphenyl-20-(4-ethynylphenyl)porphyrin (5).....	22
3.3.3 Tris(4-iodophenyl)amine (6).....	23
3.3.4 Compounds 7 and 8	23
3.3.5 Compound 1	24
Part 2: Synthesis of Surface Anchoring Units	24
3.3.6 Compound 10	24
Part 3: Synthesis of Triphenylamine-porphyrin Compounds for DSSCs	25
3.3.7 Compound 12	25
3.3.8 Compound 13	25
3.3.9 Compound 2	26
3.3.10 Compound 3	26
CHAPTER IV RESULTS AND DISCUSSION	28
4.1 Triphenylamine-porphyrin Compound for BHJ-SCs.....	28
4.1.1 Synthesis.....	28
4.1.2 Investigation of Photophysical and Electrochemical Properties of 1	30
4.1.3 Fabrication of compound 1 for BHJ-SCs.....	32
4.2 Triphenylamine-porphyrin Compounds for DSSCs.....	33
4.2.1 Synthesis of compound 2	33
4.2.2 Synthesis of compound 3	34
CHAPTER V CONCLUSION	37
REFERENCES	38
APPENDICES	42
Appendix A.....	43
Appendix B.....	71
VITA	92

LIST OF CHARTS

Chart		Page
1-1	Triphenylamine-porphyrin derivatives.....	2
2-1	Structures of some naturally occurring porphyrin derivatives.....	11
2-2	Porphyrin macrocycle.....	11
2-3	Triphenylamine molecule.....	15
2-4	Hole-transporting materials with triphenylamine core.....	16
2-5	Triphenylamine core derivatives.....	17
2-6	Triphenylamine-based compounds.....	18
2-7	Tetra-(4-carboxyphenyl)porphyrin (M-TCPP).....	19

LIST OF FIGURES

Figure		Page
2-1	Air Mass (AM), the ratio of the mass of atmosphere through which beam radiation passes to the mass it would pass through if the sun were at zenith.....	4
2-2	Photocurrent-photovoltage curve of a solar cell.....	5
2-3	Schematic layout of a BHJ-SC.....	7
2-4	The light-to-electricity conversion in bulk-heterojunction solar cells...	8
2-5	Operation principle and energy level scheme of a DSSC.....	9
2-6	Typical UV-Visible absorption spectrum of porphyrins.....	12
4-1	Comparative energy diagram of compound 1 -based BHJ-Sc.....	31
4-2	Result of photoluminescence study of the films.....	32
4-3	A schematic cell structure of a bulk heterojunction solar cell based on 1	32
A-1	¹ H-NMR spectrum of Compound 4	44
A-2	¹³ C-NMR spectrum of Compound 4	45
A-3	Mass spectrum of Compound 4	46
A-4	¹ H-NMR spectrum of Compound 5	47
A-5	¹³ C-NMR spectrum of Compound 5	48
A-6	Mass spectrum of Compound 5	49
A-7	¹ H-NMR spectrum of Compound 6	50
A-8	¹ H-NMR spectrum of Compound 7	51
A-9	¹³ C-NMR spectrum of Compound 7	52
A-10	Mass spectrum of Compound 7	53
A-11	¹ H-NMR spectrum of Compound 8	54
A-12	¹³ C-NMR spectrum of Compound 8	55
A-13	Mass spectrum of compound 8	56
A-14	¹ H-NMR spectrum of Compound 1	57

Figure		Page
A-15	¹³ C-NMR spectrum of Compound 1	58
A-16	Mass spectrum of compound 1	59
A-17	¹ H-NMR spectrum of Compound 10	60
A-18	¹³ C-NMR spectrum of Compound 10	61
A-19	¹ H-NMR spectrum of compound 12	62
A-20	Mass spectrum of compound 12	63
A-21	¹ H-NMR spectrum of compound 13	64
A-22	Mass spectrum of compound 13	65
A-23	¹ H-NMR spectrum of compound 2	66
A-24	¹³ C-NMR spectrum of compound 2	67
A-25	Mass spectrum of compound 2	68
A-26	Mass spectrum of compound 14	69
B-1	Absorption spectrum of compound 4	71
B-2	Emission spectrum of compound 4	72
B-3	Absorption spectrum of compound 5	73
B-4	Emission spectrum of compound 5	74
B-5	Absorption spectrum of compound 7	75
B-6	Emission spectrum of compound 7	76
B-7	Absorption spectrum of compound 8	77
B-8	Emission spectrum of compound 8	78
B-9	Absorption spectrum of compound 1	79
B-10	Calibration curve for quantitative determination of compound 1 in THF ($\lambda_{\text{abs}} = 425 \text{ nm}$).....	80
B-11	Calibration curve for quantitative determination of compound 1 in THF ($\lambda_{\text{abs}} = 555 \text{ nm}$).....	81

Figure		Page
B-12	Calibration curve for quantitative determination of compound 1 in THF ($\lambda_{\text{abs}} = 594 \text{ nm}$).....	82
B-13	Emission spectrum of compound 1	83
B-14	Absorption spectrum of compound 13	84
B-15	Emission spectrum of compound 13	85
B-16	Absorption spectrum of compound 2	86
B-17	Calibration curve for quantitative determination of compound 2 in THF ($\lambda_{\text{abs}} = 425 \text{ nm}$).....	87
B-18	Calibration curve for quantitative determination of compound 2 in THF ($\lambda_{\text{abs}} = 557 \text{ nm}$).....	88
B-19	Calibration curve for quantitative determination of compound 2 in THF ($\lambda_{\text{abs}} = 596 \text{ nm}$).....	89
B-20	Emission spectrum of compound 2	90

LIST OF SCHEMES

Scheme		Page
2-1	Formation of TPP under Rothmund condition.....	13
2-2	Synthesis of TPP from pyrrole using Adler-Longo's procedure.....	14
2-3	Synthesis of TPP using Lindsey's procedure.....	14
2-4	Synthesis of trisporphyrin conjugates by the Pd(0)-catalyzed Sonogashira coupling reaction.....	18
4-1	Synthesis of triphenylamine-porphyrin compound 1	29
4-2	Synthesis of Triphenylamine-Porphyrin Compounds 2 for DSSCs.....	34
4-3	Synthesis of triphenylamine-porphyrin Compound 3 for DSSCs.....	36

LIST OF ABBREVIATIONS

calcd	:	calculated
^{13}C -NMR	:	carbon-13 nuclear magnetic resonance spectroscopy
δ	:	chemical shift
CDCl_3	:	deuterated chloroform
CHCl_3	:	chloroform
J	:	coupling constant
$^\circ\text{C}$:	degree Celsius
CDCl_3	:	deuterated chloroform
d	:	doublet (NMR)
DMSO	:	hexadeuterated dimethylsulfoxide
DBU	:	1,8-diazabicyclo[5.4.0]undec-7-ene
EtOAc	:	ethyl acetate
EtOH	:	ethanol
g	:	gram (s)
Hz	:	hertz (s)
h	:	hour (s)
MS	:	mass spectrometry
MALDI-TOF-MS	:	matrix-assisted laser desorption ionization mass spectrometry
CH_2Cl_2	:	methylene chloride
μL	:	microliter (s)
MeOH	:	methanol
mg	:	milligram (s)
min	:	minute
mL	:	milliliter (s)
mmol	:	millimole (s)
ϵ	:	molar absorptivity
m	:	multiplet (NMR)
nm	:	nanometer

ppm	:	parts per million
PCBM	:	phenyl-C61-butyric acid methyl ester
PEDOT:PSS	:	polyethylenedioxythiophene:polystyrenesulfonate
P3HT	:	poly(3-hexyl thiophene)
$\text{PdCl}_2(\text{PPh}_3)_2$:	bis(triphenylphosphine)palladium(II) dichloride
$\text{Pd}_2(\text{dba})_3$:	tris(dibenzylideneacetone) dipalladium(0)
$\text{P}(o\text{-tol})_3$:	tri(<i>o</i> -tolyl)phosphine
$^1\text{H-NMR}$:	proton nuclear magnetic resonance spectroscopy
rt	:	room temperature
TEA	:	triethylamine
THF	:	tetrahydrofuran
TPA	:	triphenylamine
UV/Vis	:	ultraviolet and visible spectroscopy
obsd	:	observed
λ_{em}	:	emission wavelength
λ_{ex}	:	excitation wavelength
λ_{abs}	:	absorption wavelength

CHAPTER I

INTRODUCTION

Due to the rapid growth of global economies and industries, demand for energy to fuel its impressive industrial expansion is increased. Several sustainable and rational energy plans based on the renewable energy such as wind, natural gas, water, solar energy has been set forth to secure future energy sufficiency.

Solar energy is one of the biggest sources of the available renewable energy on earth and can be harvested by a solar cell that converts it directly into electricity. Nowadays, inorganic solar cells, especially silicon-based one, take the majority part in the market. However, the interests in organic dyes are drastically increasing owing to the possibility of low-cost cell fabrication and the development of extremely light and flexible devices. Some organic compounds such as porphyrins demonstrated satisfactory photochemical and electrochemical properties for being used as photoactive compounds in the optoelectronic devices. At the same time, triphenylamine and its derivatives are widely studied for optoelectronic application due to their excellent charge transfer properties.⁽¹⁻³⁾ To combine their beneficial properties together, we aim to synthesize a photoactive compound containing both porphyrin and triphenylamine units in the same molecule. These compounds are expected to have extremely high absorption in the visible region at 400–420 nm from characteristic of porphyrins and suitable energy band gap for solar cells. Moreover, triphenylamine acts as linker between the porphyrin absorbers to obtain the compounds having enhanced charge transfer. Finally, these compounds should have high solubility in common organic solvents, *i.e.* CH₂Cl₂, THF, toluene.

1.1 Objectives of Research

The objectives of this research are to synthesize triphenylamine-porphyrin derivatives **1–3** (Chart 1-1), and to investigate their photophysical and electrochemical properties for the potential use in organic solar cells.

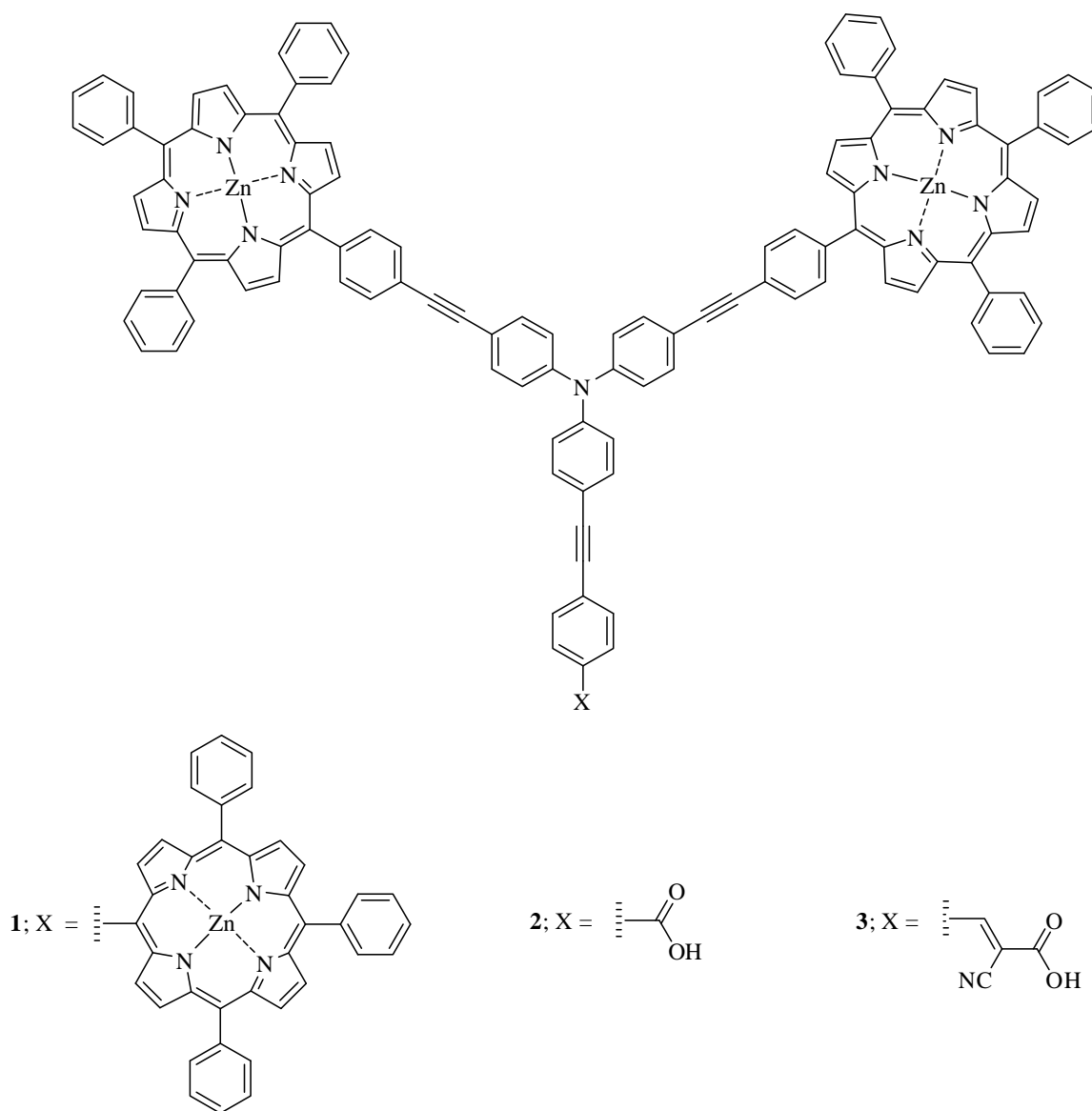


Chart 1-1. Triphenylamine-porphyrin derivatives.

1.2 Scope of Research

Three novel porphyrinic compounds were synthesized by a statistical Sonogashira coupling reaction between tris(4-iodophenyl)amine and 5,10,15-triphenyl-20-(4-ethynylphenyl)porphyrin. The completely coupled product having a triphenylamine core and three porphyrin moieties will be used as a photo-sensitizer in a bulk heterojunction solar cell. The diporphyrin-substituted derivative was subjected to a further Sonogashira coupling of the remaining iodo group on the triphenylamine core with a surface

anchoring group, *i.e.* carboxylic acid or cyanoacrylic acid group, to obtain a porphyrin-triphenylamine product for a dye-sensitized solar cell. The photophysical and electrochemical properties of all of these compounds were investigated to evaluate their potential of being used in organic solar cells. These compounds will be fully characterized by spectroscopic techniques, *i.e.* mass spectrometry, ^1H -NMR and ^{13}C -NMR spectroscopy and UV-Visible and fluorescence spectrophotometry.

CHAPTER II

THEORY AND LITERATURE REVIEWS

THEORY

2.1 Solar Cells

A solar cell is a solid state device that converts the energy of sunlight directly into electricity by the photovoltaic effect. Cells are described as photovoltaic cells when the light source is not necessarily sunlight. These are used for detecting light or other electromagnetic radiation near the visible range, for example infrared detectors, or measurement of light intensity.

2.1.1 Measurements for Solar Cell Performance⁽⁴⁾

For effective comparison, all must thus be expressed under standard illumination conditions. The standard test condition (STC) for solar cells is an Air Mass 1.5 spectrum (AM 1.5G), an incident power density of 1000 Wm^{-2} , which is defined as the standard “1 sun” (Figure 2-1).

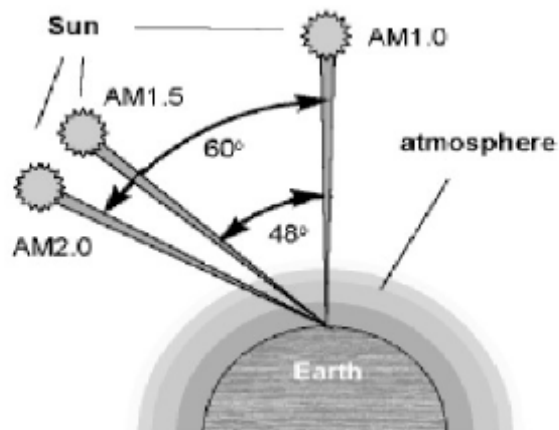


Figure 2-1. Air Mass (AM), the ratio of the mass of atmosphere through which beam radiation passes to the mass it would pass through if the sun were at zenith.⁽⁴⁾

The solar cell performance is given by two key parameters, the first is the incident photon to current conversion efficiency (IPCE) for monochromatic radiation. The other is overall white light-to-electricity conversion efficiency (η). The IPCE value is the ratio of the observed photocurrent divided by the incident photon flux, uncorrected for reflective losses during optical excitation through the conducting glass electrode (Equation 1).

$$\text{IPCE} = \frac{\text{no. of electron flowing through the external circuit}}{\text{no. of photons incident}} \quad (1)$$

The IPCE value can be considered as the effective quantum yield of the device. It relates to light harvesting efficiency, the charge injection and the charge collection efficiency. The overall efficiency of the photovoltaic cell can be obtained as a product of the short circuit photocurrent density (J_{sc}), the open circuit voltage (V_{oc}), the fill factor (FF) and the intensity of the incident light (I_S) according to Equation 2.

$$\eta = (J_{sc} V_{oc} \text{FF}) / I_S \quad (2)$$

J_{sc} and V_{oc} are determined from the photocurrent-photovoltage curve of the cell (Figure 2-2). The fill factor was calculated according to Equation 3.

$$\text{FF} = J_{max} V_{max} / J_{sc} V_{oc} \quad (3)$$

where J_{max} and V_{max} are determined from the point of the curve that the product of I and V is maximum.

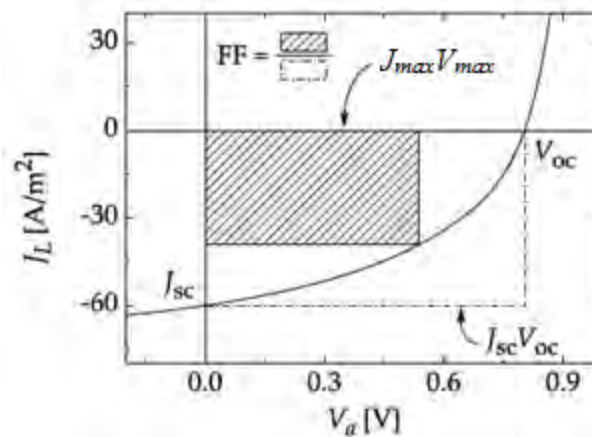


Figure 2-2. Photocurrent-photovoltage curve of a solar cell.⁽⁴⁾

2.1.2 Generation of Solar Cells

1. First Generation

The first generation started with the introduction of silicon-wafer (c-Si) based solar cells over three decades ago. This solar cell consists of a large-area and single p-n junction diode. The solar cell came out of a market environment with little concern for cost, capital efficiency and the product cost/performance ratio. Despite continued incremental improvements, silicon-wafer cells have a built-in disadvantage of fundamentally high materials cost and poor capital efficiency. Because silicon does not absorb light very strongly, silicon wafer cells have thickness and wafer are fragile, their intricate handling complicates processing all the way up to the panel product.

2. Second Generation

The second generation came about a decade ago with the first commercial thin-film solar cells. This established that new solar cells based on a stack of layers 100 times thinner than silicon wafers can make a solar cell that is just as good.⁴ Because of this solar cell based on the use of thin-film deposits of semiconductors, contributes greatly to reduced mass and cost of material for cell design. But the efficiencies of thin-film solar cells are lower compared with silicon solar cells. Besides, amorphous silicon is not stable and the solar cells have increased toxicity. There are 4 types of this generation; amorphous silicon (a-Si), polycrystalline silicon (poly-Si), cadmium telluride (CdTe) and copper indium gallium diselenide (CIGS) alloy.

3. Third Generation

The third generation, organic compounds are used in solar cells. Beside the organic solar cells have low-cost, the organic compound are designed and synthesized to get high efficiency convention. The devices include nanocrystal solar cells, photoelectrochemical (PEC) cells (Grätzel cells), polymer solar cells and dye sensitized solar cell (DSSC). The disadvantages of this generation are lower efficiency compared with silicon solar cells, decreased efficiency over time due to environmental effects and high band gap of organic compounds.

4. Fourth Generation

A hybrid between nanocrystal and polymer is the fourth generation of solar cell. This cells use polymers with nanopaticles mixed together to make a single multispectrum

layer. Significant advantages in these cells have followed the development of elongated nanocrystal rods and branched nanocrystals. Incorporation of large nanostructures into polymers required optimization of blend morphology using solvent mixtures. The advantages of solar cells in this generation are solution processable, low materials cost, self-assembly and printable nanocrystals on a polymer film. But the solar cells have disadvantages such as lower efficiency compared with silicon solar cells, potential degradation problems and optimize matching conductive polymers and nanocrystal.

2.1.3 Bulk-Heterojunction Solar Cells (BHJ-SCs)

A typical bulk-heterojunction solar cells (BHJ-SC) consists of an active layer sandwiched between two electrodes; cathode and anode, one if not both is transparent (Figure 2-3). The most popular transparent anode used nowadays is a glass substrate coated with indium-tin-oxide (ITO) having a high work function. To reduce the roughness of this ITO layer and increase the work function even further, a layer of poly(3,4-ethylene dioxythiophene):poly(styrene sulfonate) (PEDOT:PSS) is spin-casted on top, followed by the active layer. The top electrode usually consists of a low work function metal or lithium fluoride (LiF) topped with a layer of aluminum, all of which are deposited by thermal deposition in vacuum through a shadow mask.

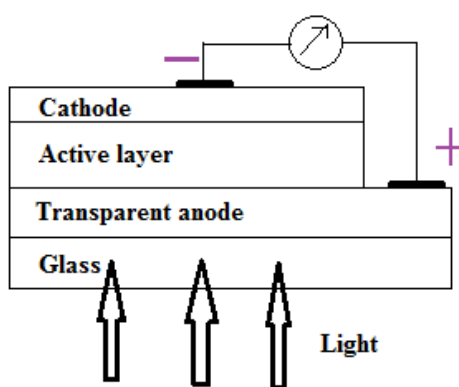


Figure 2-3. Schematic layout of a BHJ-SC.

As regards the main process of photovoltaic energy conversion by bulk-heterojunction solar cells (Figure 2-4), the foremost process is light absorption by active layer (organic compound), resulting in electrons in donor phase excited from the highest

occupied molecular orbital (HOMO) to the lowest unoccupied molecular orbital (LUMO). Then, the separated electrons from exciton transfer to the LUMO energy level of acceptor phase and diffuse to cathode. Finally, the electron transfers complete the electric circuit, leading to the electricity.

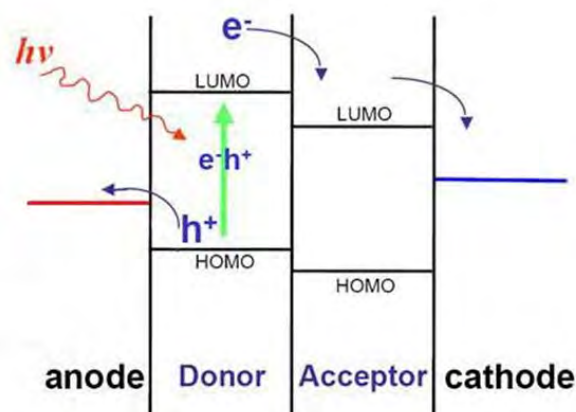


Figure 2-4. The light-to-electricity conversion in bulk-heterojunction solar cells.

2.1.4 Dye-sensitized Solar Cells (DSSCs)

Dye-sensitizer solar cells (DSSCs) were invented by Gratzel, M. and O'regan, B. in 1991.⁽⁵⁾ These cells are interesting in both of academic and commercial communities because of the good prospects to fabricate these cells at lower cost than conventional devices and their high light-to-electricity efficiency. In the present, overall solar to current conversion efficiencies of DSSCs of up to 11% have been reached.⁽⁵⁾ However, this record is still lower than the efficiency of silicon-based solar cells, therefore great efforts have been taken to improve the performance of the DSSCs.

The DSSCs consists of a photosensitizer linked (usually, via $-\text{COOH}$, $-\text{PO}_3\text{H}_2$ or $-\text{B}(\text{OH})_2$ functional groups) to the semiconductor surface and a metallic counter electrode arranged in a sandwich configuration. The inter-electrode space is filled with an electrolyte containing a redox mediator.^(6,7) In several researches, the researchers used a polypyridine complex of Ru as the dye sensitizer, nanocrystalline TiO_2 as the semiconductor and the I_2/I_3^- solution as the redox mediator.⁽⁸⁻¹⁰⁾

Operation of the DSSC starts from optical excitation with visible light that leads to excitation of the dye to an excited state (S^*) (Figure 2-5). Then electron transfer occurs by electrons injecting into the conduction band of the semiconductor. The

oxidized dye is subsequently reduced back to the ground state (S^0/S^+) by the electron donor present in the electrolyte. The electrons in the conduction band are collected at the electrode and subsequently pass through the external circuit to arrive at the counter electrode where they effect the reverse reaction of the redox mediator.^(6,7)

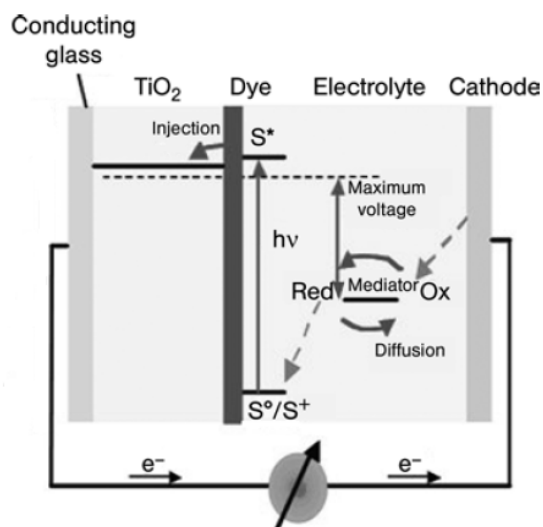


Figure 2-5. Operation principle and energy level scheme of a DSSC.⁽¹¹⁾

Requirements for higher cell voltage and conversion efficiency of DSSC are:

1. Dye sensitizer

The dye should absorb all of the visible and near IR photons of the sunlight incident on earth. Besides, dye sensitizer needs carboxylate or phosphonate or appropriate group(s) in order to ensure grafting of the dye over semiconductor oxide surface, thus increase efficiency of electron injection into the conduction band of the interface and to minimize energetic losses during the electron transfer reaction.

2. Electrolyte

The redox electrolyte regenerates the sensitizer, provided that the respective redox potentials are compatible. Efficient charge injection from the excited state of the dye into the conduction band of TiO_2 depends on the redox potential of the dye in the excited state. In addition, its reduction potential should be sufficiently positive that it can be regenerated via electron donation from the redox electrolyte.

3. Interface

The films which made of a network of nanocrystalline should produce a junction of high contact area to allow for efficient light harvesting by the adsorbed monolayer of the dye sensitizer.^(6,12)

2.2 Porphyrin

The porphyrins are a class of naturally occurring macrocyclic aromatic compounds and ubiquitous in our world. The word “porphyrin” is derived from the Greek “porphura” meaning purple.⁽¹³⁾ On account of their large π -conjugated system, all porphyrins are intensely colored. They have been called the pigments and the colors of life. This auspicious designation reflects their importance in numerous biological functions. Indeed, life as we understand it relies on the full range of biological processes that are either performed by or catalyzed by porphyrin-containing substances. Complexes of many metals with various porphyrins play a key role in biological activities as for instance iron complexes in the haemoprotein and cytochrome C, magnesium complexes in the chlorophylls, and a cobalt complex in Vitamin B₁₂ (Chart 2-1).

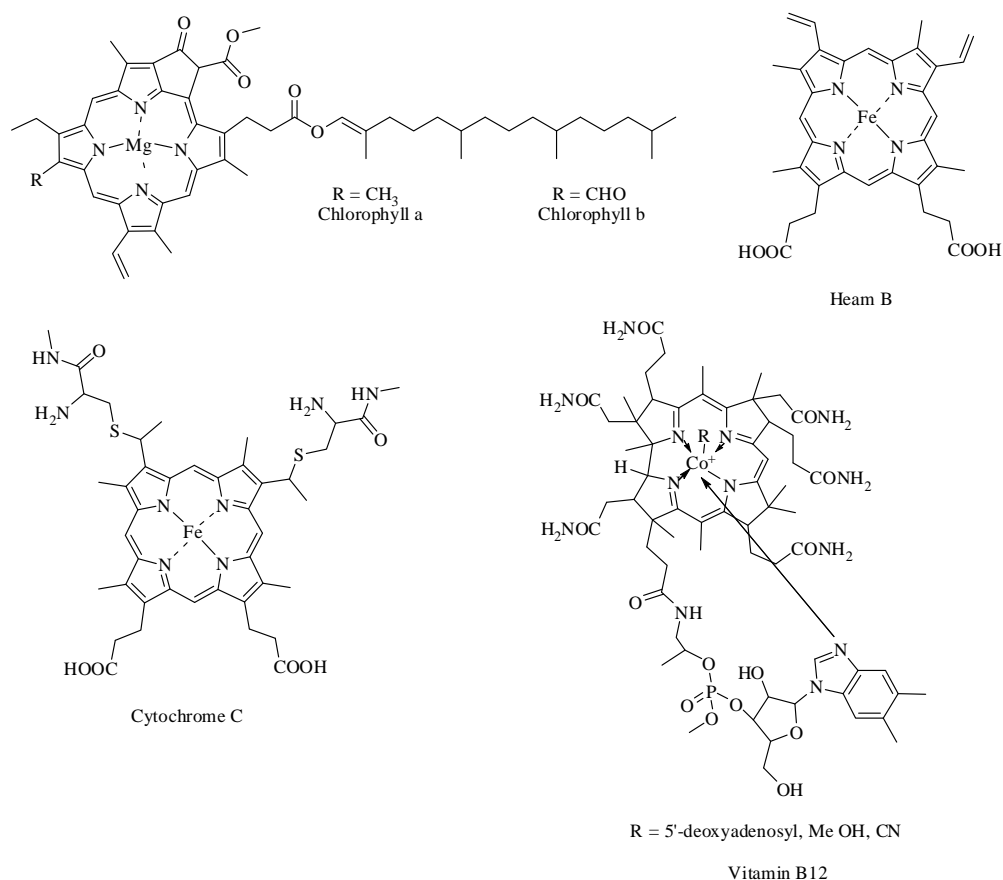


Chart 2-1. Structures of some naturally occurring porphyrin derivatives.

The porphyrin macrocycle consists of four pyrrole rings joined by four interpyrrolic methine bridges to give a highly conjugated macrocycle (Chart 2-2). The aromaticity of porphyrin has been well established both by its chemical and physical properties. These tetrapyrrolic systems have a closed loop of edgewise overlapping p-orbitals which interact favorably to stabilize the olefins: the 22 π electrons available porphyrins make up six different 18e-delocalization pathway which follows Hückel's $4n+2$ rule for aromaticity. A lower number of delocalization pathways result in less aromatic character that produces differences in spectroscopic properties.

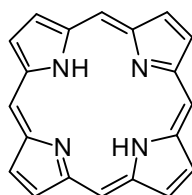


Chart 2-2. Porphyrin macrocycle.

Characteristic of porphyrin and their derivatives are highly colored absorbing strongly in the visible region near 400 nm (molar extinction coefficients are about 10^5 L·cm⁻¹·mol⁻¹). The main intense absorption band is known as Soret band or B band. And several weaker absorption bands between 450–700 nm known as Q bands (Figure 2-6). A variation in the peripheral substituents of the porphyrin ring normally results in a slight change in the intensity and wavelength of the absorption bands. However, as long as a cyclic 18 π electron-path exists, the intense Soret band is really a major characteristic of their optical spectra.

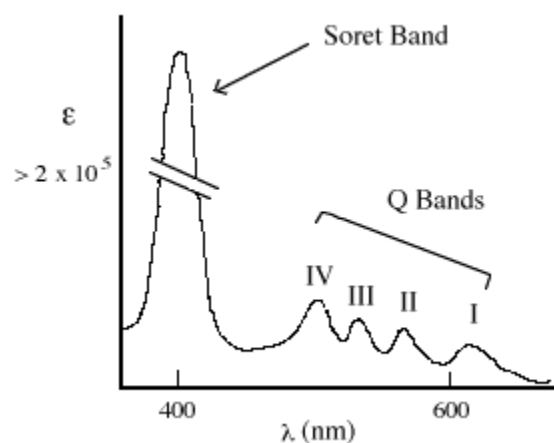
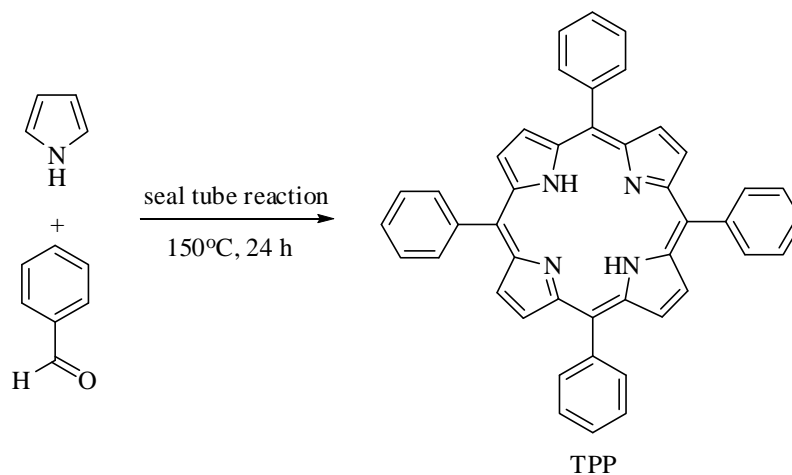


Figure 2-6. Typical UV-Visible absorption spectrum of porphyrins.

The porphyrin macrocycle and its derivatives are amphoteric. Pyrrolic nitrogen atoms at the centre of the porphyrin are responsible for this interesting characteristic. The NHs can be deprotonated with strong bases, while the two-imine nitrogens can be protonated with acid. However, metallated porphyrins lack this amphoteric quality because the nitrogens are chelated to the metal with both covalent and dative bonds. The NMR spectrum of the aromatic tetrapyrrole shows anisotropic effect. The ring current generated by the applied field induces a local magnetic field similar to that in benzene. The NH protons inside the porphyrin ring system are therefore shifted upfield to as high as -5 ppm in porphyrins, whereas the deshielded *meso*-protons appear at very low field ($\delta \sim 10$ ppm). The pyrrolic protons are also deshielded and tend to resonate at δ 8 to 9, versus $\delta \sim 6$ ppm in pyrrole. These porphyrin systems make their NMR spectra challenge spectra.

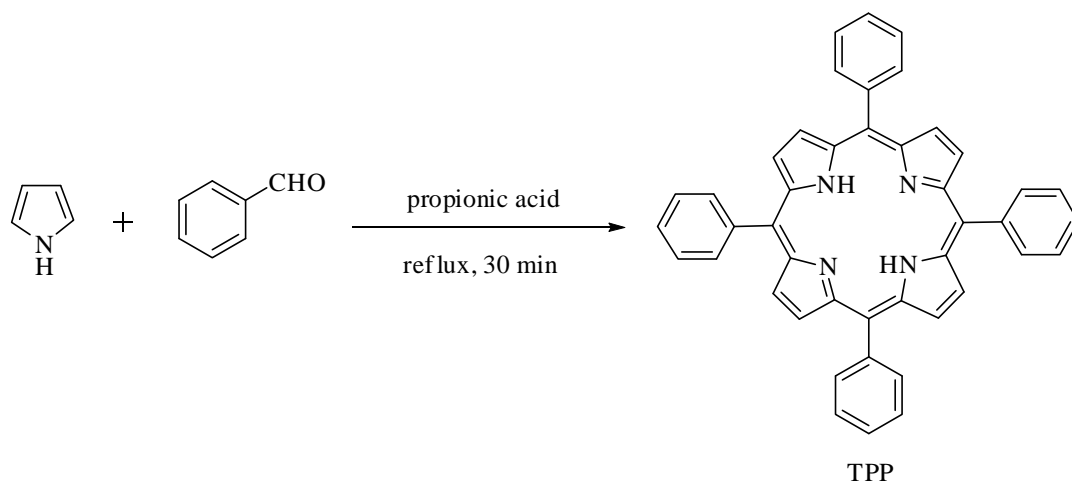
2.2.1 Porphyrin Synthesis

Porphyrin and their derivatives has stimulated large amounts of research into synthesis, purification and structure determination. One of the simplest porphyrins is tetraphenylporphyrin (TPP) obtained from the condensation of pyrrole and benzaldehyde under an acidic condition. The first route was reported by Rothmund, P. who reported the porphyrin formation in sealed glass tubes at high temperature (Scheme 2-1).⁽¹⁴⁾ However, the yields were low and the strong conditions meaning that only a limited number of aromatic aldehydes survived the procedure.



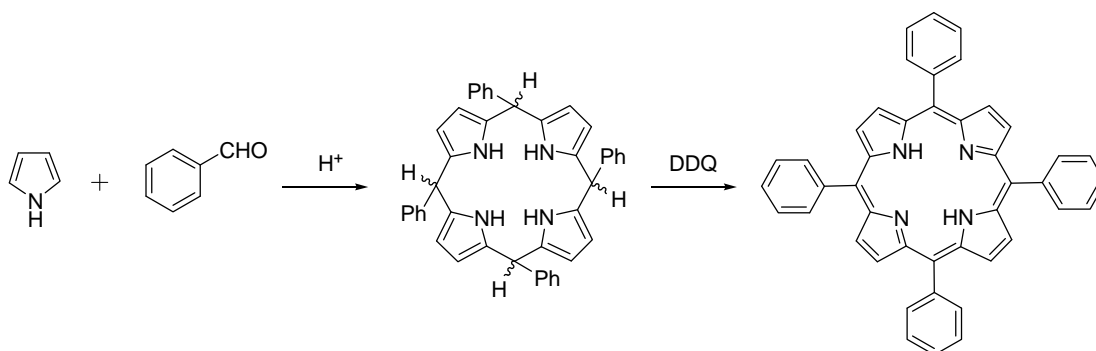
Scheme 2-1. Formation of TPP under Rothmund condition.

About three decades later, Adler, Longo and their colleagues described the involving use of refluxed propionic acid instead of sealed tubes chemistry to reproducibly obtain TPP and derivatives in 20–25% yield (Scheme 2-2).⁽¹⁵⁾ This procedure has been widely used when large amounts of porphyrins are needed and the corresponding aldehydes are able to survive under the condition of refluxing propionic acid.



Scheme 2-2. Synthesis of TPP from pyrrole using Adler-Longo's procedure.

The porphyrin synthesis was greatly developed by Lindsey's group who used mild reaction conditions and obtained high yields of a wide variety of *meso*-tetraarylporphyrins.⁽¹⁶⁾ The porphyrins were formed from two-step reaction of arylaldehydes and pyrrole in the presence of mild acid. In the first step, the acid-catalyzed condensation reaction is carried out in the presence of trace acid catalyst, usually $\text{BF}_3 \cdot \text{OEt}_2$ or TFA, yielding tetraarylporphyrinogen. In the second step, the porphyrinogen intermediate is irreversibly oxidized by a quinone derivative, such as 2,3-dichloro-5,6-dicyanobenzoquinone (DDQ), to afford the desired tetraarylporphyrin (Scheme 2-3).



Scheme 2-3. Synthesis of TPP using Lindsey's procedure.

2.2.2 Uses and Applications of Porphyrin Derivatives

There are a lot of interesting applications of porphyrins in chemical and biomedical research, for example:

1. Optoelectronic devices, such as solar cells⁽¹⁷⁾
2. Organic light emitting diodes⁽¹⁸⁾
3. Dyes for food, cloth, printing⁽¹⁹⁾
4. Electrochemical and photocatalysts⁽²⁰⁾
5. Photodynamic Therapy (PDT)⁽²¹⁾
6. Optical sensors^(22,23)
7. Organic semiconductors⁽²⁴⁾

2.3 Triphenylamine

Triphenylamine (Chart 2-3) is a tertiary amine with structural formula $(C_6H_5)_3N$. Triphenylamine is IUPAC name and the other names are *N,N,N*-triphenylamine, *N,N*-diphenylbenzeneamine, *N,N*-diphenylaniline and a common abbreviation is TPA. Its derivatives have useful properties in electrical conductivity and electroluminescence and are used in OLEDs as hole-transporters.

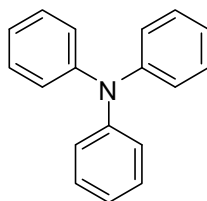


Chart 2-3. Triphenylamine molecule.

Triphenylamine derivatives have been widely investigated for almost two decades. Considerable effort in synthesis chemistry, in particular by Shirota and co-worker⁽³⁾, has led to the development of many classes of triphenylamine-based compounds as hole-transporting or electroluminescent materials (Chart 2-4). Owing to the noncoplanarity of the three phenyl substituents, triphenylamine derivatives can be viewed as 3D systems. The combination of triphenylamine with linear π -conjugated systems could be expected to lead to amorphous materials with isotropic optical and charge-transfer properties.⁽²⁵⁾

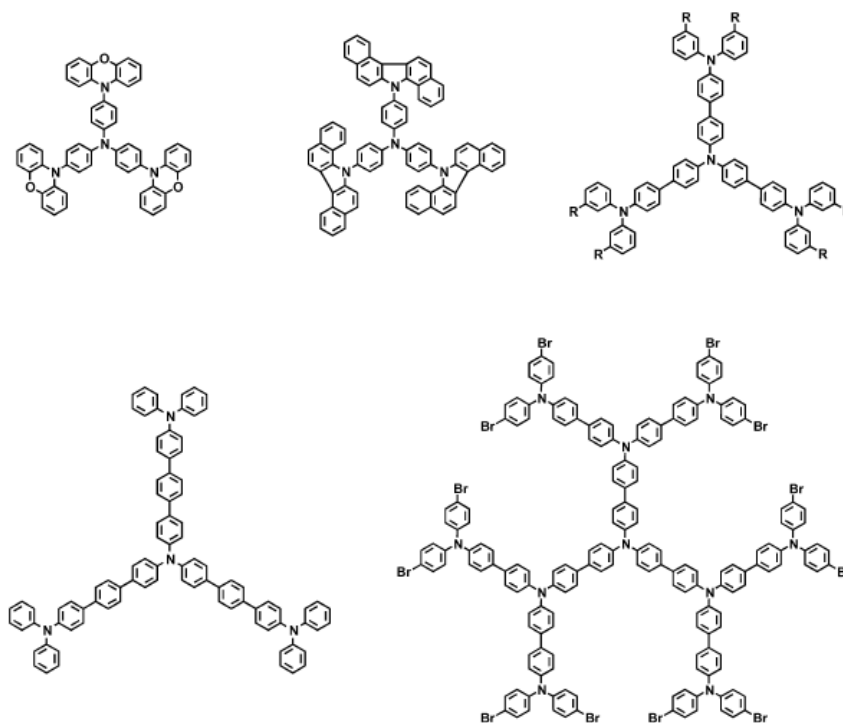


Chart 2-4. Hole-transporting materials with triphenylamine core.

For many years, triphenylamine derivatives have been shown to be promising materials for two-photon absorption. Triphenylamine is an electron-rich, propeller-shaped molecule exhibiting a C_3 symmetry thus displaying an octupolar feature. By introduction of electron-withdrawing groups on the three position para to the central nitrogen, very efficient two-photon absorption fluorophores were recently obtained.⁽²⁶⁾

Triphenylamine has been shown to be a good framework in enhancing nonlinear responses. Because of good coplanarity of the central nitrogen and the three surrounding carbon atoms connecting to it, the triphenylamine unit can maintain uninterrupted conjugation between central nitrogen lone pair electrons and the arms, as well as function as a strong electron donor to the conjugation system.⁽²⁷⁾

LITERATURE REVIEWS

Roquet *et. al.*⁽²⁵⁾ reported star-shaped molecules based on a triphenylamine core derivatized with various combinations of thienylenevinylene conjugated branches and electron-withdrawing indanedione or dicyanovinyl groups (Chart 2-5) that have been designed for many advantages such as the hole-transport properties due to triphenylamine

derivatives, extension the absorption spectrum of the donor and a high oxidation potential.

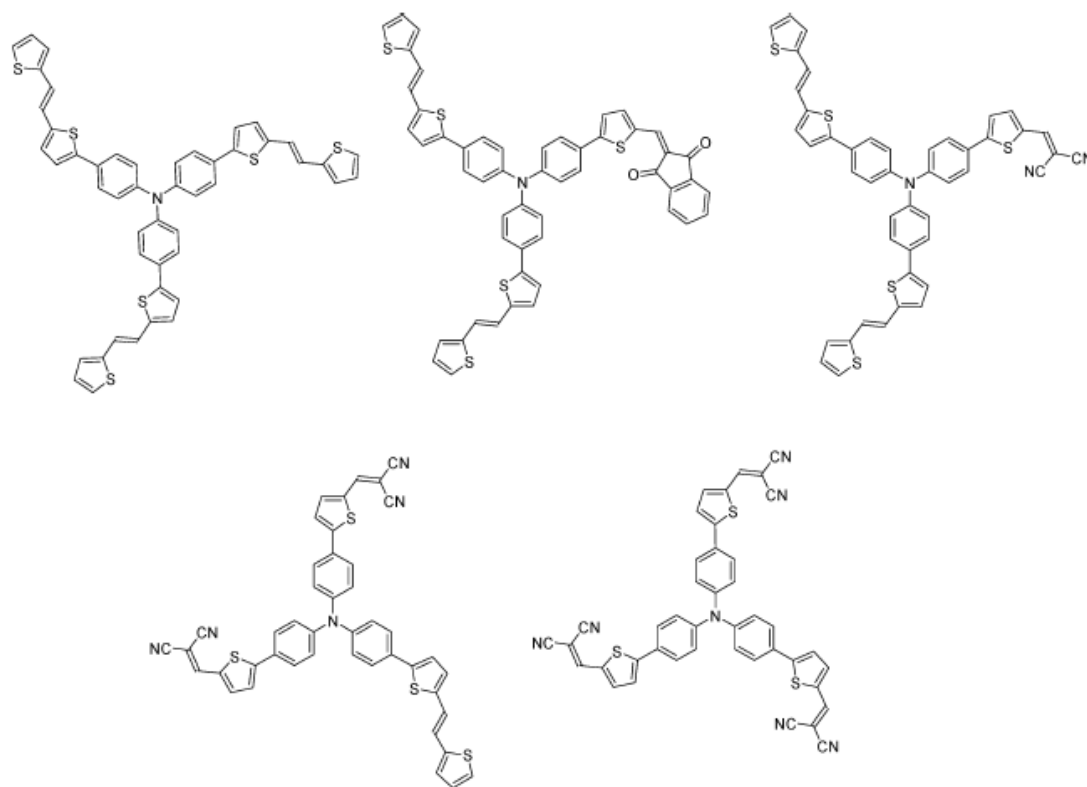


Chart 2-5. Triphenylamine core derivatives.

Cravino *et. al.*⁽²⁸⁾ reported a star-shaped tris[4-(2-thienyl)phenyl]amine core modified by peripheral electron-withdrawing dicyanovinyl groups (Chart 2-6) which used as donor materials for the heterojunction solar cells. Triphenylamine-based compounds could be act as material for hole transport and electroluminescence. Spectroscopic and electrochemical analysis indicated that this molecule leads to an extensive toward longer wavelength and to an increase of the oxidation potential.

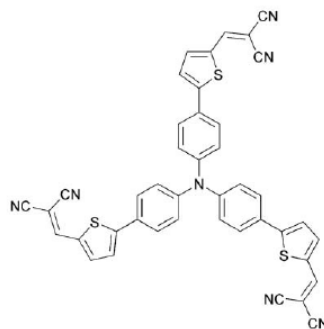
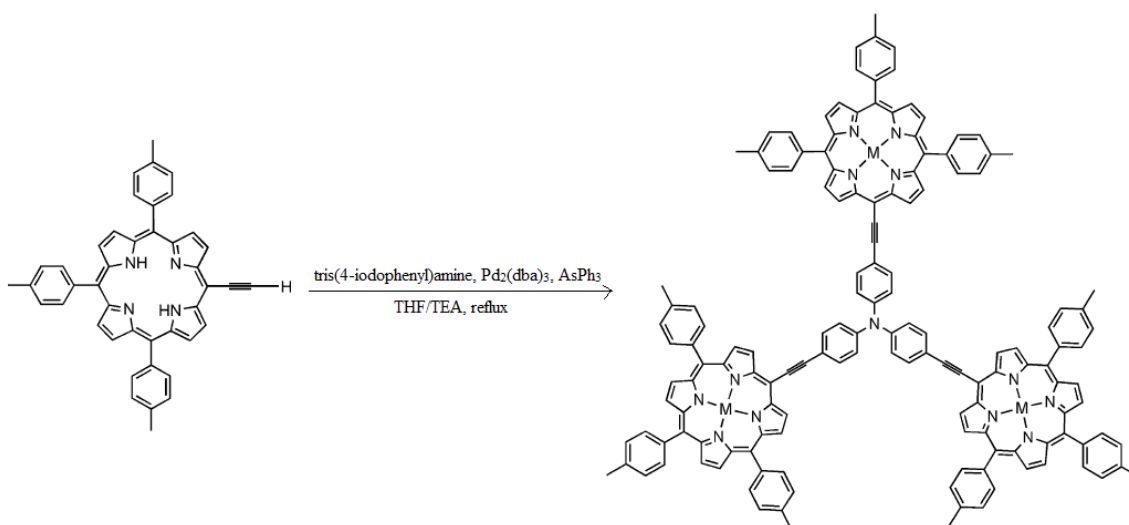


Chart 2-6. Triphenylamine -based compound.

Seo *et. al.*⁽²⁹⁾ reported octopolar trisporphyrin conjugates, derived from the a triphenylamine core with three ethynyl-porphyrin wings. The target molecule was synthesized by the Pd(0)-catalyzed Sonogashira coupling reaction of tris(4-iodophenyl)amine with 5,10,15-tri-(*p*-tolyl)-20-ethynylporphyrin (Scheme 2-4).



Scheme 2-4. Synthesis of trisporphyrin conjugates by the Pd(0)-catalyzed Sonogashira coupling reaction.

Campbell *et. al.*⁽³⁰⁾ investigated the porphyrins as a dyes in DSSCs. Various porphyrins have been used for the photosensitization of wide band gap semiconductors; like NiO, ZnO and TiO₂. These porphyrins shown long-lived π^* singlet excited states and only weak singlet/triplet mixing. A LUMO level of porphyrins reside above the conduction band of the TiO₂ and a HOMO level lies below the redox couple in the

semiconductor/dye/electrolyte surface. The tetra-(4-carboxyphenyl)porphyrin (TCPP) was used in this work and compared with its Zn-chelated derivative (Zn-TCPP) (Chart 2-7). The result revealed that the device based on TCPP gave higher energy conversion efficiency than that based on Zn-TCPP.

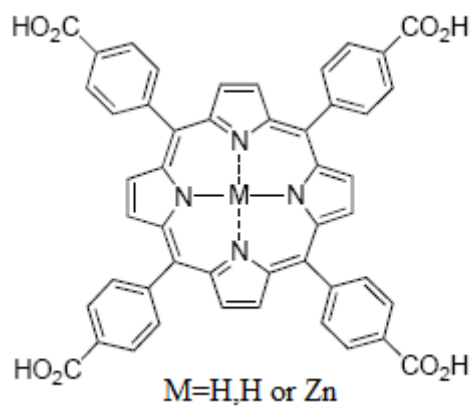


Chart 2-7. Tetra-(4-carboxyphenyl)porphyrin (M-TCPP).

CHAPTER III

EXPERIMENTAL

3.1 Chemicals

1. Benzaldehyde : Merck
2. Pyrrole : Merck
3. 4-((Trimethylsilyl)-ethynyl)benzaldehyde : Aldrich
4. Boron trifluoride diethyl etherate : Merck
5. 2,3-Dichloro-4,5-dicyanobenzoquinone (DDQ) : Aldrich
6. Triethylamine : Merck
7. Methylene Chloride, commercial grade : Lab-Scan
8. Hexanes, commercial grade : Lab-Scan
9. Ethyl acetate, commercial grade : Lab-Scan
10. Tetrahydrofuran : Lab-Scan
11. Methanol : Merck
12. Ethanol : Merck
13. Potassium carbonate : AnalaR
14. Sodium sulfate (anhydrous) : Merck
15. Triphenylamine : Aldrich
16. Mercuric oxide : Hopkin & Williams
17. Iodine : Merck
18. Toluene : Labscan
19. Tris(dibenzylideneacetone) dipalladium(0) : Aldrich
20. Tri(*o*-tolyl)phosphine : Aldrich
21. Chloroform : Labscan
22. Zinc acetate dihydrate : Sigma-Aldrich
23. Magnesium sulfate (anhydrous) : Sigma-Aldrich
24. 4-Iodobenzoic acid : Aldrich
25. Bis(triphenylphosphine)palladium(II) dichloride : Aldrich

26. Copper(I) iodide	: Fuka
27. Trimethylsilylacetylene	: Aldrich
28. Potassium fluoride	: Wako
29. Hydrochloric acid	: Merck
30. Sodium hydrogen carbonate	: Merck
31. Cyanoacetic acid	: Merck
32. Ammonium acetate	: J.T. Baker Inc.
33. Acetic acid	: Merck
34. Sized-exclusion resin; Bio-Beads 200-400 Mesh	: Bio-Rad Laboratories
35. Celite; 30-80 Mesh	: BDH
36. Aluminium oxide G; type 60/E	: Merck
37. Deuterated chloroform	: Merck
38. Hexadeuterated dimethylsulfoxide	: Merck
39. 1,8-Diazabicyclo[5.4.0]undec-7-ene	: Fluka

3.2

Analytical Instruments

^1H -NMR and ^{13}C -NMR spectra were obtained in deuterated chloroform (CDCl_3) and hexadeuterated dimethylsulfoxide ($\text{DMSO-}d_6$) using Varian Mercury and Blüker NMR spectrometers operated at 400 MHz for ^1H and 100 MHz for ^{13}C nuclei (Varian Company, CA, USA and Blüker company, Germany). Chemical shifts (δ) are reported in parts per million (ppm) relative to the residual CHCl_3 peak (7.26 ppm for ^1H -NMR and 77.0 ppm for ^{13}C -NMR) and $\text{DMSO-}d_6$ peak (2.50 ppm for ^1H -NMR and 39.5 ppm for ^{13}C -NMR). Coupling constants (J) are reported in Hertz (Hz).

Mass spectra were obtained using a matrix-assisted laser desorption ionization mass spectrometry (MALDI-MS) technique and dithranol as a matrix.

Absorption spectra were measured in tetrahydrofuran by a Varian Cary 50 UV-Vis spectrophotometer. Emission spectra were recorded in tetrahydrofuran on Varian spectrofluorometer.

3.3 Experimental Procedure

Part 1: Synthesis of Triphenylamine-porphyrin Compound for BHJ-SCs

3.3.1 5,10,15-Triphenyl-20-(4-[2-(trimethylsilyl)ethynyl]phenyl) porphyrin (4)

Following a literature procedure⁽³¹⁾ with slight modification, a mixture of benzaldehyde (1269.5 mg, 11.976 mmol), pyrrole (1172.1 mg, 17.494 mmol) and 4-((trimethylsilyl)-ethynyl)benzaldehyde (808.7 mg, 3.998 mmol) in CH₂Cl₂ (1600 mL) was stirred at room temperature until homogeneous solution was obtained. BF₃·OEt₂ (0.67 mL, 5.3 mmol) was then added in the solution and the reaction mixture was stirred at room temperature. After 1 h, 2,3-dichloro-4,5-dicyanobenzoquinone (DDQ) (2740.6 mg, 12.073 mmol) was added and the reaction was continued for additional 1 h. The resulting mixture was treated with triethylamine (0.8 mL) at room temperature for 5 min and then filtered through a silica pad (CH₂Cl₂). Then solvent was removed and crude product was purified by column chromatography [silica gel, Ethyl acetate/hexanes (1:10)] to give the title compound as a purple solid (236.7 mg, 8%). ¹H-NMR (CDCl₃) δ -2.82 (s, 2H), 0.36 (s, 9H), 7.70–7.79 (m, 9H), 7.86 (d, *J* = 8.0 Hz, 2H), 8.15 (d, *J* = 8.1 Hz, 2H), 8.19 (d, *J* = 6.3 Hz, 6H), 8.78–8.86 (m, 8H) (**Figure A-1**); ¹³C-NMR (CDCl₃) δ 0.2, 95.7, 105.2, 119.3, 120.4, 120.5, 122.7, 126.9, 127.9, 130.5, 130.7, 131.2, 134.6, 134.7, 142.3, 142.7 (**Figure A-2**); MALDI-TOF-MS *m/z* obsd 710.125, calcd 710.938 (M = C₄₉H₃₈N₄Si) (**Figure A-3**); λ_{abs} 417, 513, 549, 593, 647 nm (**Figure B-1**); λ_{em} (λ_{ex} = 417 nm) 659, 720 nm (**Figure B-2**).

3.3.2 5,10,15-Triphenyl-20-(4-ethynylphenyl)porphyrin (5)

Adapted from a previous published procedure,⁽³²⁾ **4** (129.3 mg, 0.1819 mmol) in tetrahydrofuran/methanol (20.2 mL, 3:1) was treated with potassium carbonate (56.5 mg, 0.409 mmol) at room temperature. After 4 h, solvent was removed under reduced pressure. The reaction mixture was then redissolved in CH₂Cl₂ and washed with water. The organic phase was combined, dried over Na₂SO₄ and concentrated to dryness. After the removal of solvent, the crude mixture was purified by a silica column [CH₂Cl₂/hexanes (1:3)], affording **5** as a purple solid (109.3 mg, 94%). ¹H-NMR (CDCl₃) δ -2.81 (s, 2H), 3.31 (s, 1H), 7.70–7.80 (m, 9H), 7.88 (d, *J* = 8.0 Hz, 2H), 8.15–

8.23 (m, 8H), 8.79–8.87 (m, 8H) (**Figure A-4**); ^{13}C NMR (CDCl_3) δ 30.2, 78.7, 84.2, 119.4, 120.8, 120.9, 122.1, 127.2, 128.2, 131.0, 131.5, 134.9, 135.0, 142.6, 143.3 (**Figure A-5**); MALDI-TOF-MS m/z obsd 638.227, calcd 638.757 ($M = \text{C}_{46}\text{H}_{30}\text{N}_4$) (**Figure A-6**); λ_{abs} 417, 513, 549, 590, 647 nm (**Figure B-3**); λ_{em} ($\lambda_{\text{ex}} = 417$ nm) 661, 720 nm (**Figure B-4**).

3.3.3 Tris(4-iodophenyl)amine (6)

Following a standard procedure,⁽³³⁾ a mixture of triphenylamine (0.3941 g, 1.106 mmol), HgO (1.511 g, 6.972 mmol) and I_2 (2.267 g, 8.923 mmol) in EtOH (20.0 mL) was stirred overnight at room temperature. The solvent was removed and the product was separated from mercuric salts with boiling toluene. Then, the solution was filtered through the short Al_2O_3 column and precipitated with methanol to obtain **6** as a yellow-brown solid (0.4808 g, 70%). ^1H -NMR (CDCl_3) δ 6.79 (d, $J = 8.8$ Hz, 6H), 7.51 (d, $J = 8.8$ Hz, 6H) (**Figure A-7**). Other spectral data are consistent with those reported in the literature.

3.3.4 Compounds 7 and 8

Following a previously published procedure⁽³⁴⁾ with slight modification, a mixture of **5** (296.1 mg, 0.4636 mmol) and **6** (70.8 mg, 0.114 mmol) in toluene/TEA [5:1] (19.6 mL) was stirred under nitrogen atmosphere until a homogeneous solution was obtained. After that, tris(dibenzylideneacetone) dipalladium(0) (19.0 mg, 0.0207 mmol) and tri(*o*-tolyl)phosphine (35.5 mg, 0.117 mmol) was added and the reaction mixture was stirred under nitrogen atmosphere at 40 °C. After 24 h, the reaction mixture was filtered through a silica pad (toluene). After the removal of solvent under reduced pressure, the resulting crude mixture was separated by a three-column process: a silica column [CH_2Cl_2 /hexanes (1:1)], a size-exclusion column (tetrahydrofuran) and then a silica column [CH_2Cl_2 /hexanes (1:1)] and triturated with hexanes to obtain **7** (88.6 mg, 36%) and **8** (22.6 mg, 12%) as magenta solids. Compound **7**: ^1H -NMR (CDCl_3) δ -2.80 (s, 6H), 7.58–7.98 (m, 45H), 8.11–8.52 (m, 24H), 8.74–9.12 (m, 24H) (**Figure A-8**); ^{13}C NMR (CDCl_3) δ 29.6, 117.2, 118.4, 120.5, 124.4, 126.9, 127.9, 128.7, 129.3, 130.1, 130.3, 131.2, 133.3, 134.3, 134.7, 141.9, 142.3 (**Figure A-9**); MALDI-TOF-MS m/z obsd

2156.927, calcd 2155.542 ($M = C_{156}H_{99}N_{13}$) (**Figure A-10**); λ_{abs} 420, 515, 550, 590, 647 nm (**Figure B-5**); λ_{em} ($\lambda_{\text{ex}} = 420$ nm) 654, 719 nm (**Figure B-6**). **Compound 8**: $^1\text{H-NMR}$ (CDCl_3) δ -2.76 (s, 4H), 7.02–7.83 (m, 30H), 7.94 (d, $J = 7.7$ Hz, 4H), 8.14–8.29 (m, 16H), 8.81–8.93 (m, 16H) (**Figure A-11**); $^{13}\text{C NMR}$ (CDCl_3) δ 89.3, 90.5, 117.9, 120.3, 122.9, 123.5, 123.8, 125.7, 126.7, 126.9, 127.8, 129.7, 129.9, 131.4, 131.8, 132.1, 132.9, 133.0, 134.1, 134.55, 134.61, 138.6, 142.1, 146.9, 147.5 (**Figure A-12**); MALDI-TOF-MS m/z obsd 1519.852 [$(M-I)^+$], 1645.721 [M^+], calcd 1644.698 ($M = C_{110}H_{70}IN_9$) (**Figure A-13**); λ_{abs} 418, 518, 548, 594, 646 nm (**Figure B-7**); λ_{em} ($\lambda_{\text{ex}} = 418$ nm) 652, 719 nm (**Figure B-8**).

3.3.5 Compound 1

Adapted from a previously published procedure,⁽³²⁾ a solution of **7** (88.6 mg, 0.0411 mmol) in CHCl_3 (15.0 mL) was treated with a solution of $\text{Zn}(\text{OAc})_2 \cdot 2\text{H}_2\text{O}$ (364.8 mg, 1.662 mmol) in methanol (5.0 mL). After refluxing for 2 h, the reaction mixture was concentrated to dryness, redissolved in CH_2Cl_2 and then washed with water. The organic phase was combined and dried over anhydrous MgSO_4 . After the removal of solvent under reduced pressure, the crude product was purified by column chromatography [silica gel, $\text{CH}_2\text{Cl}_2/\text{hexanes}$ (2:1)], affording **1** as a magenta solid (90.7 mg, 94%). $^1\text{H-NMR}$ (CDCl_3) δ 7.66 (d, $J = 8.4$ Hz, 6H), 7.71–7.86 (m, 33H), 7.96 (d, $J = 7.8$ Hz, 6H), 8.18–8.30 (m, 24H), 8.93–9.03 (m, 24H) (**Figure A-14**); $^{13}\text{C NMR}$ (CDCl_3) δ 89.5, 90.4, 118.2, 121.27, 121.34, 122.7, 124.3, 126.6, 127.5, 129.8, 131.7, 132.1, 132.2, 133.1, 134.4, 134.5, 142.8, 142.9, 146.9, 149.9, 150.2, 150.28, 150.31 (**Figure A-15**); MALDI-TOF-MS m/z obsd 2346.904, calcd 2345.725 ($M = C_{156}H_{93}N_{13}Zn_3$) (**Figure A-16**); $\lambda_{\text{abs}}(\epsilon)$ 425(646,540), 555(32,448), 594(17,883) nm (**Figure B-9–12**); λ_{em} ($\lambda_{\text{ex}} = 425$ nm) 607, 655 nm (**Figure B-13**).

Part 2: Synthesis of Surface Anchoring Units

3.3.6 Compound 10

Following a previously published procedure⁽³⁵⁾ with slight modification, a mixture of 4-((trimethylsilyl)-ethynyl)benzaldehyde (510.2 mg, 2.522 mmol), cyanoacetic acid (231.7 mg, 2.724 mmol) and ammonium acetate (69.7 mg, 0.905 mmol) in acetic acid

was stirred under a nitrogen atmosphere at 120 °C for 24 h. After the removal of solvent under reduced pressure, the crude product was redissolved in tetrahydrofuran/methanol (27.0 mL, 3:1) and treated with potassium carbonate (120.0 mg, 0.8683 mmol) at room temperature for 4 h. After the removal of solvent, the resulting crude mixture was redissolved in CH₂Cl₂ and washed with water. The organic phase was combined, dried over anhydrous MgSO₄ and concentrated to dryness, affording **10** as a yellow solid (344.6 mg, 70%). ¹H NMR (DMSO-*d*₆) δ 4.48 (s, 1H), 7.66 (d, *J* = 8.0 Hz, 2H), 8.02 (d, *J* = 8.0 Hz, 2H), 8.33 (s, 1H) (**Figure A-17**); ¹³C NMR δ 82.7, 84.3, 104.5, 115.8, 125.8, 130.6, 131.6, 132.3, 153.1, 162.9 (**Figure A-18**).

Part 3: Synthesis of Triphenylamine-porphyrin Compounds for DSSCs

3.3.7 Compound 12

Following a literature procedure⁽³⁶⁾ with slight modification, a mixture of **6** (167.2 mg, 0.2684 mmol) and **11**³⁷ (32.5 mg, 0.222 mmol) in THF (7 mL) was stirred under nitrogen atmosphere until a homogeneous solution was obtained. After that, bis(triphenylphosphine)palladium(II) dichloride (1.9 mg, 0.0027 mmol) and Copper(I) iodide (2.1 mg, 0.011 mmol) was added and the reaction mixture was stirred under nitrogen atmosphere at room temperature. After 20 h, the reaction mixture was redissolved in CH₂Cl₂ and washed with water. The organic phase was combined and dried over anhydrous MgSO₄. After the removal of solvent under reduced pressure, the crude product was precipitated in MeOH/CH₂Cl₂ to obtain **12** as a brown solid (69.1 mg, 48%). ¹H-NMR (CDCl₃) 6.78–6.94 (m, 6H), 7.24–7.46 (m, 4 H), 7.56–7.74 (m, 6H) (**Figure A-19**); MALDI-TOF-MS *m/z* obsd 388.508 [(M-2I)⁺], 640.740 [(M-H)⁺], calcd 641.238 (M = C₂₇H₁₇I₂NO₂) (**Figure A-20**).

3.3.8 Compound 13

Following a previously published procedure⁽³⁴⁾ with slight modification, a mixture of **5** (178.1 mg, 0.2788 mmol) and **12** (44.0 mg, 0.0686 mmol) in tetrahydrofuran/TEA (13.7 mL, 5:1) was stirred under nitrogen atmosphere until a homogeneous solution was obtained. After that, tris(dibenzylideneacetone) dipalladium(0) (29.6 mg, 0.0323 mmol) and tri(*o*-tolyl)phosphine (84.5 mg, 0.278 mmol) was added and the reaction mixture was

stirred under nitrogen atmosphere at 50 °C. After 41 h, the reaction mixture was redissolved in CH₂Cl₂ and washed with water. The organic phase was combined and dried over anhydrous MgSO₄. After the removal of solvent under reduced pressure, the crude mixture was purified by silica column [EtOAc] and triturated with methanol to obtain **13** as a magenta solid (13.4 mg, 12%). ¹H-NMR (CDCl₃) δ -2.82 (s, 4H), 6.94–7.24 (m, 8H), 7.35–7.99 (m, 30 H), 8.00–8.48 (m, 16H), 8.50–9.10 (m, 16H) (**Figure A-21**); MALDI-TOF-MS m/z obsd 1663.882 [(M+H)⁺], calcd 1662.928 (M = C₁₁₉H₇₅N₉O₂) (**Figure A-22**); λ_{abs} 419, 515, 547, 590, 648 nm (**Figure B-14**); λ_{em} (λ_{ex} = 419 nm) 652, 719 nm (**Figure B-15**).

3.3.9 Compound 2

Adapted from a previously published procedure,⁽³²⁾ a solution of **13** (12.6 mg, 0.00758 mmol) in CHCl₃ (6.0 mL) was treated with a solution of Zn(OAc)₂·2H₂O (20.7 mg, 0.0943 mmol) in methanol (2.0 mL) was stirred overnight at room temperature. The reaction mixture was concentrated to dryness, redissolved in CH₂Cl₂ and then washed with water. The organic phase was combined and dried over anhydrous MgSO₄. After the removal of solvent under reduced pressure, the crude product was purified by column chromatography [silica gel, MeOH/CH₂Cl₂ (2:98)], affording **2** as a magenta solid (11.3 mg, 83%). ¹H-NMR (CDCl₃) δ 7.45–7.50 (m, 4H), 7.51–7.64 (m, 10 H), 7.66–7.77 (m, 20H), 7.89 (d, *J* = 7.6 Hz, 4H), 7.96–8.04 (m, 2H), 8.14–8.21 (m, 16H), 8.91 (d, *J* = 10.0 Hz, 16H) (**Figure A-23**); ¹³C NMR δ 89.7, 90.5, 118.6, 120.4, 121.4, 121.5, 122.8, 124.1, 124.5, 125.9, 126.7, 127.7, 129.95, 130.3, 131.6, 131.9, 132.2, 132.4, 133.2, 134.6, 134.7, 143.0, 143.1, 147.0, 150.1, 150.4, 150.5 (**Figure A-24**); MALDI-TOF-MS m/z obsd 1791.114 [(M+H)⁺], calcd 1789.716 (M = C₁₁₉H₇₁N₉O₂Zn₂) (**Figure A-25**); λ_{abs}(ε) 425(476,010), 557(20,336), 596(8,478) nm (**Figure B-16–19**); λ_{em} (λ_{ex} = 425 nm) 604, 654 nm (**Figure B-20**).

3.3.10 Compound 3

Adapted from a previously published procedure,⁽³⁴⁾ a mixture of **8** (44.1 mg, 0.0268 mmol) and **10** (35.5 mg, 0.180 mmol) in tetrahydrofuran/TEA (14.0 mL, 5:1) was stirred under nitrogen atmosphere until a homogeneous solution was obtained. After that,

tris(dibenzylideneacetone) dipalladium(0) (9.1 mg, 0.0099 mmol) and tri(*o*-tolyl)phosphine (15.7mg, 0.0516 mmol) was added and the reaction mixture was stirred under nitrogen atmosphere at 50 °C. After 40 h, the reaction mixture was redissolved in CH₂Cl₂ and washed with water. The organic phase was combined and dried over anhydrous MgSO₄. After the removal of solvent under reduced pressure to obtain crude of **14** which exhibited the expected molecular ion peak of **14**. MALDI-TOF-MS m/z obsd 1714.632, calcd 1713.973 (M = C₁₂₂H₇₆N₁₀O₂) (**Figure A-26**). The crude was used in the metallation step without further purification. The result will be reported elsewhere.

CHAPTER IV

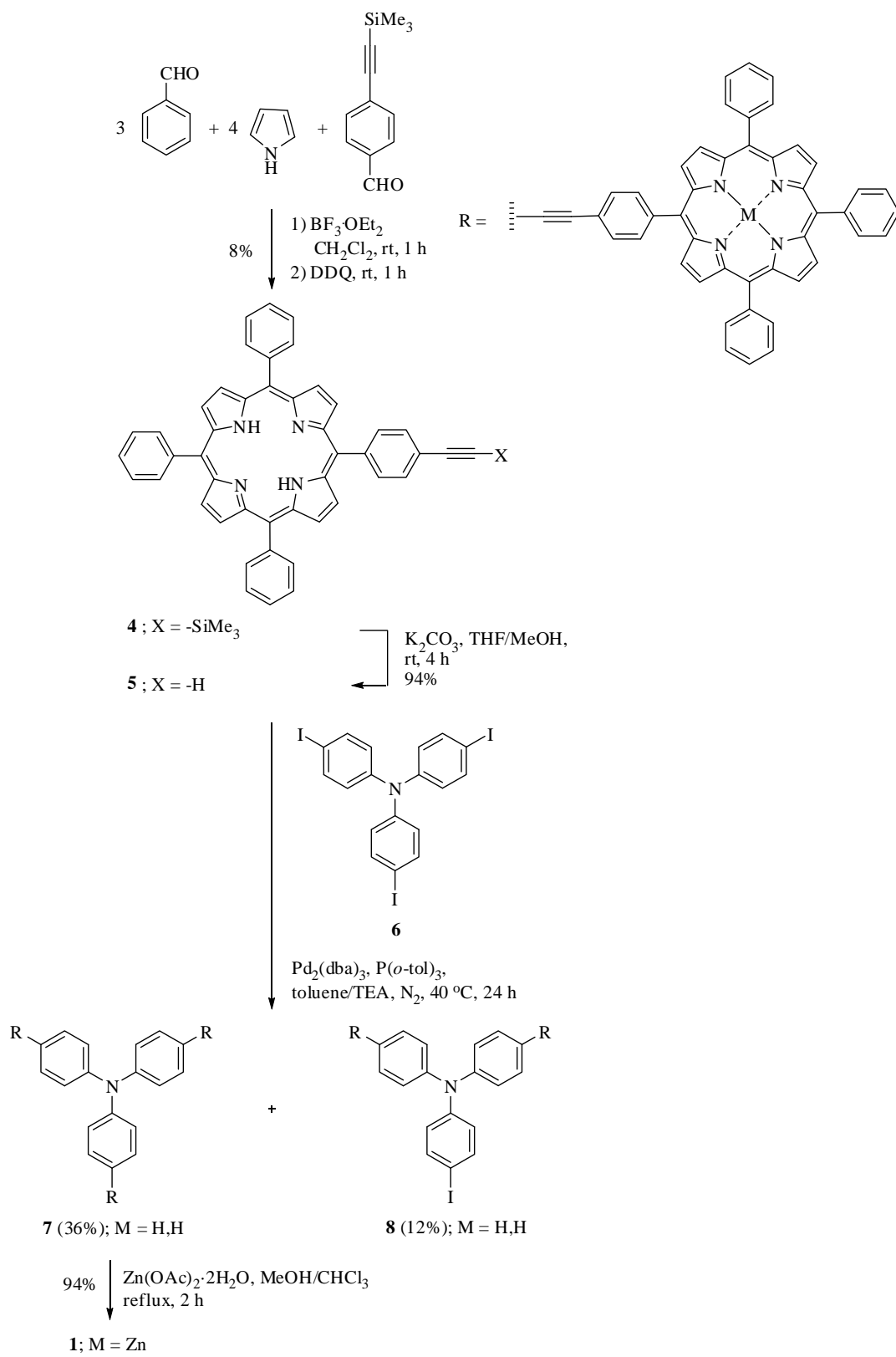
RESULTS AND DISCUSSION

Key concepts of the molecular design of the organic light sensitizers in this project are (i) the collaboration between highly photoactive porphyrin and hole transporting triphenylamine for broad absorption range and efficient charge transfer, and (ii) the use of the surface anchoring groups to enhance the electronic communication between the organic compounds and the electrode surface. Preparation of a series of triphenylamine-porphyrin derivatives was pursued and is separately described according to their applications as follows.

4.1 Triphenylamine-porphyrin Compound for BHJ-SCs.

4.1.1 Synthesis

Synthesis of target compound **1** for BHJ-SCs is illustrated in Scheme 4-1.



Scheme 4-1. Synthesis of triphenylamine-porphyrin compound **1**.

The synthesis started from Lindsey's condensation⁽³¹⁾ of benzaldehyde, pyrrole and 4-((trimethylsilyl)-ethynyl)benzaldehyde in the presence of $\text{BF}_3 \cdot \text{OEt}_2$ at room temperature for 1 h. Then, DDQ was added in the reaction mixture as an oxidizing agent, leading to **4** in 8% yield. The major reason of low yield is the competing reaction in the porphyrin formation step, *i.e.* a polymerization of pyrrole and the formation of other statistically possible porphyrin by-products. From $^1\text{H-NMR}$ spectrum, a characteristic inner proton peak of a free base porphyrin appeared as a singlet at $\delta -2.25$ ppm. A singlet peak indicating a trimethylsilyl group was observed at 0.41 ppm. With regard to the solubility, compound **4** is soluble in several common organic solvents, such as CH_2Cl_2 , toluene and THF. A trimethylsilyl group of **4** was readily removed by a reaction of **4** with K_2CO_3 in tetrahydrofuran/methanol at room temperature for 4 h, leading to compound **5** in 94% yield. In a $^1\text{H-NMR}$ spectrum, the singlet peak of trimethylsilyl group at 0.41 ppm was disappeared and a singlet peak of an ethynyl proton at 3.32 ppm was observed, indicating the successful deprotection.

Sonogashira coupling of compounds **5** and **6** under catalysis of tris(dibenzylideneacetone) dipalladium(0) and tri(*o*-tolyl)phosphine in toluene/TEA under nitrogen atmosphere at 40 °C for 24 h afforded the desirable compounds **7** and **8** in 36% and 12%, respectively. A mass spectrum of **7** showed a molecular ion peaks at 2156.838, while that of **8** exhibited a molecular ion at m/z 1645.721 and a fragment ion at 1519.852, resulting from the fragmentation of an iodine atom. After that **7** was zinc-metallated in the presence of $\text{Zn}(\text{OAc})_2 \cdot 2\text{H}_2\text{O}$ in refluxing chloroform/methanol for 2 h, affording to **1** in 94% yield. Upon the excitation at its maximum absorption (420 nm), the emission of **7** appeared at 654 and 719 nm, while that of **1** was observed at 607 and 655 nm upon the excitation at 425 nm. The absence of the emission at about 720 nm, together with the disappearance of the singlet signal at -2.80 ppm of the $^1\text{H-NMR}$ spectrum of **1** indicated the complete metallation of the porphyrin ring.

4.1.2 Investigation of Photophysical and Electrochemical Properties of **1**

Electrochemical properties of **1** was determined by mean of cyclic voltammetry in MeCN containing 0.1 M Bu_4NPF_6 by using a ITO-coated glass working electrode, Pt

wire counter electrode and Ag/AgCl quasi-reference electrode (QRE) with scan rate of 50 mV/s. The resulting redox potentials were externally calibrated with ferrocene/ferrocenium couple of which the potential of 0.40 V vs NHE was used. The result from cyclic voltammetry indicated that the estimated energy gap of **1** was 1.9 eV with the highest occupied molecular orbital (HOMO) level of -5.5 eV and the lowest unoccupied molecular orbital (LUMO) level of -3.6 eV. When consider together with ITO conduction band (CB), PEDOT:PSS Fermi level (FL), HOMO-LUMO level of P3HT and PCBM and Al work function (WF), the HOMO-LUMO level of **1**, the HOMO-LUMO levels of **1** should be able to serve both as donor or acceptor for the solar cells (Figure 4-1).

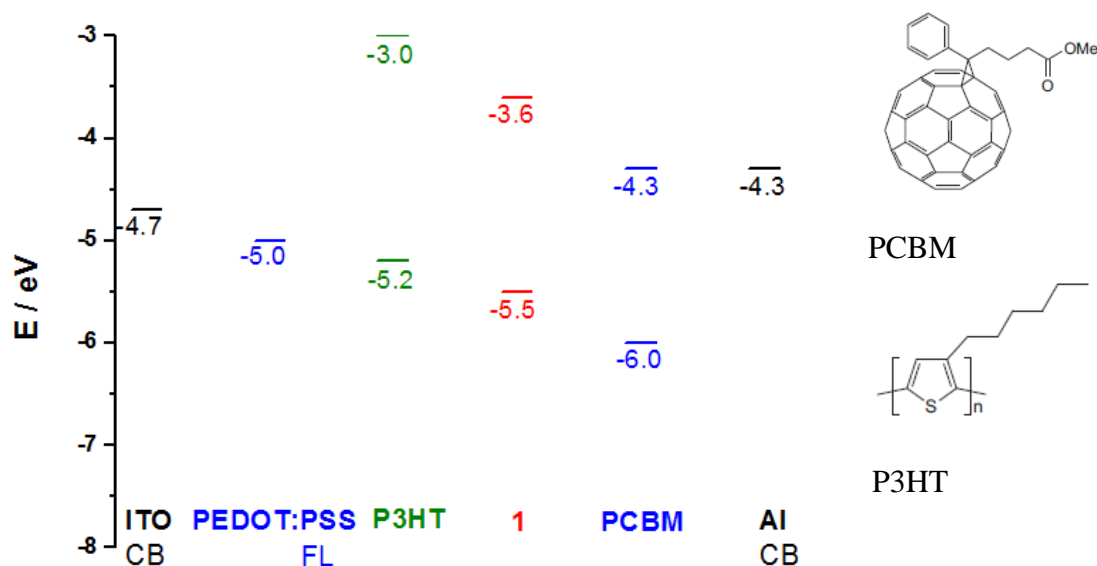


Figure 4-1. Comparative energy diagram of compound **1**-based BHJ-SC.

In order to prove the ability of **1** for serving as a donor or an acceptor material, a photoluminescence study of compound **1**:PCBM (1:1) and P3HT: **1** (1:1) blended films was performed. The films were prepared by spincoating the mixed solution (60 μ L) in chlorobenzene at 800 rounds per minute for 25 seconds. The result in Figure 4-2 showed that porphyrin emission was completely quenched by PCBM, indicating the efficient electron transfer from **1** (donor) to PCBM (acceptor). However, such emission

quenching was not observed in the case of a P3HT: **1** film, indicating that the charge transfer from P3HT (donor) to **1** (acceptor) was not efficient.

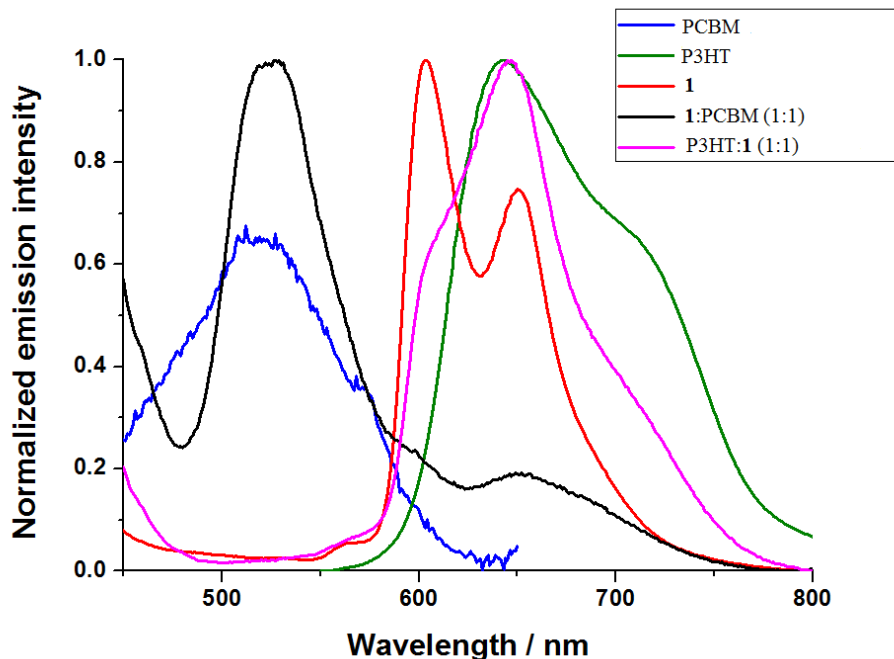


Figure 4-2. Result of photoluminescence study of the films.

4.1.3 Fabrication of Compound **1**-based BHJ-SCs.

Following a standard procedure for device fabrication⁽³⁸⁾ with slight modification, the BHJ-SCs containing the **1**:PCBM was fabricated in the schematic structure shown in Figure 4-3.

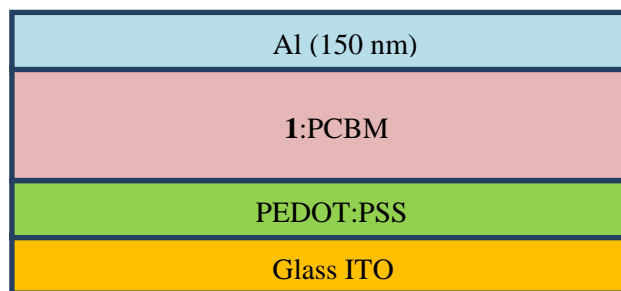


Figure 4-3. A schematic cell structure of a bulk heterojunction solar cell based on **1**.

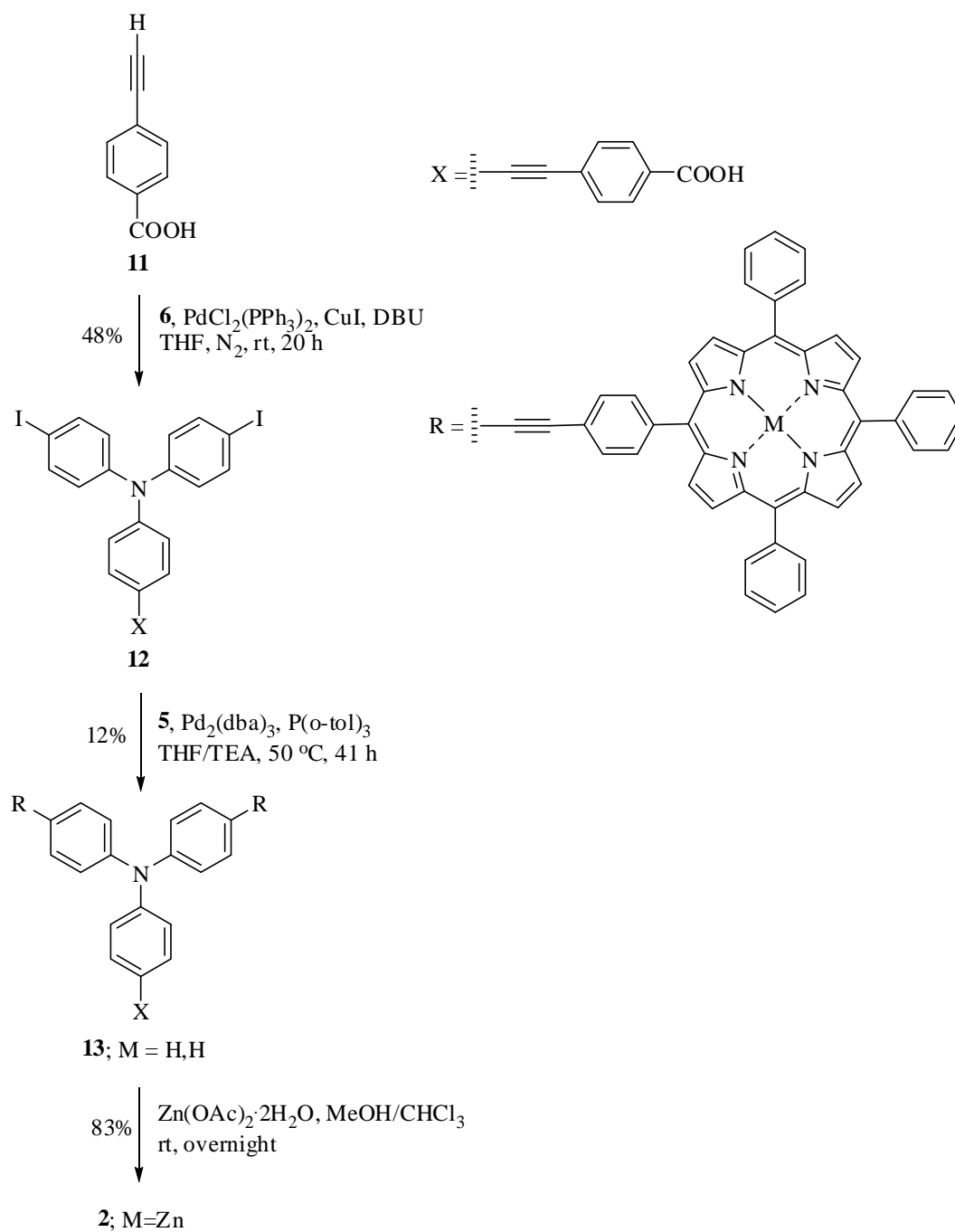
With the fixed film thickness and type of a metal top contact, PEDOT:PSS and ITO-coated glass, the **1**:PCBM ratio was varied from 4:1 to 1:14 to optimize the device

efficiency. As a result, the η was found to be 0.1 to 0.3% with the highest value when the 1:PCBM weight ratio of 1:6 was used. Based on Atomic Force Microscopy (AFM) film measurement, the roughness of the resulting film was less than 10 nm with the thickness of ~80 nm. Varying of film thickness by using the different concentration of the 1:PCBM solution mixture in the film formation process was failed to improve the cell efficiency. Further improvement of the device efficiency can be expected when other cell parameters, for example, types of top contact and PEDOT:PSS, and film formation technique is optimized.

4.2 Triphenylamine-porphyrin Compounds for DSSCs

4.2.1 Synthesis of compound **2**

In dye-sensitized solar cells, the photoactive compounds must be bound on TiO₂ surface. Therefore, a carboxyl surface anchoring groups was introduced to the triphenylamine-porphyrin compounds. Two surface anchoring units were used in this study : a 4-carboxyl group and a cyano acrylic acid group. The latter is expected to give enhanced electron injection, compare to the former, from the dye molecule into the TiO₂ electrode due to its strong electron withdrawing cyano group. The synthesis of **2** is shown in Scheme 4-2. Sonogashira coupling of compounds **6** and **11**³⁷ in the presence of bis(triphenylphosphine)palladium(II) dichloride and copper(I) iodide in THF under nitrogen atmosphere at room temperature for 20 h, leading to **12** in 48%. Then **12** was coupled with **5** under catalysis of tris(dibenzylideneacetone) dipalladium(0) and tri(*o*-tolyl)phosphine in THF/TEA under nitrogen atmosphere at 50 °C for 41 h, affording to the desirable **13** in 12%. Compound **13** was reacted with Zn(OAc)₂·2H₂O in refluxing chloroform/methanol for 2 h, affording Zn-chelated **2** in 83% yield.

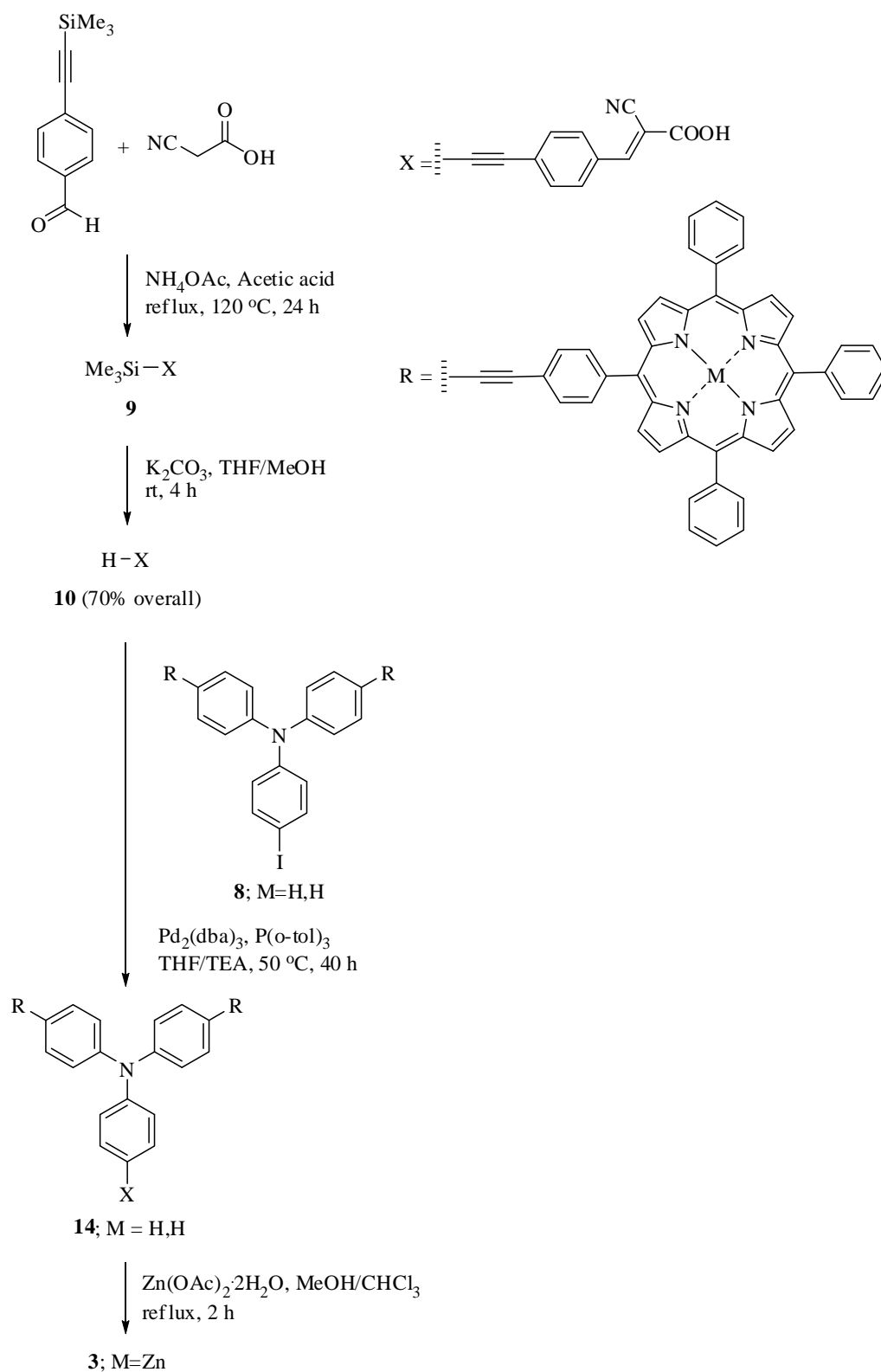


Scheme 4-2. Synthesis of triphenylamine-porphyrin compound **2** for DSSCs.

4.2.2 Synthesis of compound 3

As shown in Scheme 4-3, synthesis of the target **3** started from the preparation of the anchoring unit. 4-((Trimethylsilyl)-ethynyl)benzaldehyde was reacted with

cyanoacetic acid in the presence of NH_4OAc in refluxing acetic acid under nitrogen atmosphere for 24 h, resulting in trimethylsilyl compound **9**. Subsequent deprotection of trimethylsilyl group afforded **10** in 70% overall yield. After that compound **10** was coupled with **8** under catalysis of tris(dibenzylideneacetone) dipalladium(0) and tri(*o*-tolyl)phosphine in THF/TEA under nitrogen atmosphere at 50 °C for 40 h, leading to a crude mixture containing the desirable **14** of which the formation was confirmed by the presence of its molecular ion peak. The further metallation will be performed with this crude and reported elsewhere.



Scheme 4-3. Synthesis of triphenylamine-porphyrin compound **3** for DSSCs.

CHAPTER V

CONCLUSION

A series of novel triphenylamine-porphyrin derivatives has been successfully synthesized from Sonogashira coupling of 5,10,15-Triphenyl-20-(4-ethynylphenyl) porphyrin (**5**) and Tris(4-iodophenyl)amine (**6**) under catalysis of $\text{Pd}(\text{PPh}_3)_2\text{Cl}_2$ with and fully characterized. The completely coupled product (compound **1**), having a triphenylamine core and three porphyrin moieties exhibited satisfactory solubility in several common organic solvent. Compound **1** shown characteristic absorption peaks at about 425, 555 and 594 nm, and emission at 607 and 655 nm upon the excitation at its maximum absorption (420 nm). Based on cyclic voltammetry, the estimated energy band gaps and HOMO-LUMO levels are in the range allowing charge transport in the solar cells. The potential of charge transport was proved possible by the photoluminescence study, indicating the possible electron transfer from compound **1** (donor) to PCBM (acceptor). According to above properties, it can be concluded that compound **1** will be used as a photo-sensitizer in a bulk heterojunction solar cell. Compound **1** was fabricated for bulk heterojunction solar cells and obtained up to 0.3% energy conversion efficiency.

Similarly, compounds **2** exhibited the characteristic absorption at 425, 557 and 596 nm, and emission at 604 and 654 nm, while the synthesis of compound **3** has yet to be done. These compounds are subjected to the investigation for their potential use in dye-sensitized solar cells.

REFERENCES

- [1] Shirota, Y. Organic Materials for Electronic and Optoelectronic Devices J. Mater. Chem. 10 (2000): 1–25.
- [2] Shirota, Y. Photo- and Electroactive Amorphous Molecular Materials–Molecular Design, Synthesis, Reactions, Properties, and Applications J. Mater. Chem. 15 (2005): 75–93.
- [3] Shirota, Y., and Kageyama, H. Charge Carrier Transporting Molecular Materials and Their Applications in Devices Chem. Rev. 107 (2007): 953–1010.
- [4] Pagliaro, M., Palmisano G., and Ciriminna, R. Flexible Solar Cells Federal Republic of Germany: WILEY-VCH Verlag GmbH & Co., 2008.
- [5] O' Regan, B., and Gratzel, M. A Low Cost, High-Efficiency Solar Cell Based on Dye sensitized Colloidal TiO₂ Film Nature. 353 (1991): 737–740.
- [6] Gratzel, M., and Kalyanasundaram, K. Applications of Functionalized Transition Metal Complexes in Photonic and Optoelectronic Devices Coord. Chem. Rev. 177 (1998): 347–414.
- [7] Hagfeldt, A., and Gratzel, M. Molecular Photonics Acc. Chem. Rev. 33 (2000): 269–277.
- [8] Hara, K.; et al. Influence of Electrolyte on the Photovoltaic Performance of a Dye Sensitized TiO₂ Solar Cell Base on a Ru(II)terpyridyl Complex Photosensitizer Sol. Energy Mater. Sol. Cells 85 (2005): 21–30.
- [9] Nakashima, T., Satoh, N., Albrecht, K., and Yamamoto, K. Interface Modification on TiO₂ Electrode Using Dendrimers in Dye Sensitized Solar Cells Chem. Mater. 20 (2008): 2538–2543.
- [10] Song, L. Q.; et al. Photoinduced Intra Molecular Electron Transfer in Aniline Containing Ru(II)polypyridine Complexes J. Photochem. Photobiol. A-chem. 165 (2004): 137–142.
- [11] Grätzel, M. Dye-sensitized Solar Cells. J. Photochem. Photobiol, A. Rev. 4 (2003): 145–153.

- [12] Zhao, D., et al. Enhanced Photocatalytic Degradation of Dye Pollutants under Visible Irradiation on Al(III) Modified TiO₂: Structure, Interaction and Interfacial Electron Transfer Environ. Sci. Technol. 42 (2008): 308–314.
- [13] Milgrom, L. R. *The Colours of Life: An Introduction to the Chemistry of Porphyrins and Related Compounds* Oxford: OUP, 1975.
- [14] Rothmund, P. Formation of Porphyrins from Pyrrole and Aldehydes J. Am. Chem. Soc. 57 (1935): 2010–2011.
- [15] Adler, A. D., Longo, F. R., Finarelli, J. D., Goldmacher, J., Assour, J., and Korsakoff, L. A Simplified Synthesis for *meso*-Tetraphenylporphine J. Org. Chem. 32 (1967): 476.
- [16] Lindsey, J. S., Schreiman, I. C., Hsu, H. C., Kearney, P. C., and Marguerettaz, A. M. Rothermund and Adler-Longo Reactions Revisited: Synthesis of Tetraphenyl Porphyrins under Equilibrium Conditions J. Org. Chem. 52 (1987): 827–836.
- [17] Granstrom, M., Petritsch, K., Arias, A. C., Lux, A., Anderson, M. R., and Friend, R. H. Laminated Fabrication of Polymeric Photovoltaic Diodes Nature 395 (1998): 257–260.
- [18] Friend, R. H., et al. Electroluminescence in Conjugated Polymers Nature 397 (1999): 121–128.
- [19] Berezin, B.D., Berezin, M. B., Moryganov, A. P., Rumyantseva, S. V., and Dymnikova, N. S. Chlorophyll and Its Derivatives, Chlorins and Porphyrins, as a Promising Class of Environmentally Friendly Dyes Russian Journal of Applied Chemistry 76 (2003): 1958–1961.
- [20] Rahiman, A. K., Rajesh, K., Bharathi, K. S., Sreedaran, S., and Narayanan, V. Catalytic Oxidation of Alkenes by Manganese(III) Porphyrin-Encapsulated Al, V, Si-Mesoporous Molecular Sieves Inorg. Chim. Acta. 362 (2009): 1491–1500.
- [21] Fukushima, K., Tabata, K., and Okura, I. Photochemical Properties of Water-Soluble Fluorinated Zinc Phthalocyanines and Their Photocytotoxicity Against HeLa cells J. Porphyrins Phthalocyanines 2 (1998): 219–222.

- [22] Fang, Z., and Liu, B. A Cationic Porphyrin-Based Self-assembled Film for Mercury Ion Detection Tetrahedron Lett. 49 (2008): 2311–2315.
- [23] Mizutani, T., Wada, K., and Kitagawa, S. Porphyrin Receptors for Amines, Amino Acids, and Oligopeptides in Water J. Am. Chem. Soc. 121, (1999): 11425–11431.
- [24] Kathiravan, A., Kumar, P. S., Renganathan, R., and Anandan, S. Photoinduced Electron Transfer Reactions Between *meso*-Tetrakis(4-sulfonatophenyl) porphyrin and Colloidal Metal-Semiconductor Nanoparticles Colloids and Surfaces A: Physicochem. Eng. Aspects 333 (2002): 175–181.
- [25] Roquet, S., Cravino, A., Leriche, P., Aleveque, O., Frere, P., and Roncali, J. Triphenylamine–Thienylenevinylene Hybrid Systems with Internal Charge Transfer as Donor Materials for Heterojunction Solar Cells J. Am. Chem. Soc. 128 (2006): 3459–3466.
- [26] Lartia, R., et al. Synthetic Strategies to Derivatizable Triphenylamines Displaying High Two-photon Absorbtion J. Org. Chem. 73 (2008): 1732–1744.
- [27] Wei, P., Bi, X., Wu, Z., and Xu, Z. Synthesis of Triphenylamine-cored Dendritic Two-Photon Absorbing Chromophores Org. Lett. 7 (2005): 3199–3202.
- [28] Cravino, A., Roquet, S., Leriche, P., Aleveque, O., Frere, P., and Roncali, J. A Star-shaped Triphenylamine π -Conjugated System with Internal Charge-Transfer as Donor Material for Hetero-junction Solar Cells Chem. Commun. (2006): 1416–1418.
- [29] Seo, J.-W., Jang, S Y., Kim, D., and Kim, H-J. Octupolar Trisporphyrin Conjugates Exhibiting Strong Two-photon Absorbtion Tetrahedron 64 (2008): 2733–2739.
- [30] Campbell, W. M., Burrell, A. K., Officer, D. L., and Jolley, K. W. Porphyrins as Light Harvesters in The Dye-sensitised TiO₂ Solar Cell Coor. Chem. Rev. 248 (2004): 1363–1379.
- [31] Lindsey, J. S., Prathapan, S., Johnson, T. E., and Wagner, R. W. Porphyrin Building Blocks for Modular Construction of Bioorganic Model Systems Tetrahedron 50 (1994): 8941–8968.

- [32] Thamyongkit, P., et al. Swallowtail Porphyrin: Synthesis, Characterization and Incorporation into Porphyrin Dyads J. Org. Chem. 69 (2004): 3700–3710.
- [33] Varnavski, O. P., et al. Coherent Effects in Energy Transport in Model Dendritic Structures Investigated by Ultrafast Fluorescence Anisotropy Spectroscopy J. Am. Chem. Soc. 124 (2002): 1736–1743.
- [34] Tomizaki, K. Y., Thamyongkit, P., Loewe, R. S., and Lindsey, J. S. Practical Synthesis of Perylene-monoimide Building Blocks that Possess Features Appropriate for Use in Porphyrin-based Light-harvesting Arrays Tetrahedron 59 (2003): 1191–1207.
- [35] Chang, Y. J., and Chow, T. J. Dye-sensitized Solar Cell Utilizing Organic Dyads Containing Triarylene Conjugates Tetrahedron 65 (2009): 4726–4734.
- [36] Niamnont, N., Siripornnoppakhun, W., Rashatasakhon, P., and Sukwattanasinitt, M. A Polyanionic Dendritic Fluorophore for Selective Detection of Hg^{2+} in Triton X-100 Aqueous Media Org. Lett. 11 (2009): 2768–2771.
- [37] Jones, L. F., et al. Tuning Magnetic Properties Using Targeted Structural Distortion: New Additions to A Family of Mn_6 Single-molecule Magnets Inorg. Chim. Acta 361 (2008): 3420–3426.
- [38] Pavel, A. T., et al. Material Solubility-Photovoltaic Performance Relationship in the Design of Novel Fullerene Derivatives for Bulk Heterojunction Solar Cells Adv. Funct. Mater. 19 (2009): 779–788.

APPENDICES

APPENDIX A

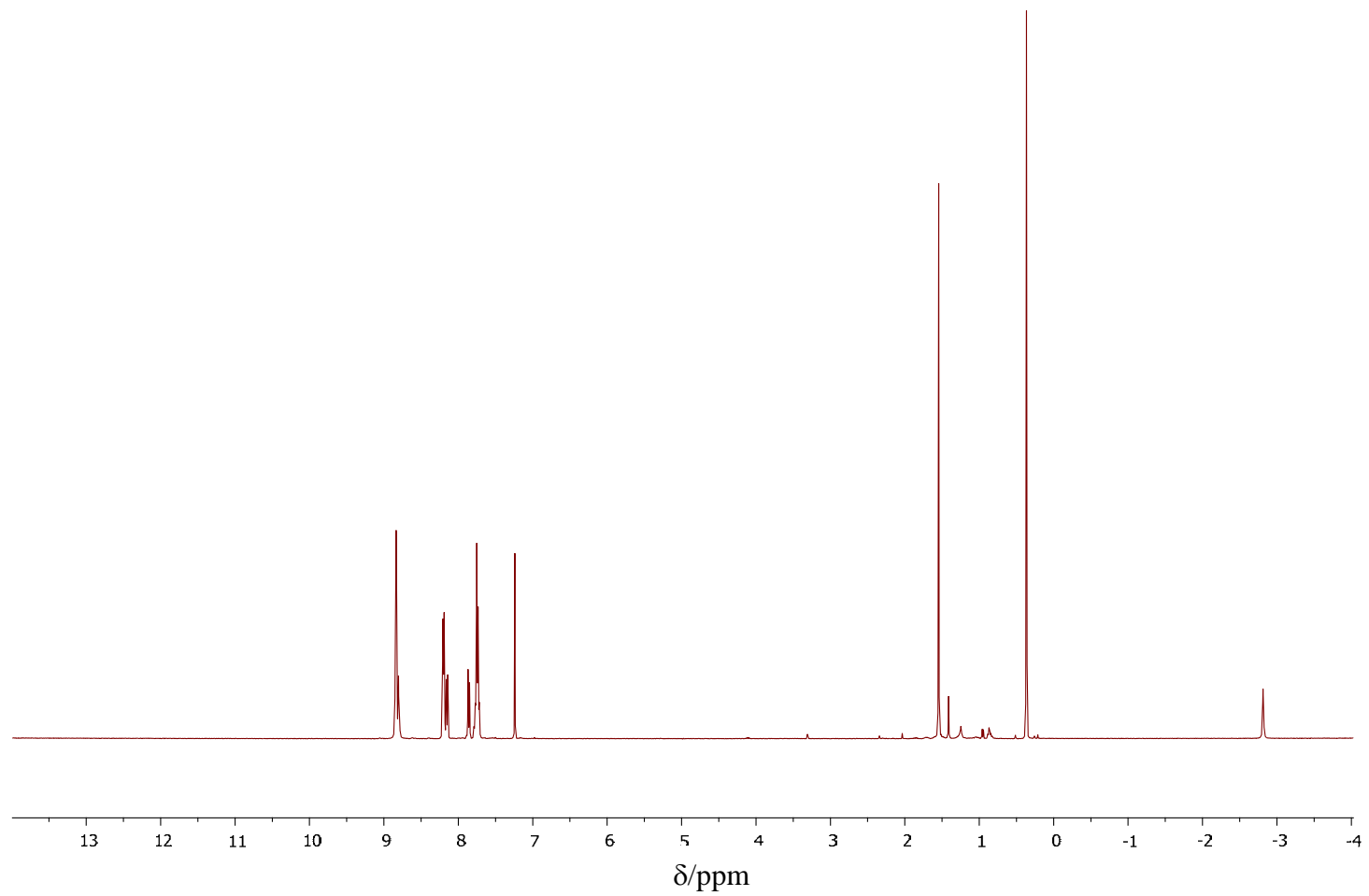


Figure A-1. $^1\text{H-NMR}$ spectrum of compound

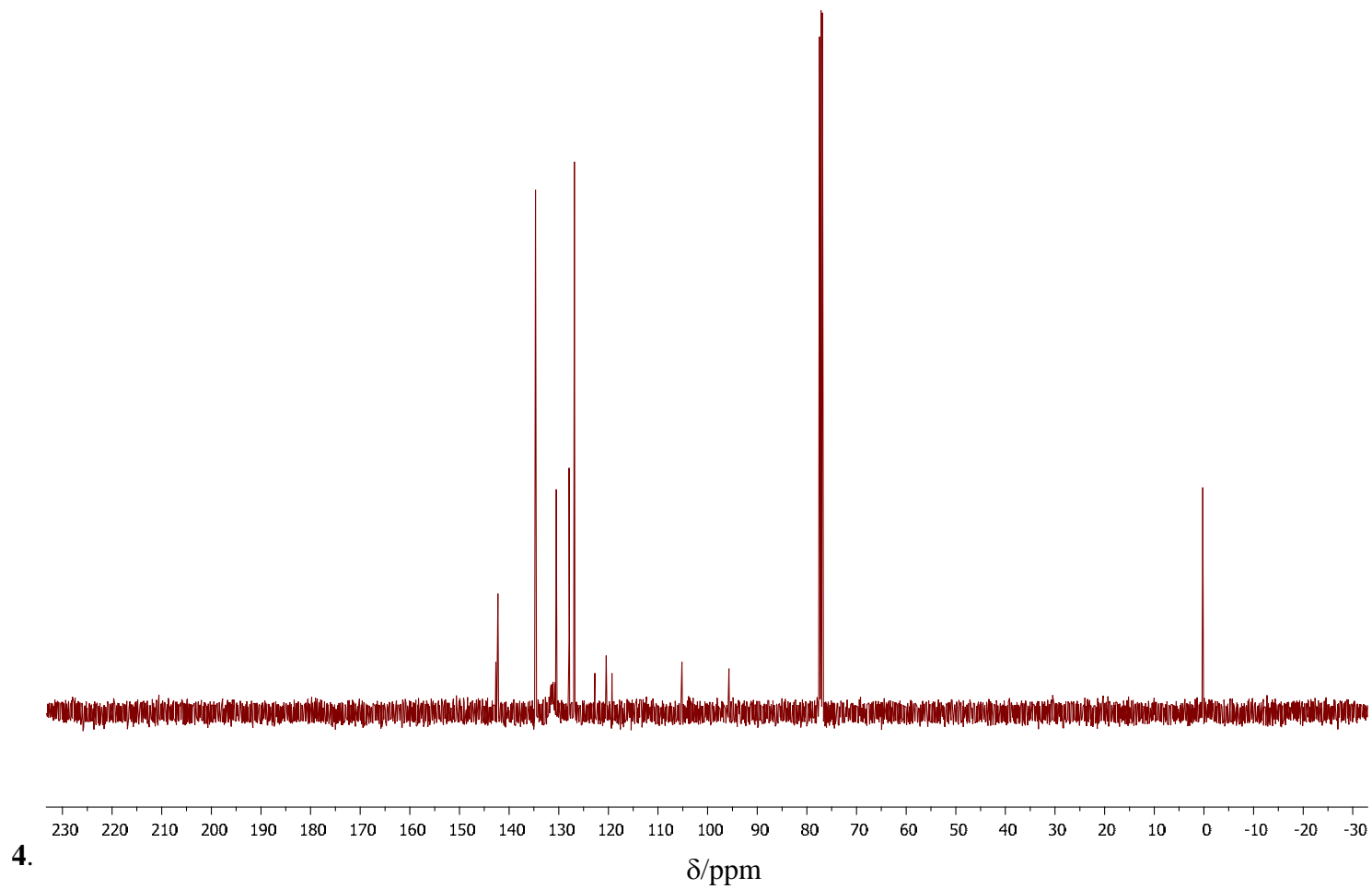


Figure A-2. ^{13}C -NMR spectrum of compound **4**.

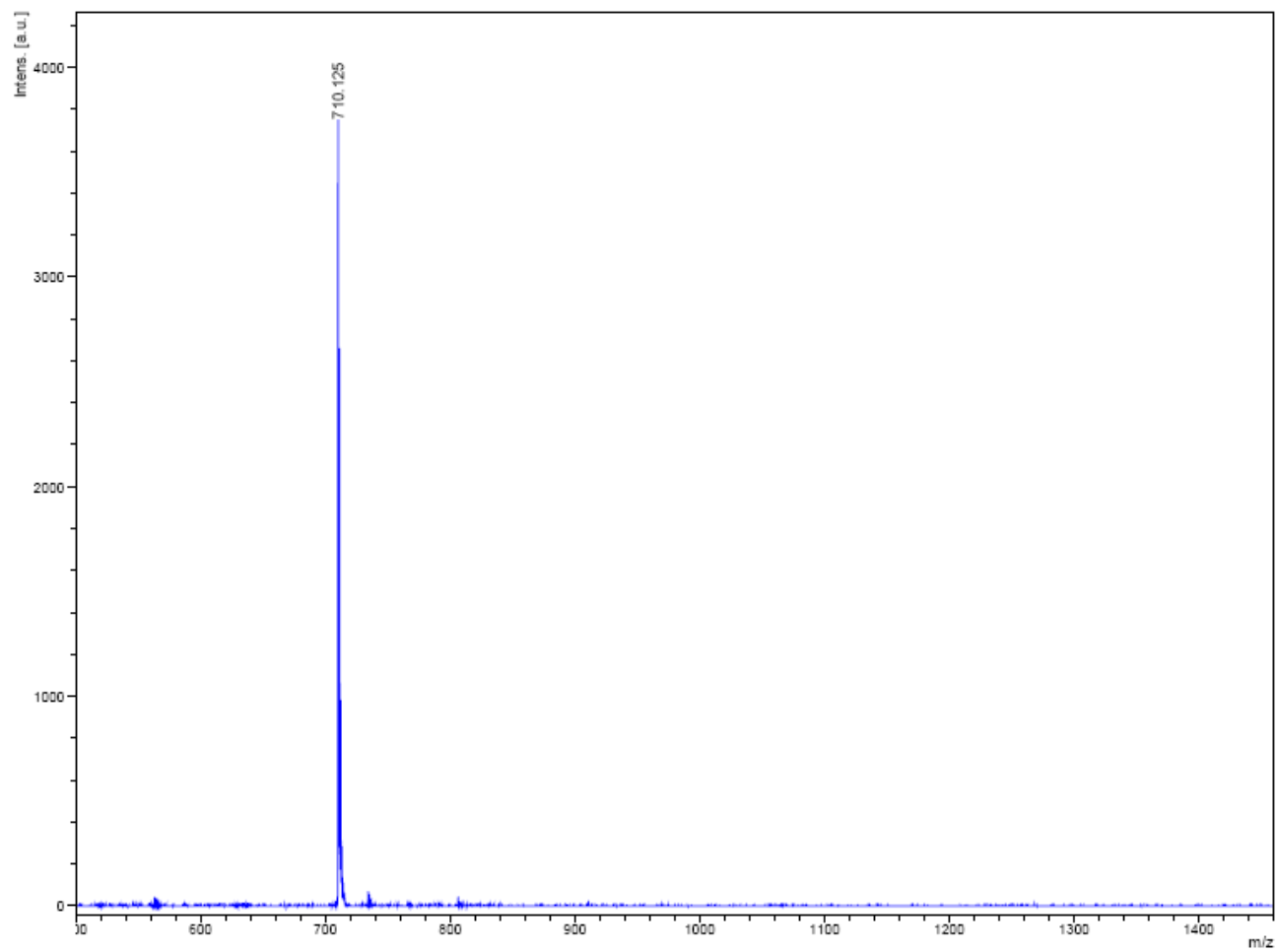


Figure A-3. Mass spectrum of compound **4**.

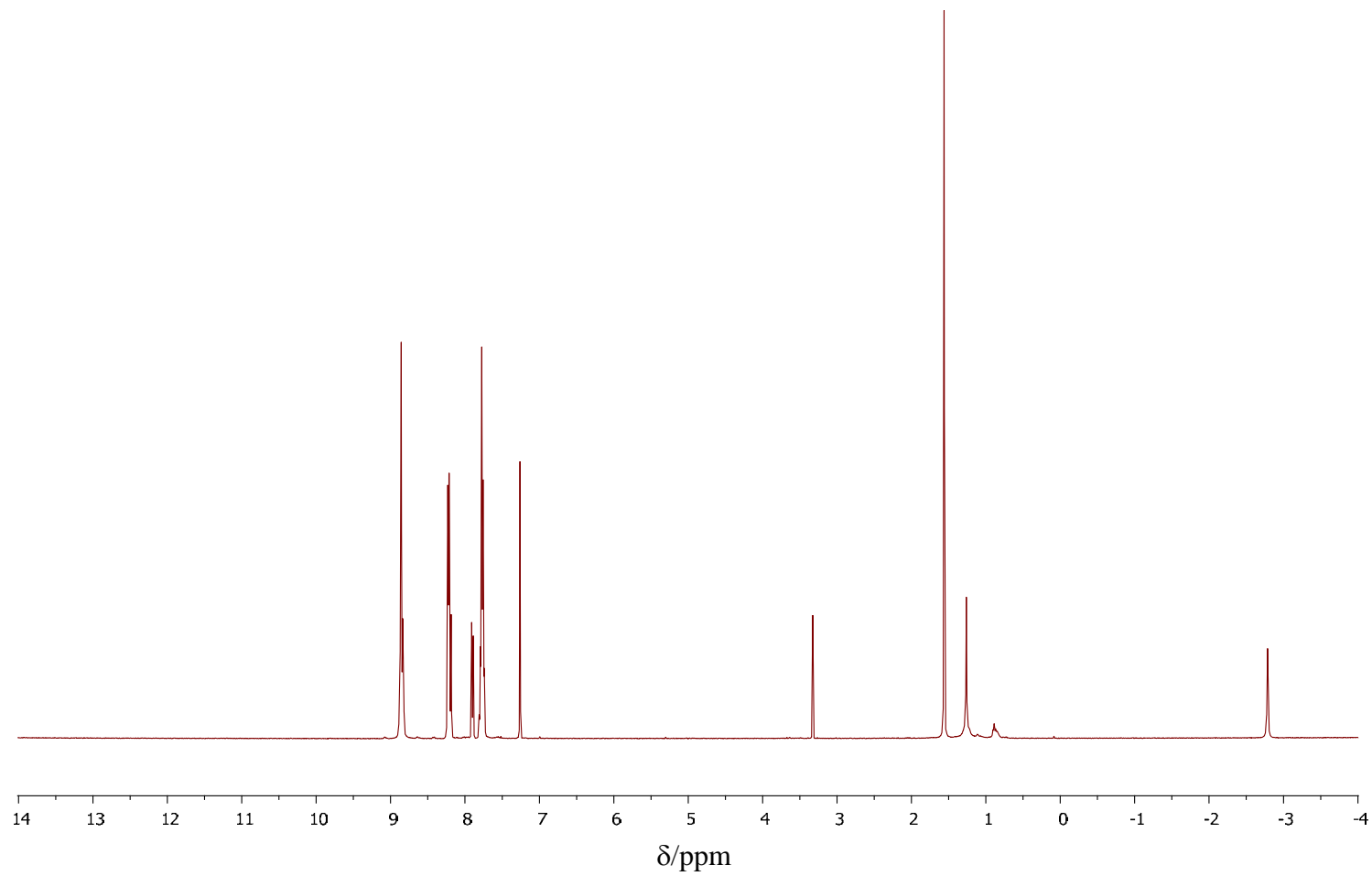


Figure A-4. $^1\text{H-NMR}$ spectrum of compound 5.

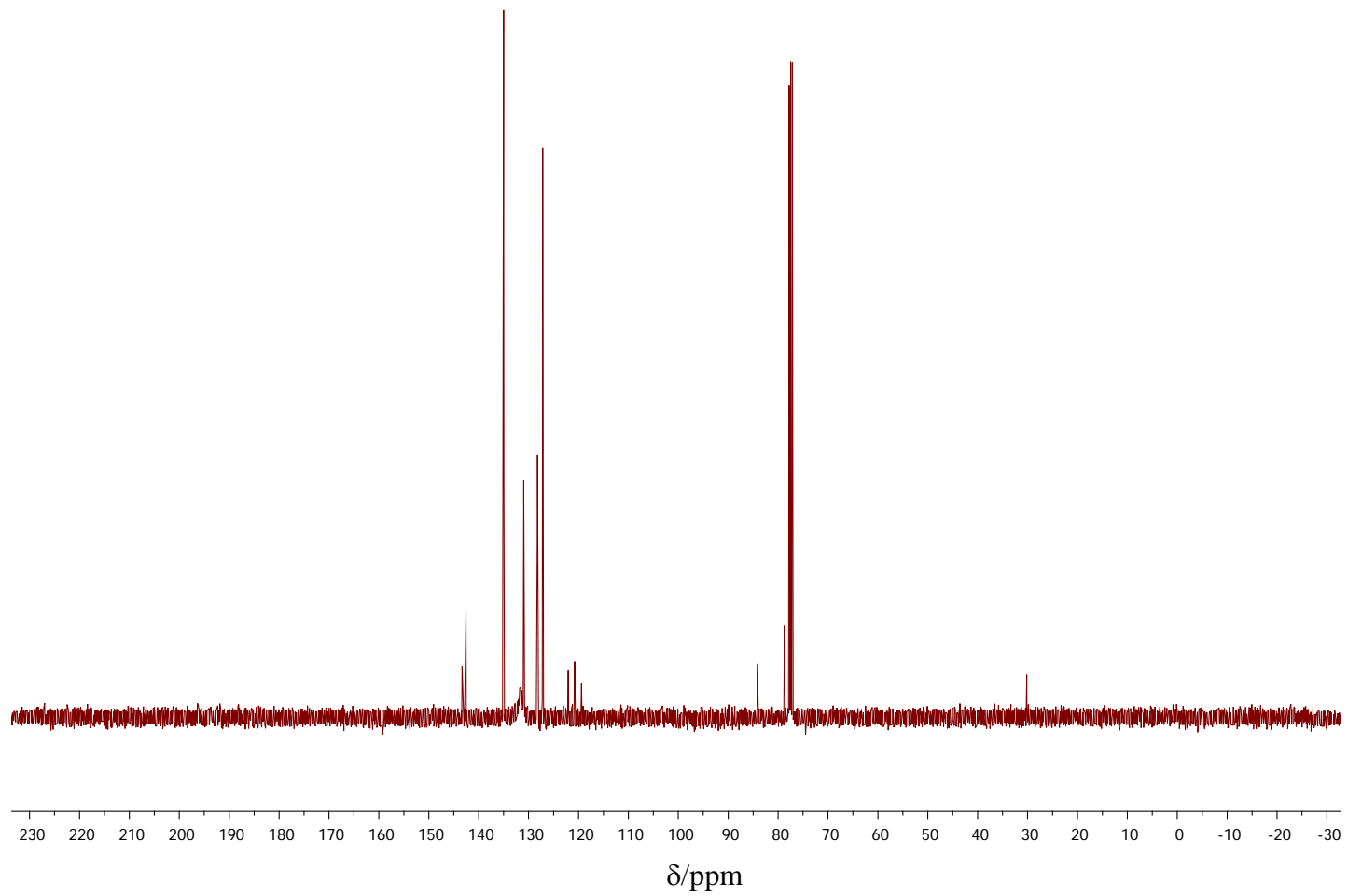


Figure A-5. ^{13}C -NMR spectrum of compound 5.

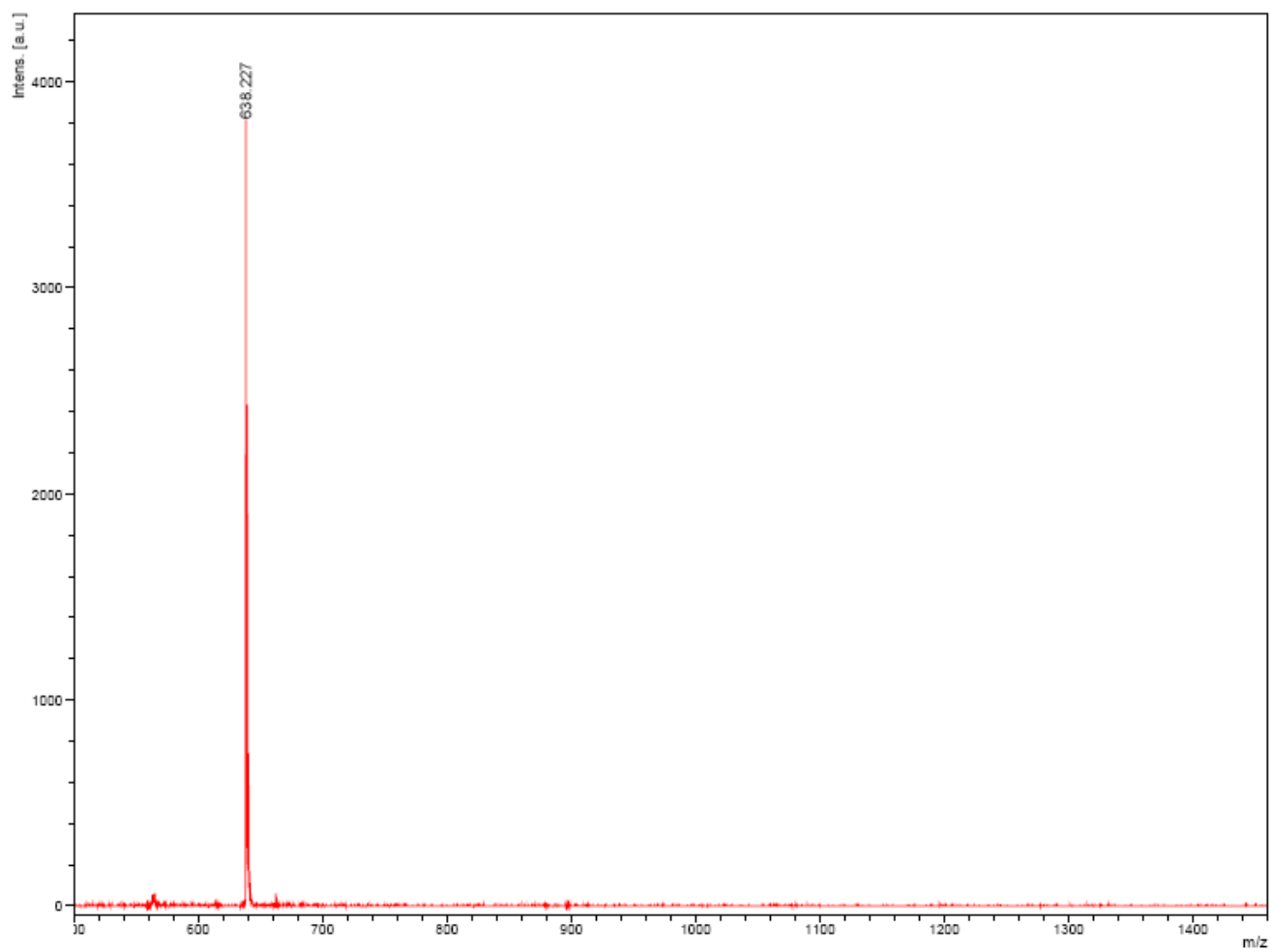


Figure A-6. Mass spectrum of compound **5**.

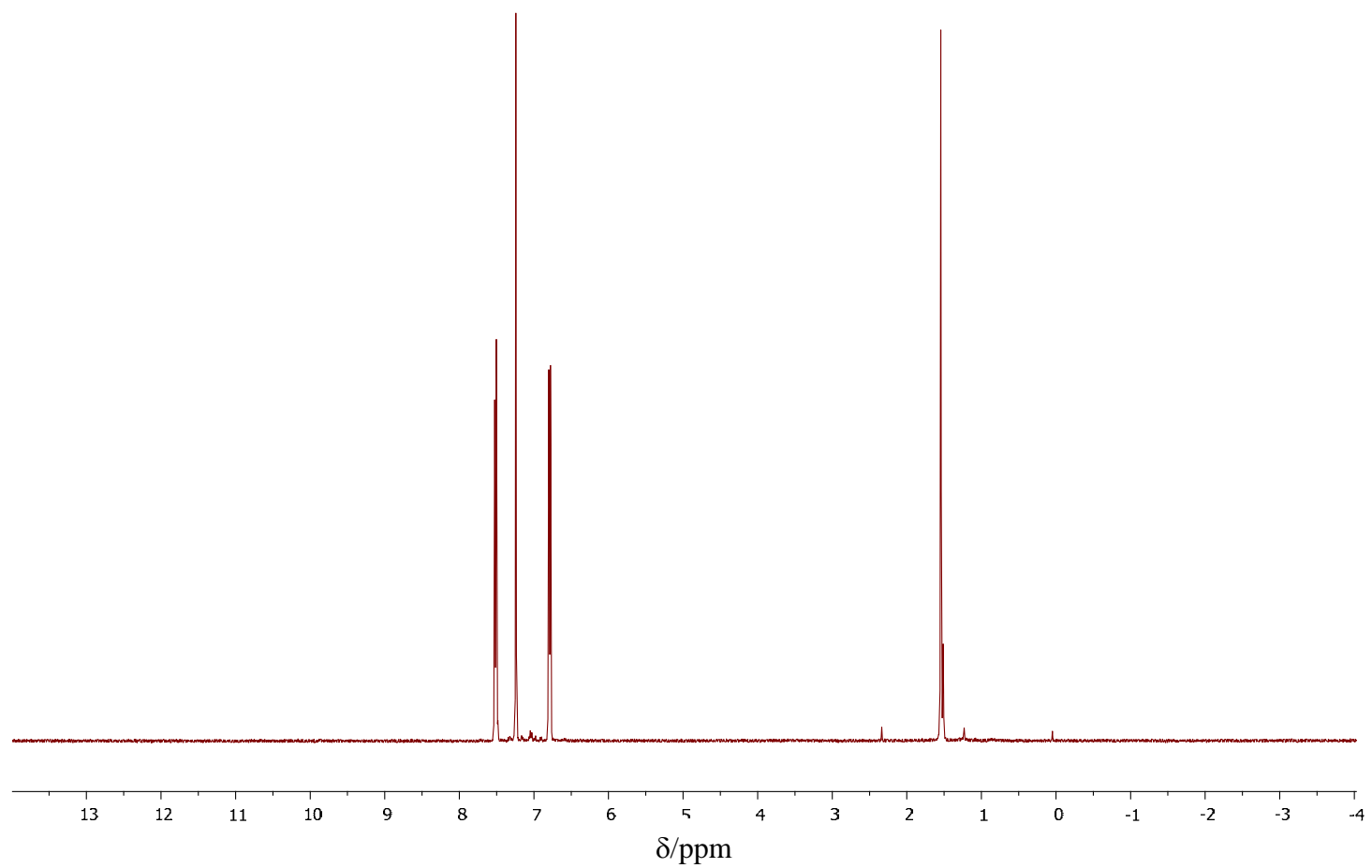


Figure A-7. $^1\text{H-NMR}$ spectrum of compound 6.

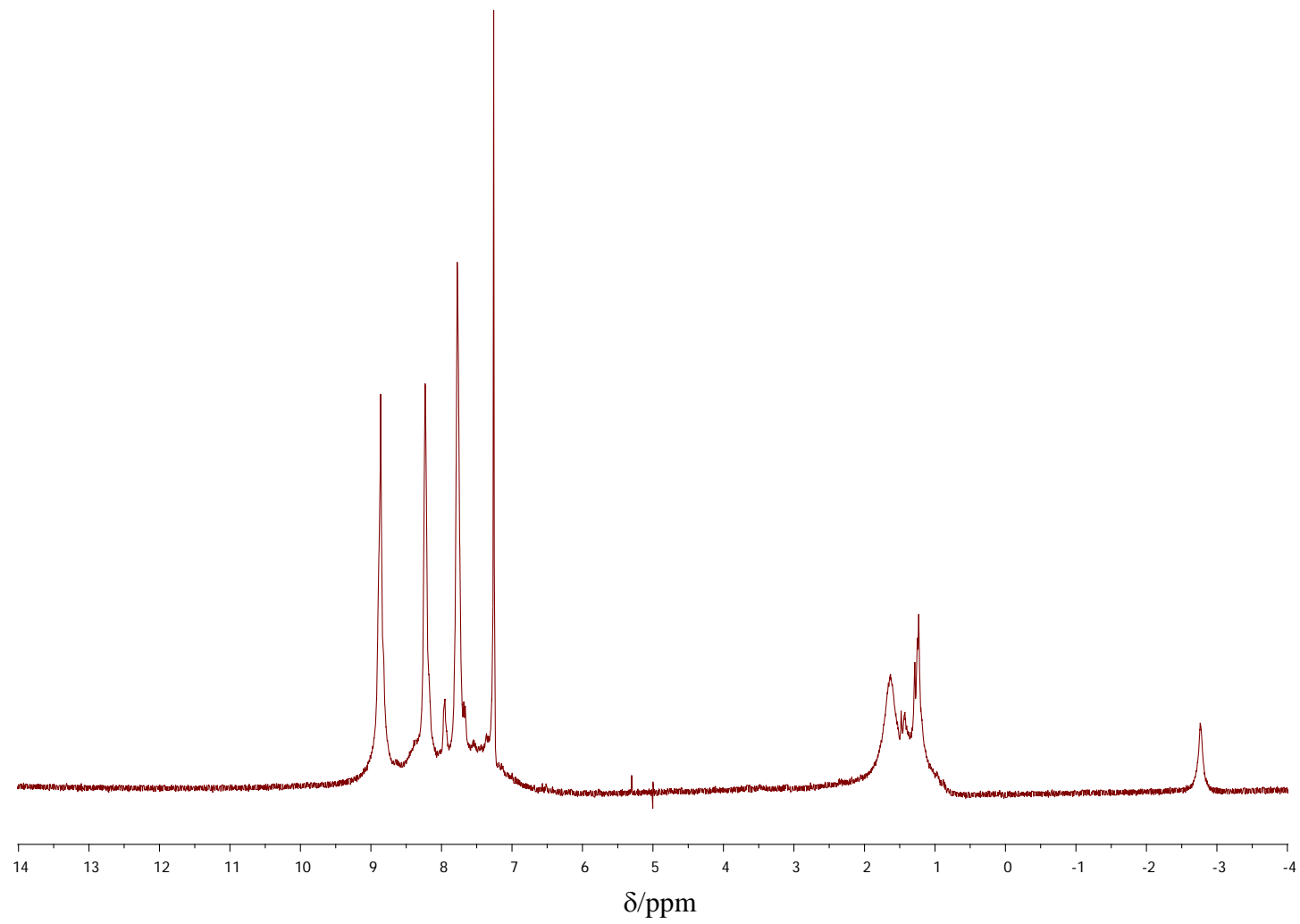


Figure A-8. $^1\text{H-NMR}$ spectrum of compound 7.

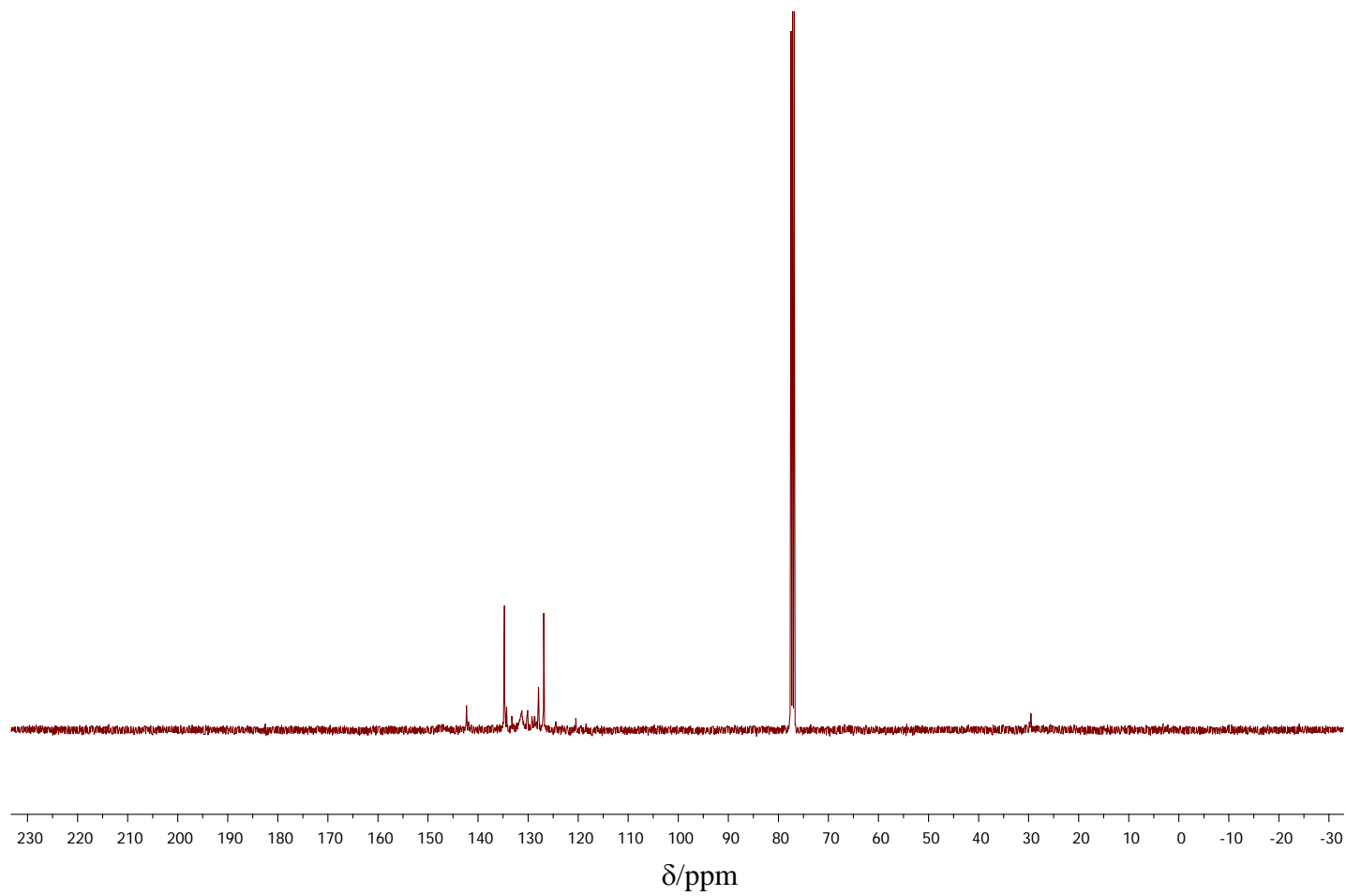


Figure A-9. ^{13}C -NMR spectrum of compound 7.

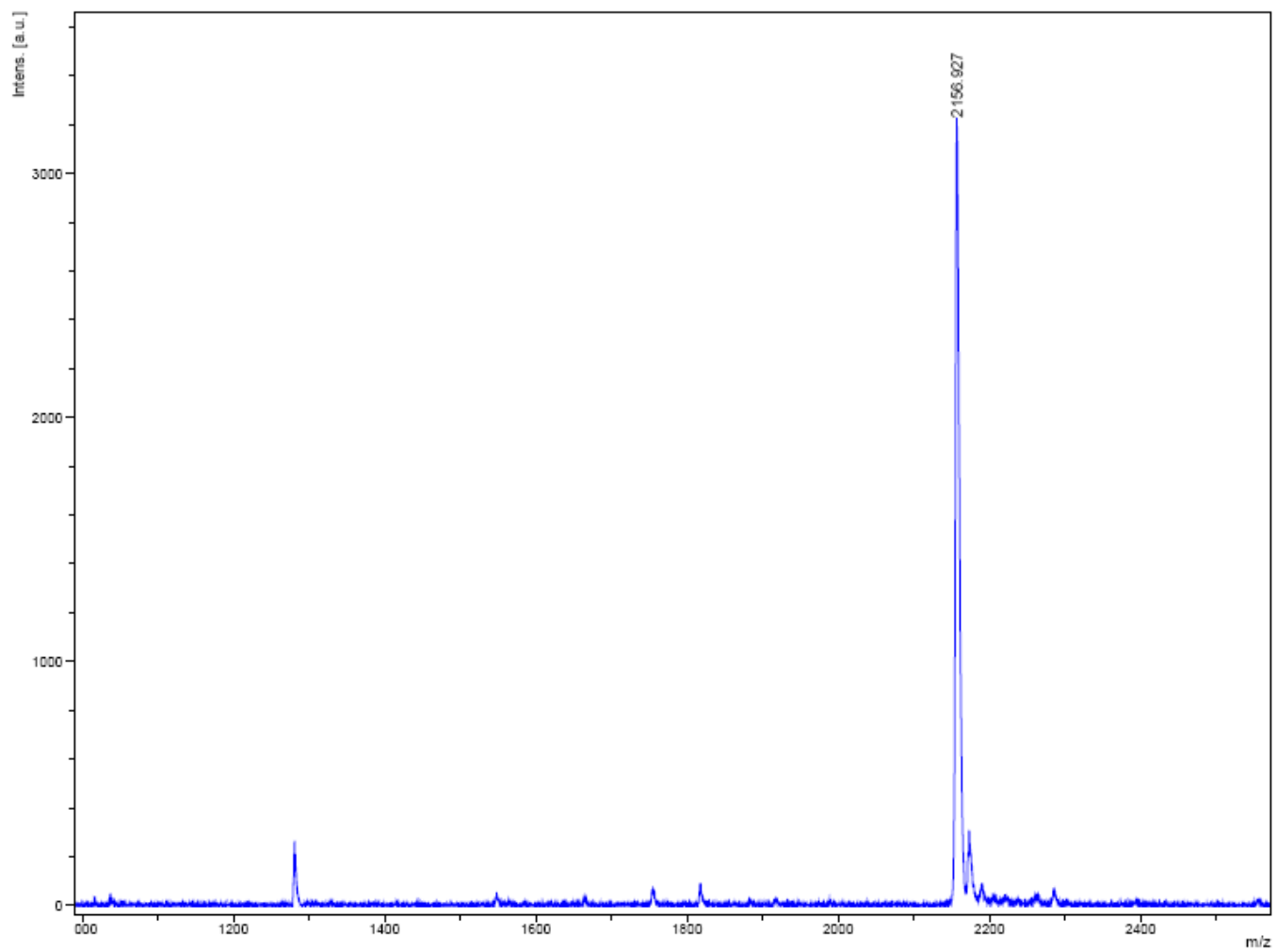


Figure A-10. Mass spectrum of compound 7.

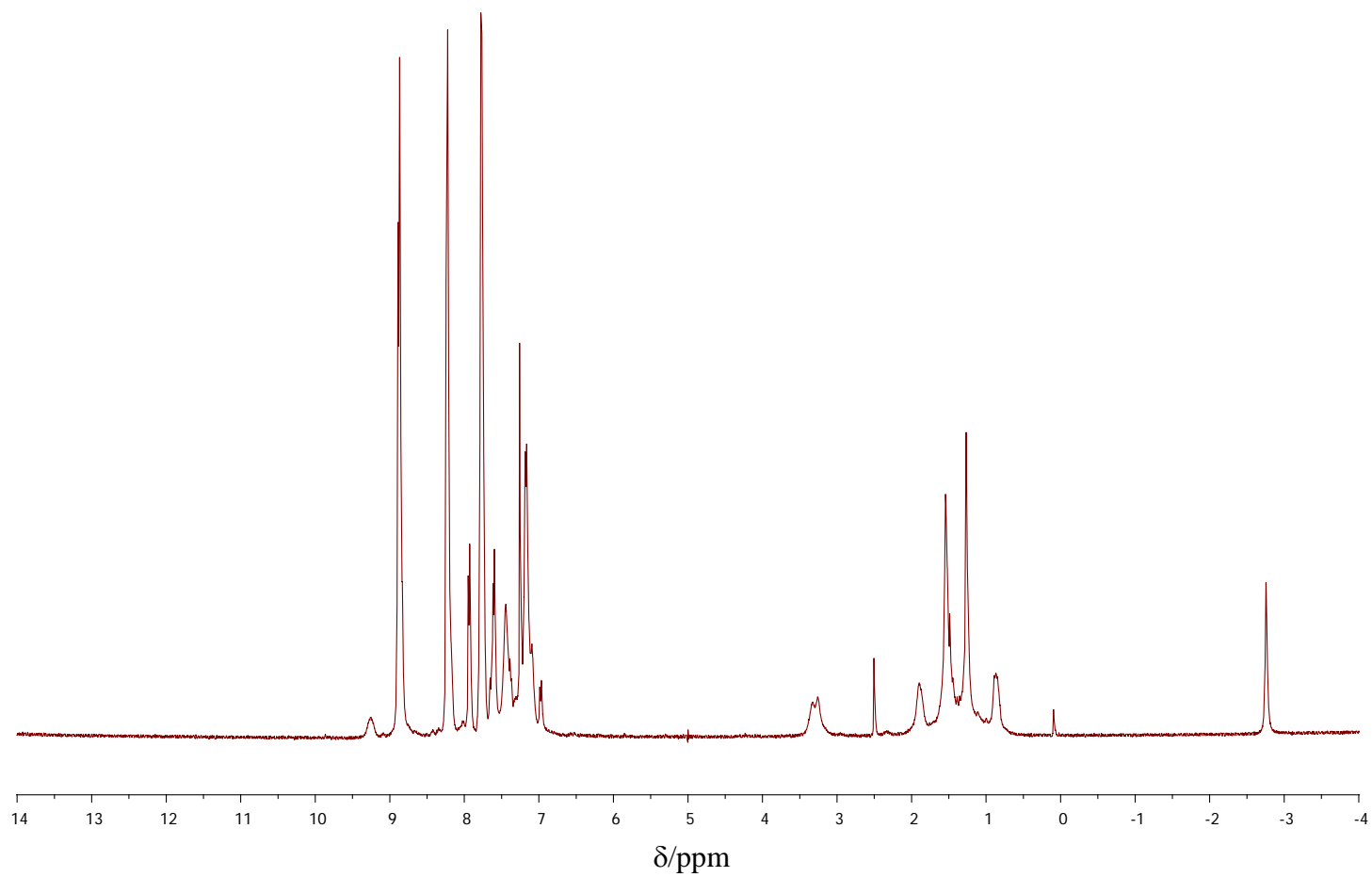


Figure A-11. $^1\text{H-NMR}$ spectrum of compound **8**.

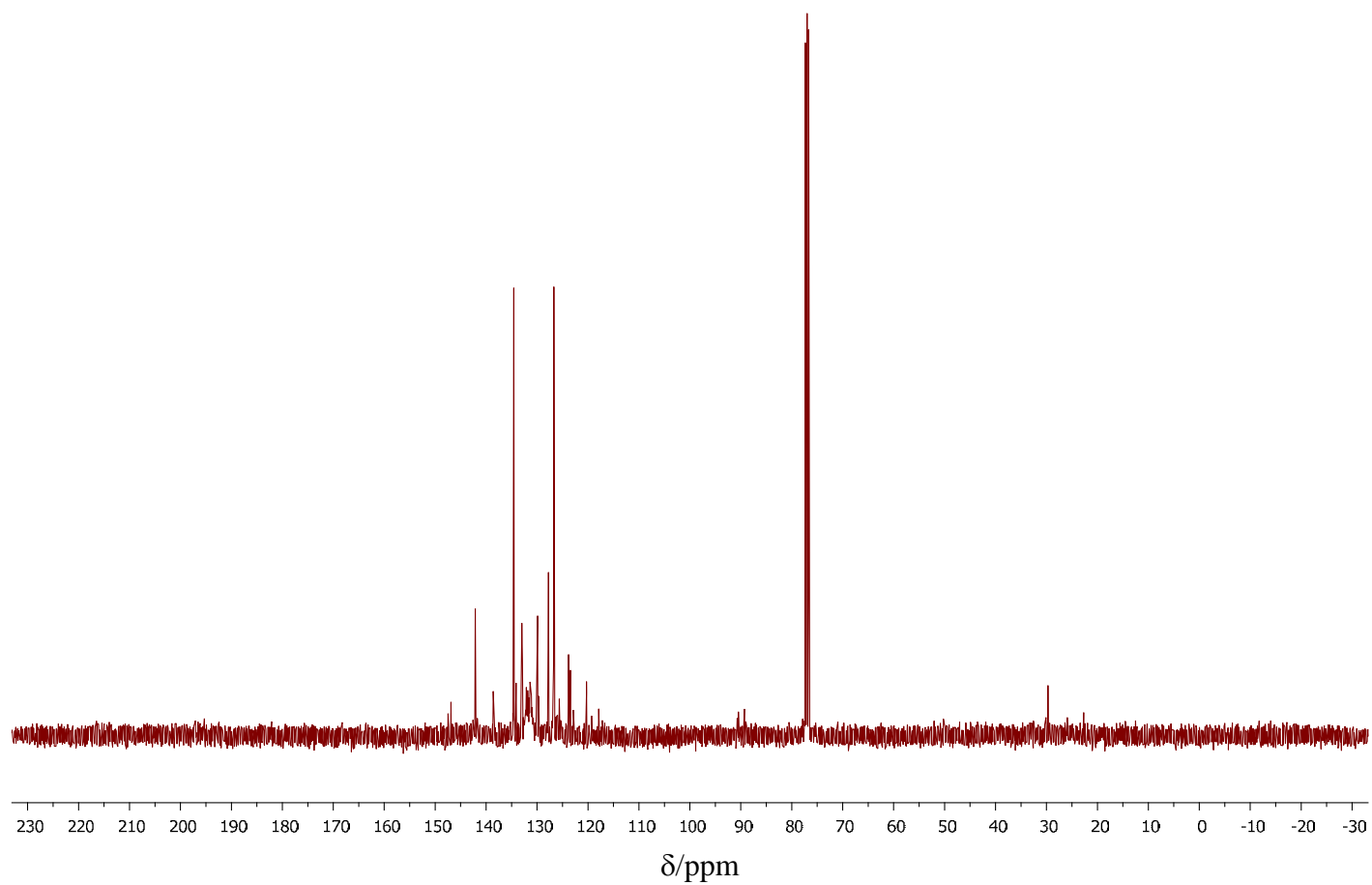


Figure A-12. ^{13}C -NMR spectrum of compound **8**.

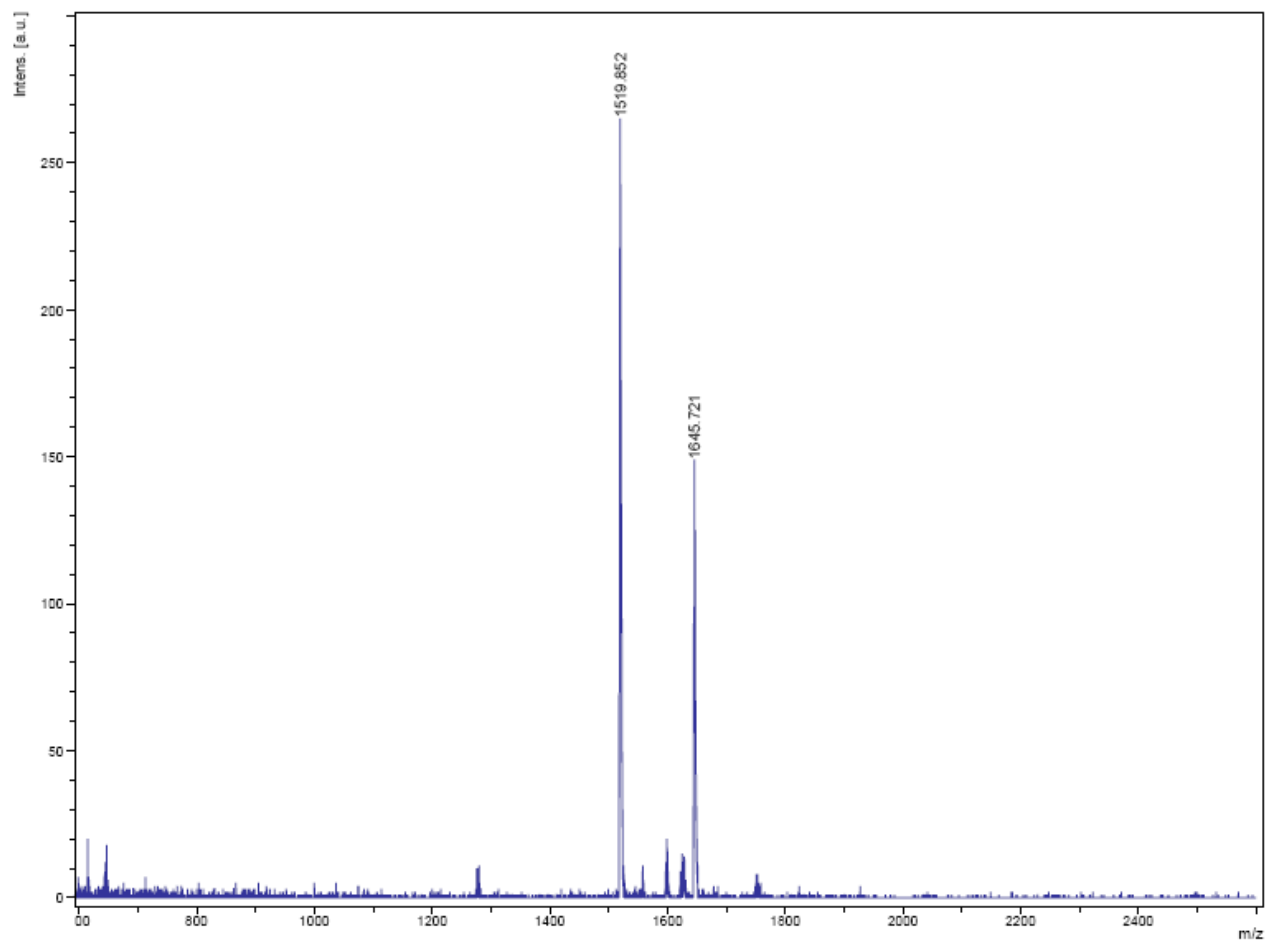


Figure A-13. Mass spectrum of compound **8**.

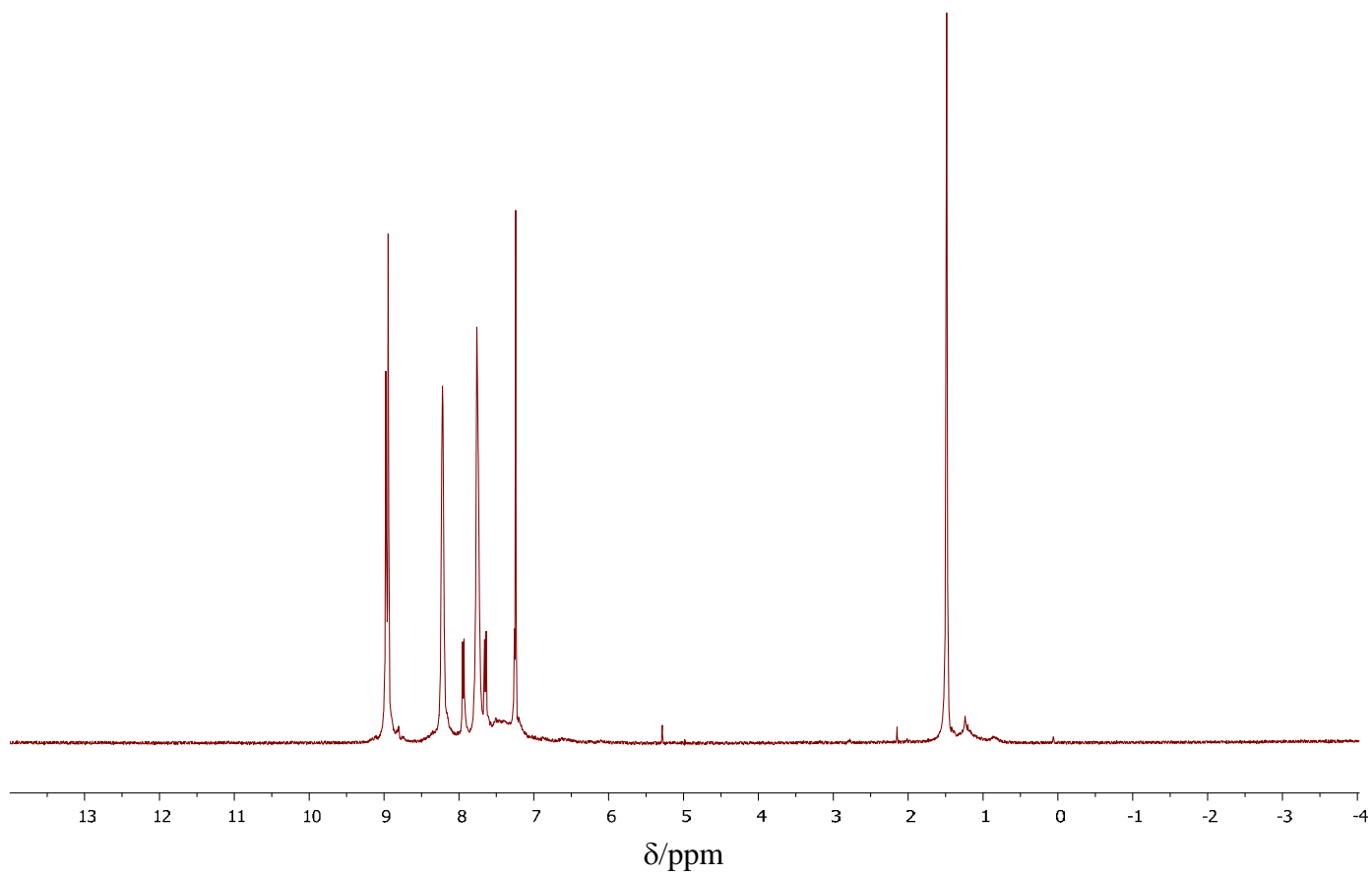


Figure A-14. $^1\text{H-NMR}$ spectrum of compound **1**.

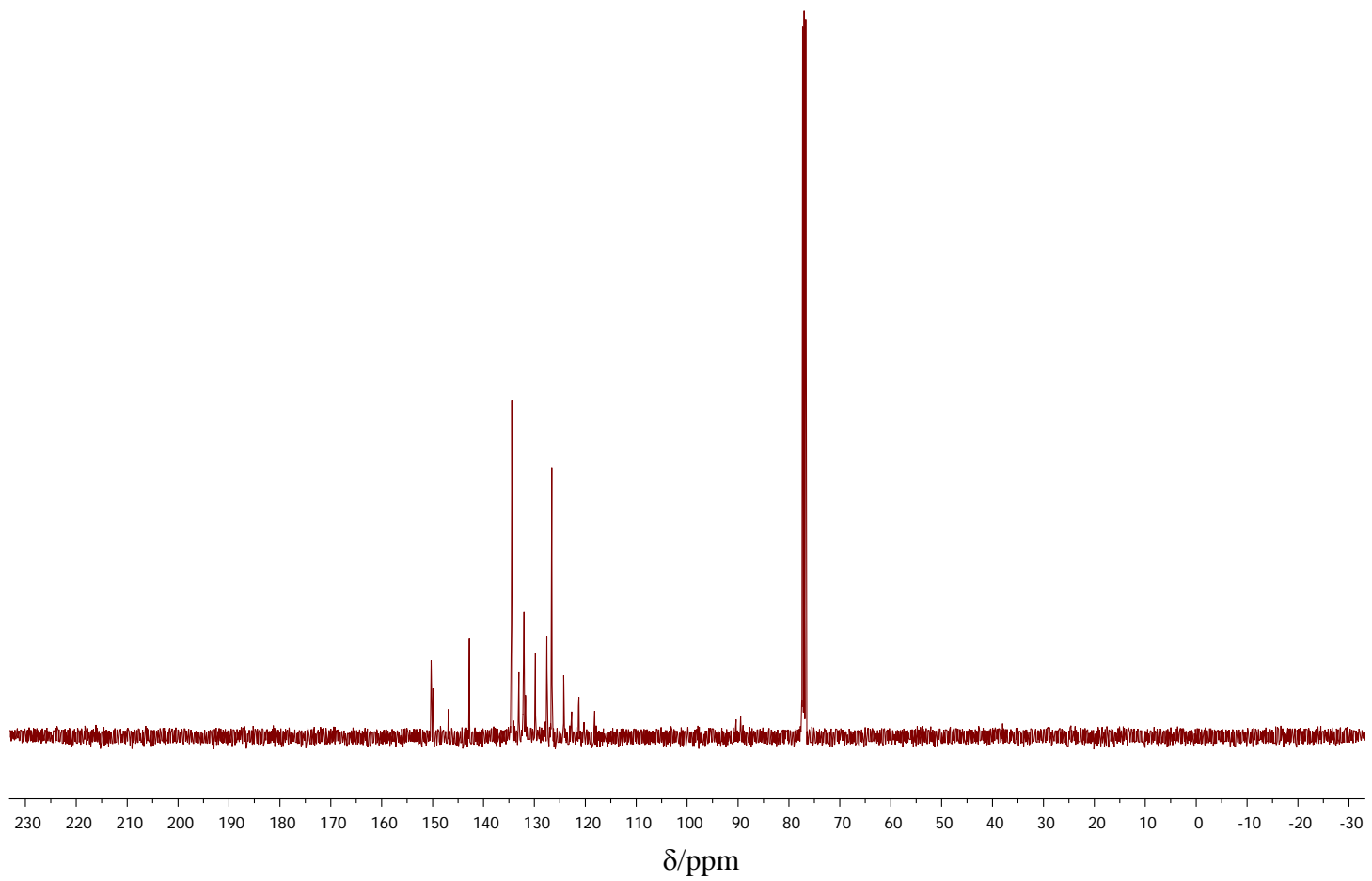


Figure A-15. ^{13}C -NMR spectrum of compound 1.

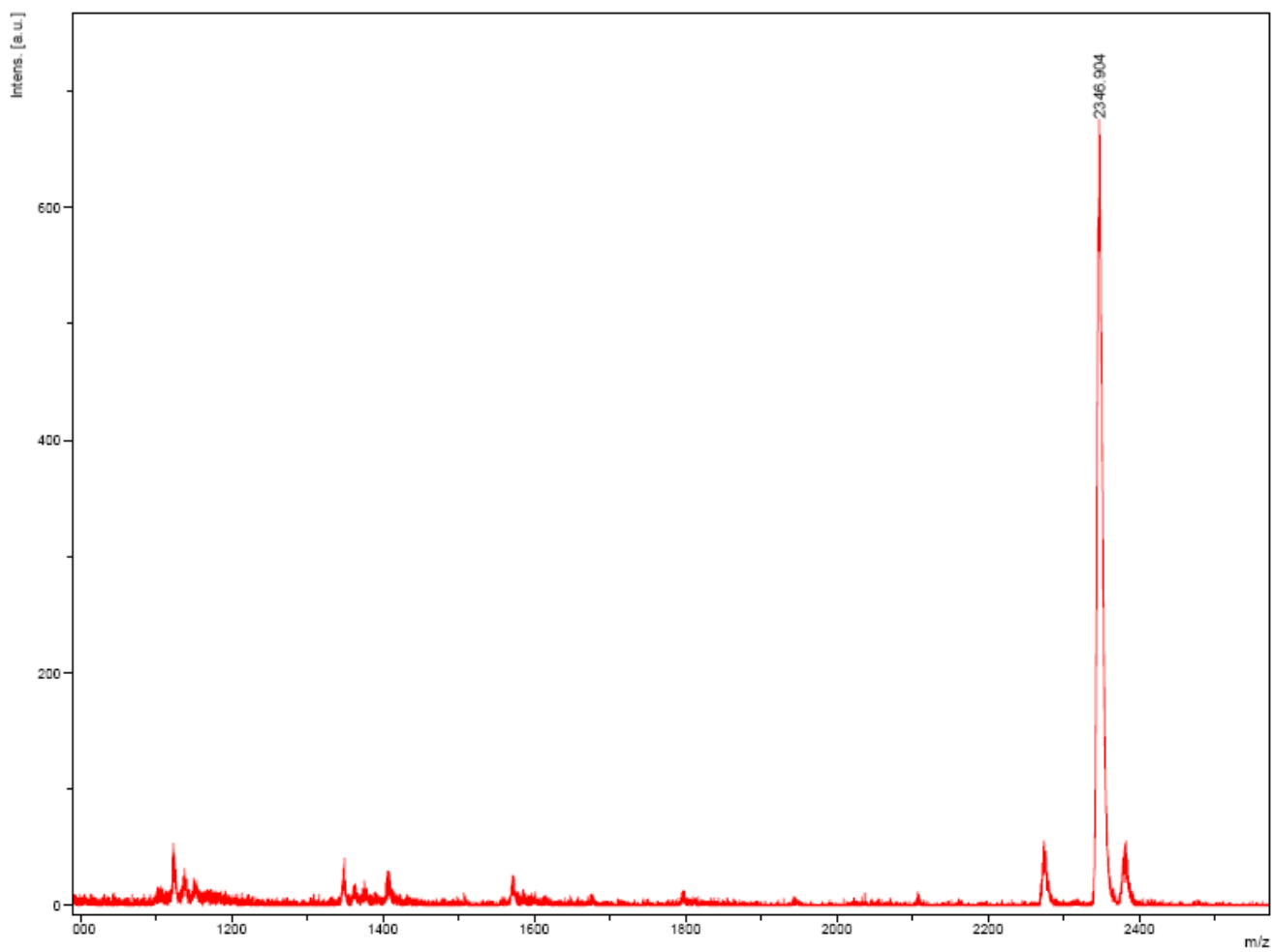


Figure A-16. Mass spectrum of compound **1**.

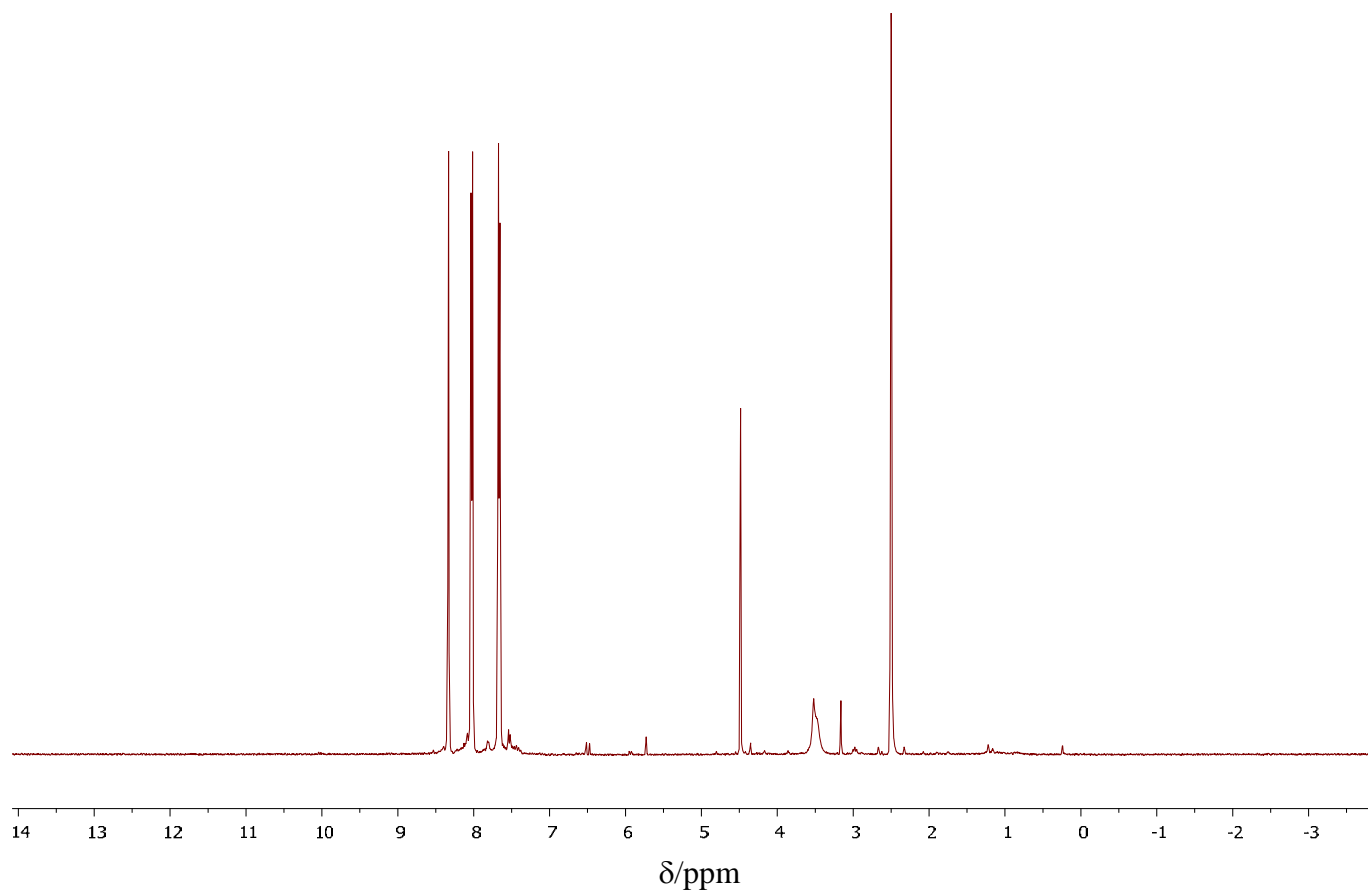


Figure A-17. $^1\text{H-NMR}$ spectrum of compound **10**.

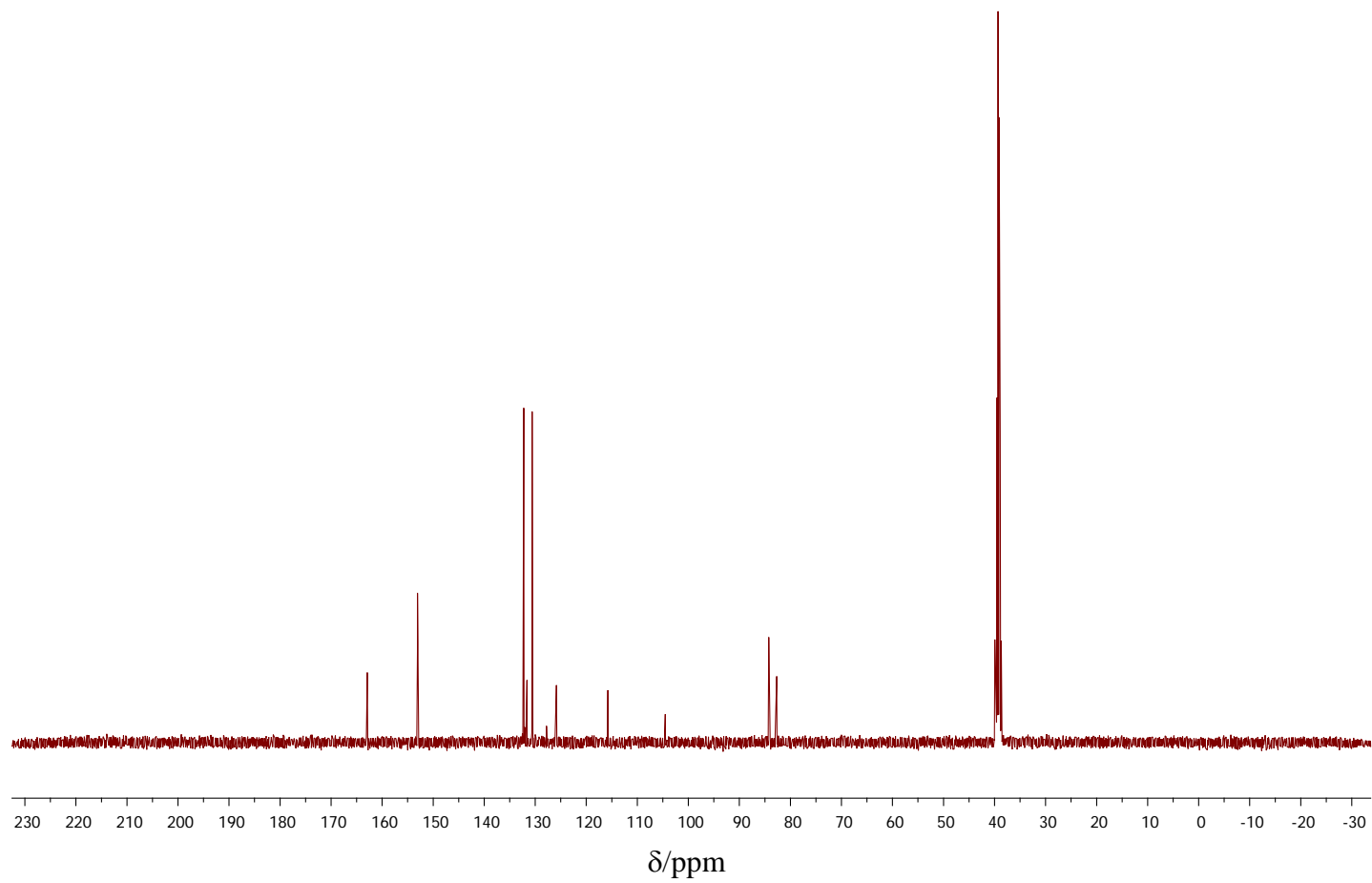


Figure A-18. ^{13}C -NMR spectrum of compound **10**.

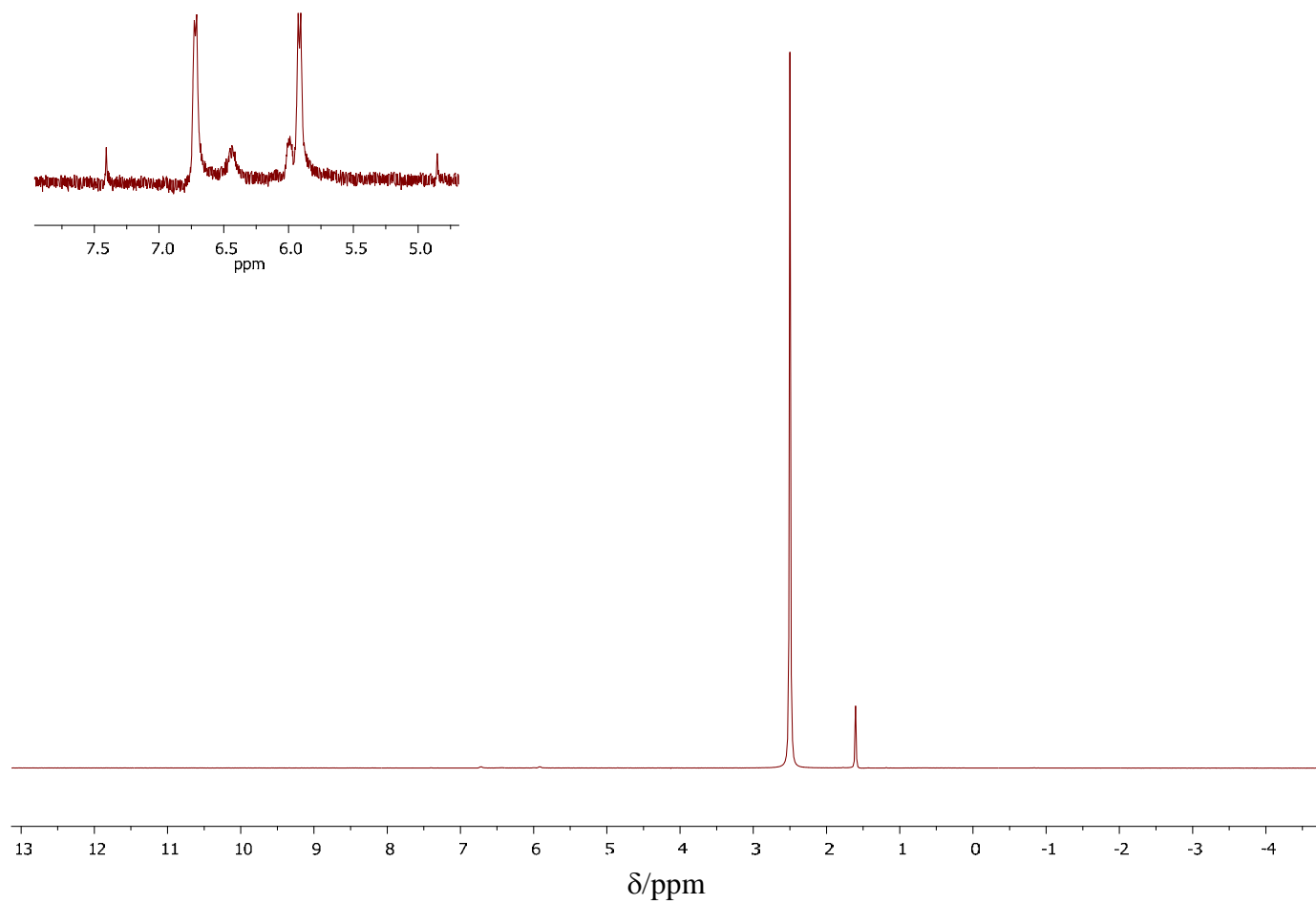


Figure A-19. $^1\text{H-NMR}$ spectrum of compound 12.

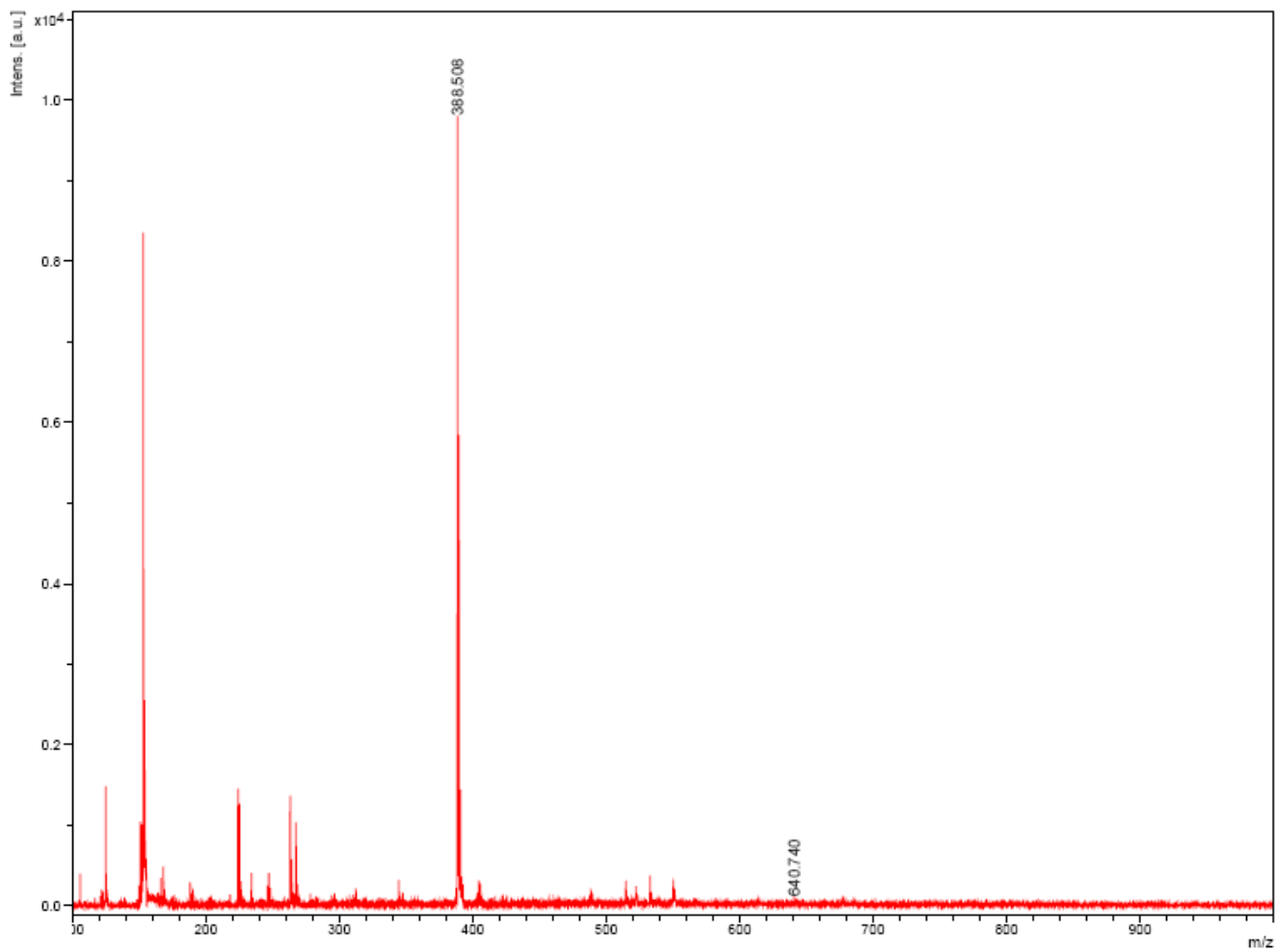


Figure A-20. Mass spectrum of compound 12.

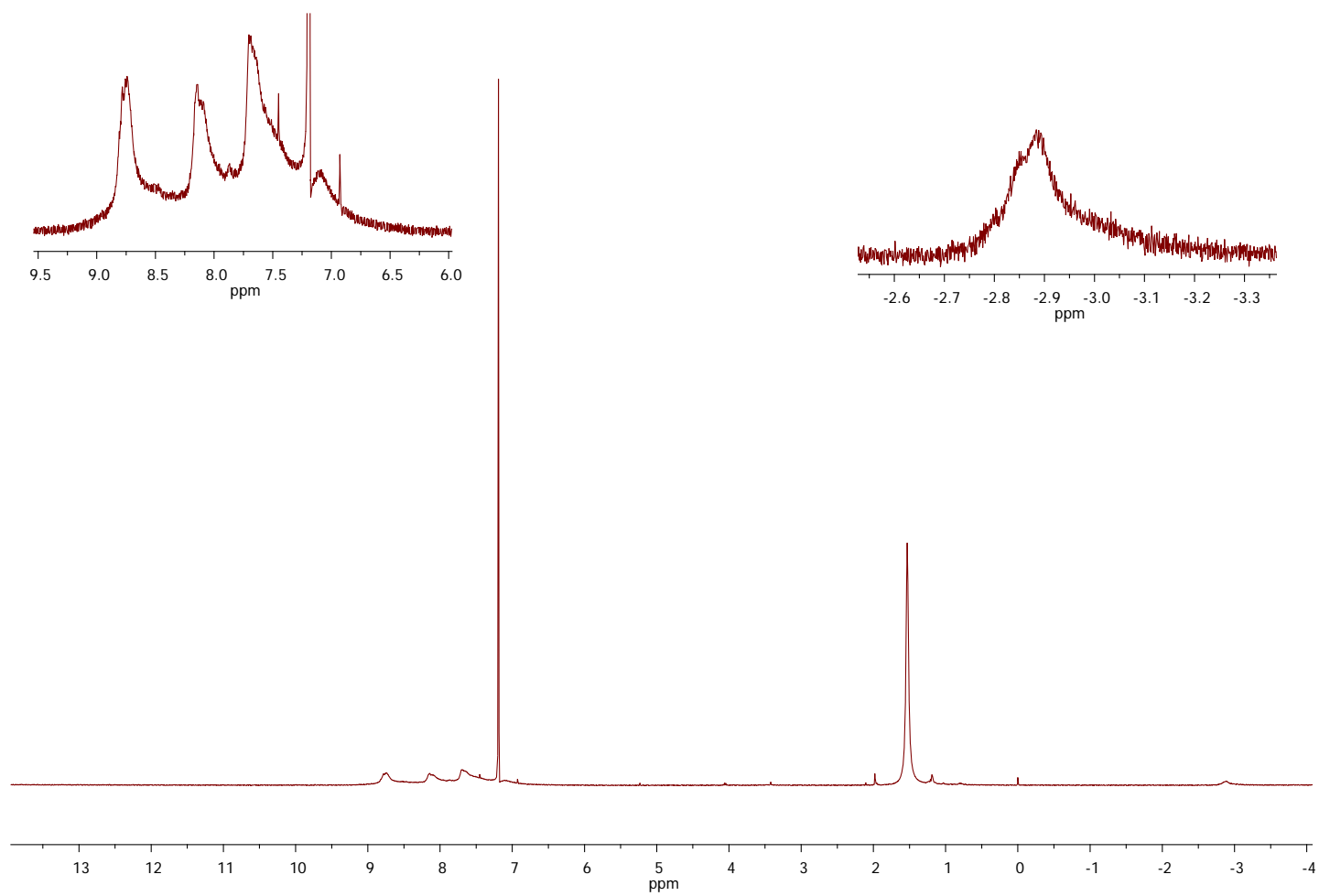


Figure A-21. $^1\text{H-NMR}$ spectrum of compound 13.

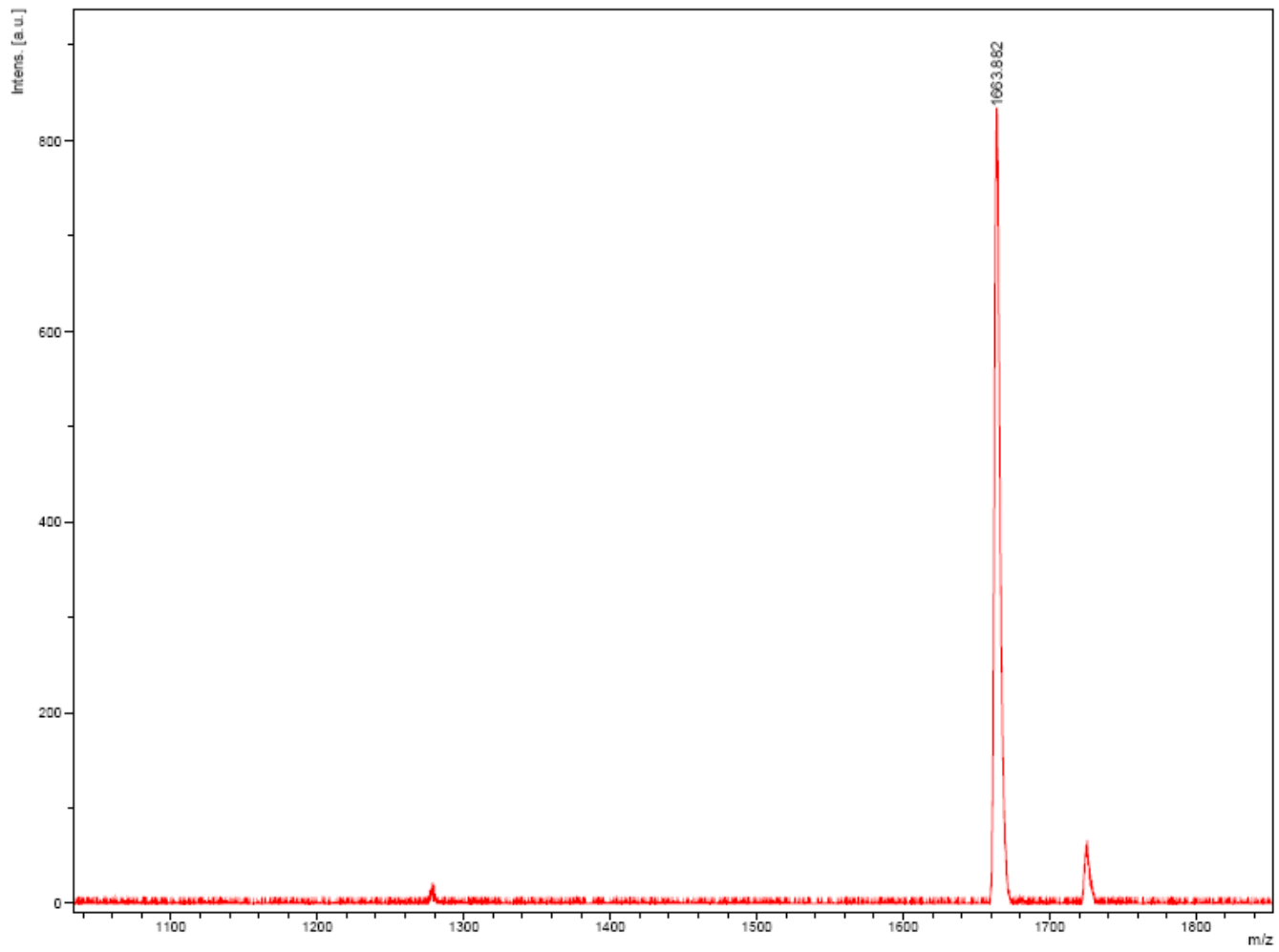


Figure A-22. Mass spectrum of compound 13.

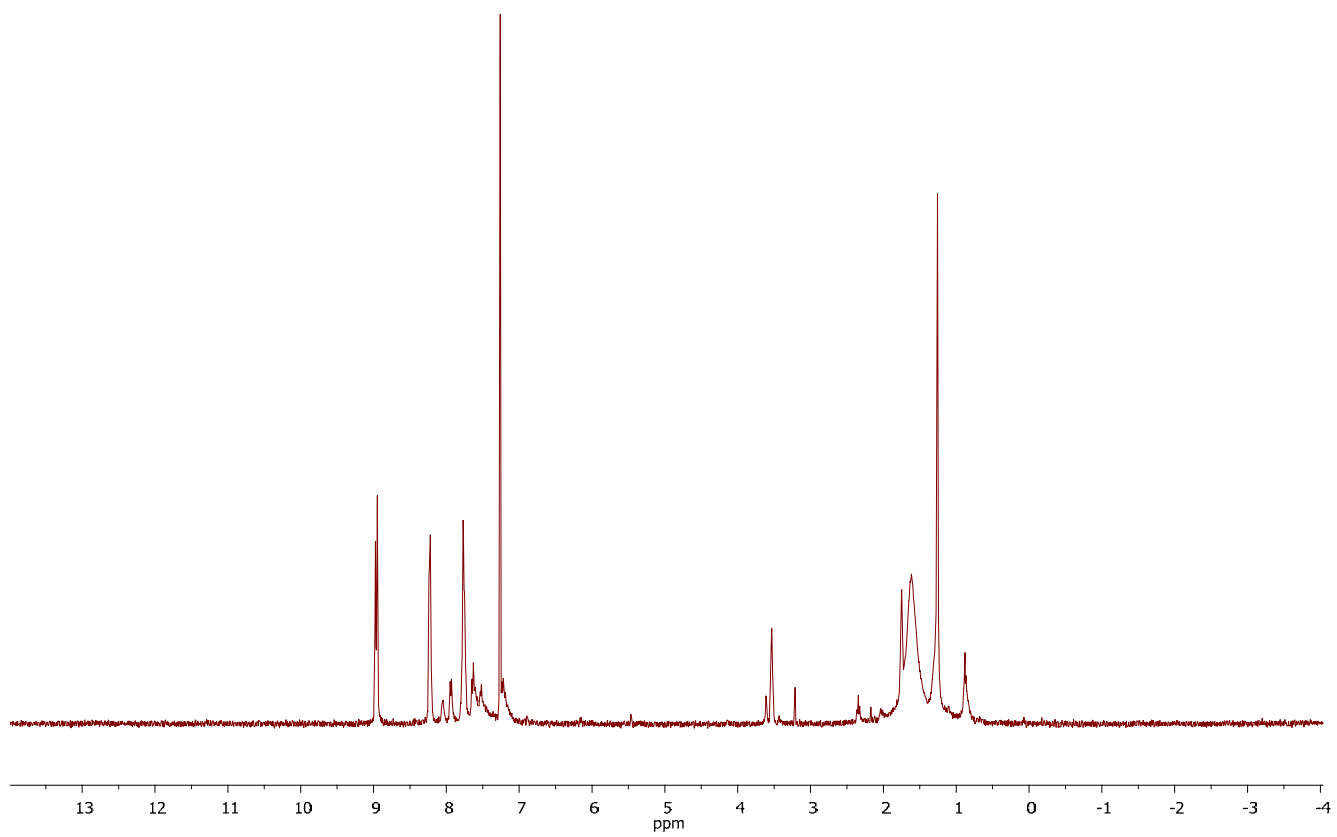


Figure A-23. $^1\text{H-NMR}$ spectrum of compound 2.

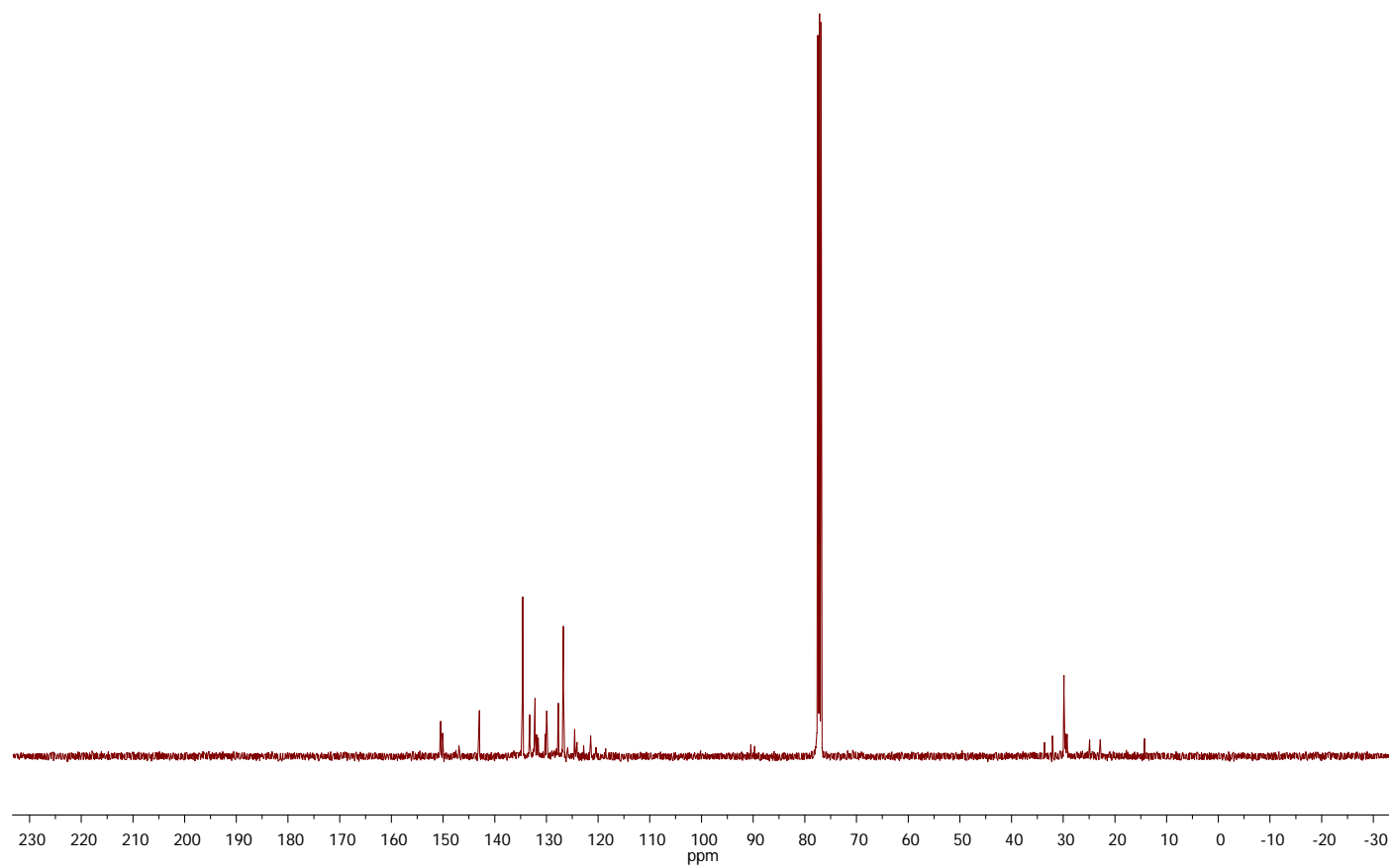


Figure A-24. ^{13}C -NMR spectrum of compound 2.

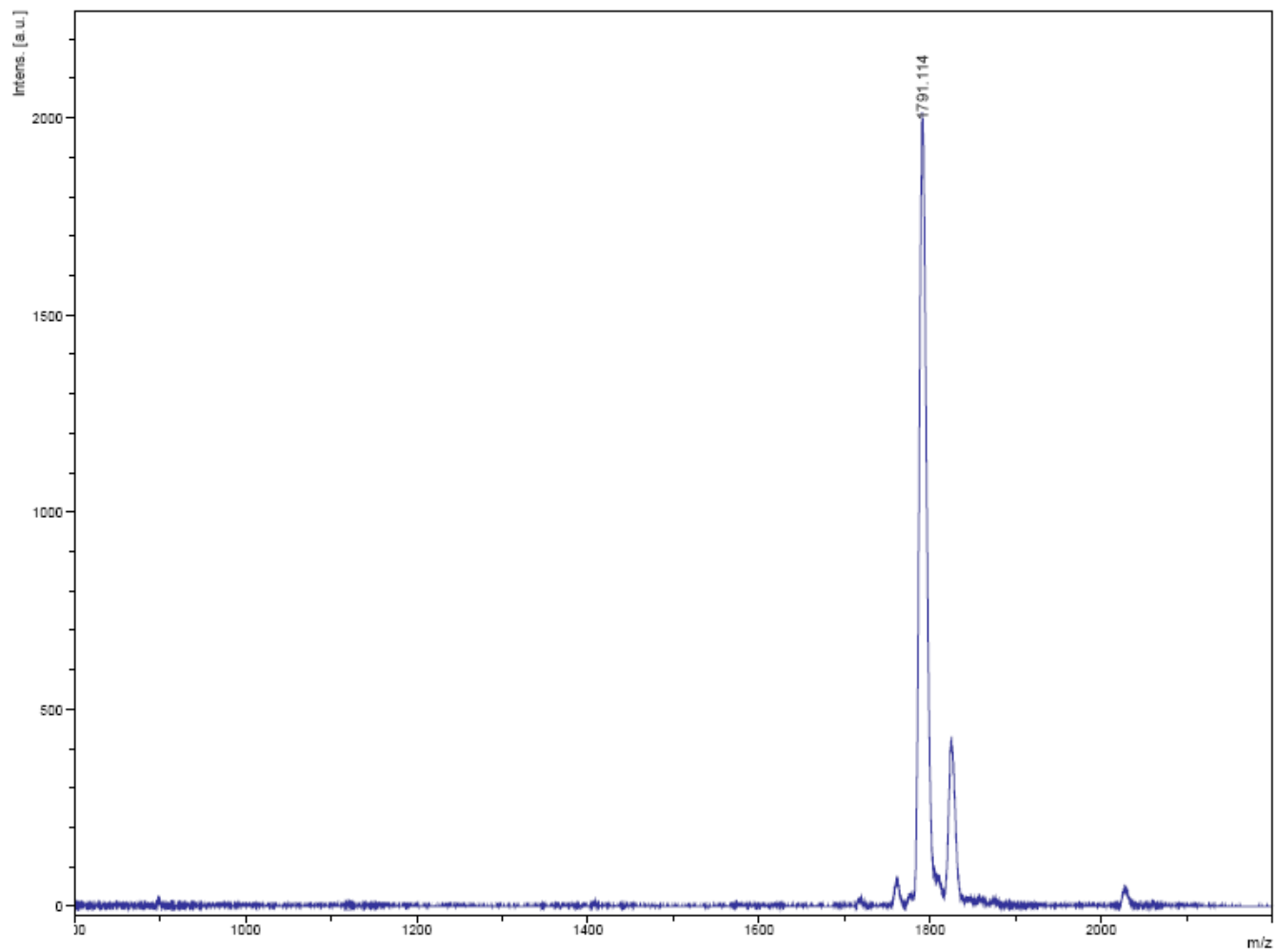


Figure A-25. Mass spectrum of compound 2.

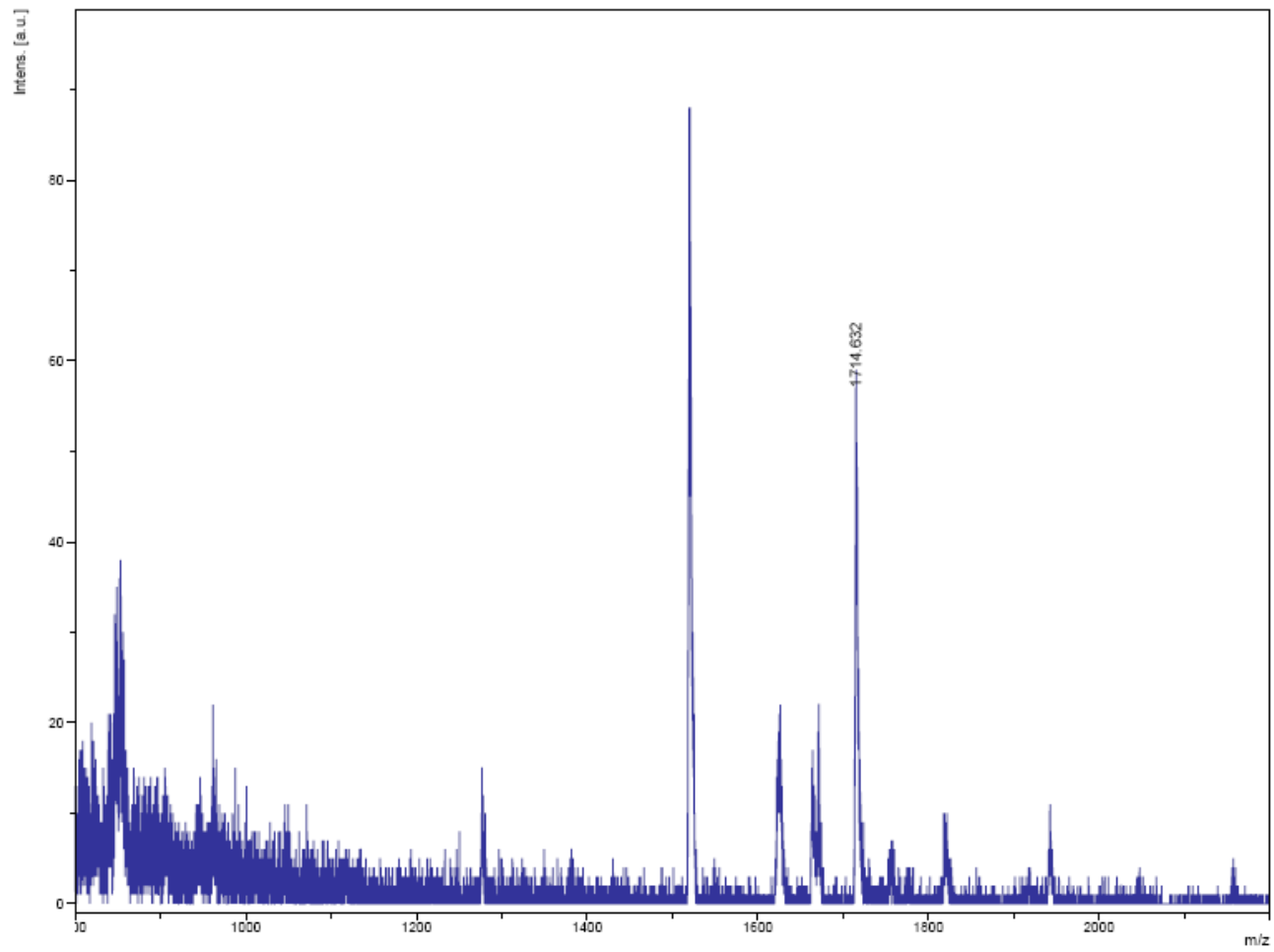


Figure A-26. Mass spectrum of compound 14.

APPENDIX B

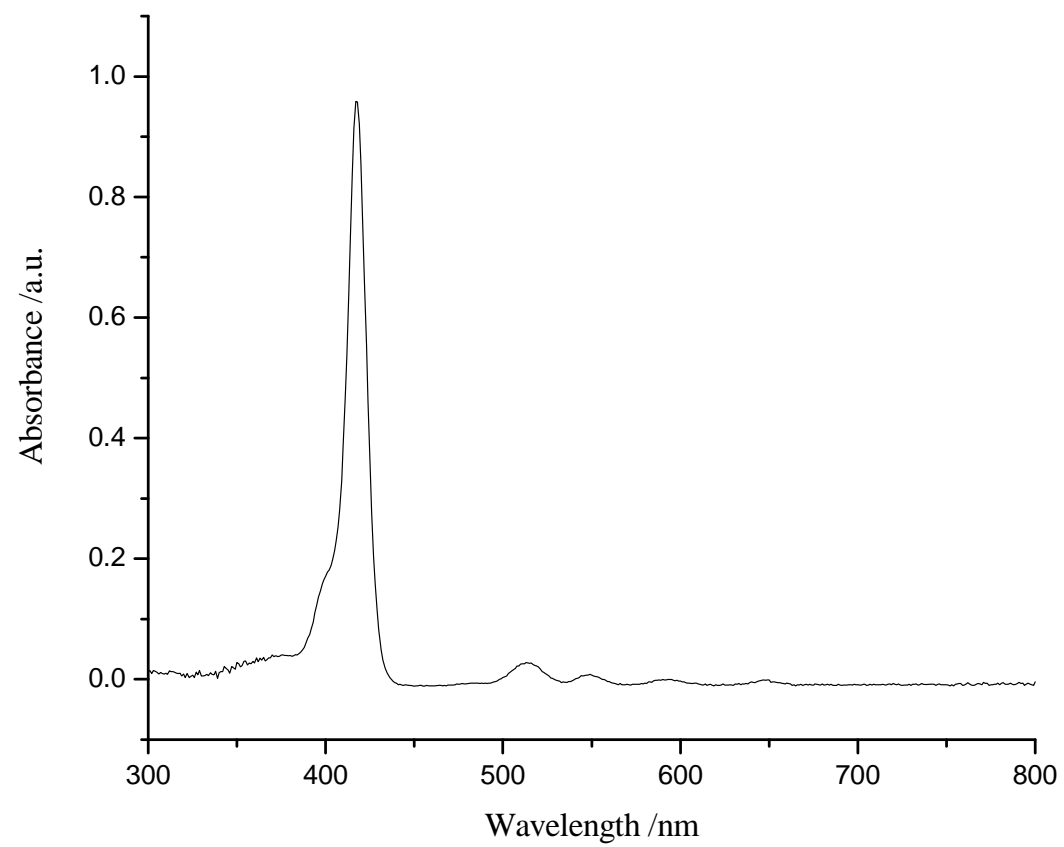


Figure B-1. Absorption spectrum of compound 4.

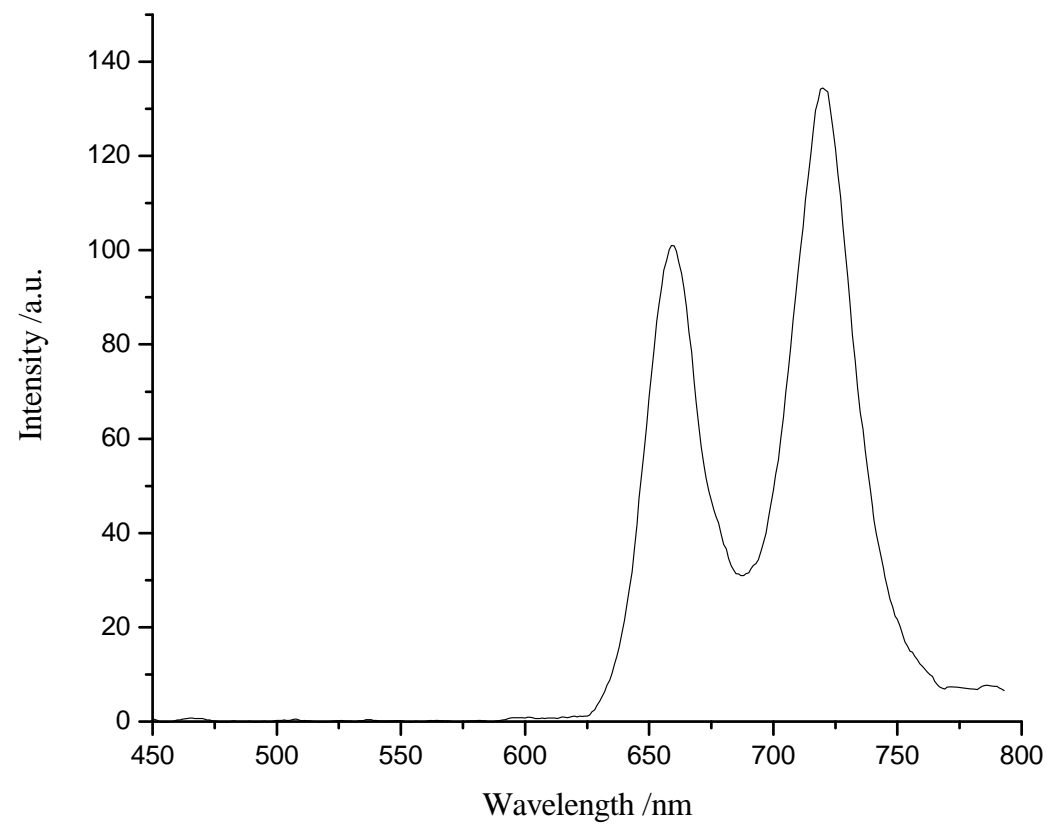


Figure B-2. Emission spectrum of compound 4.

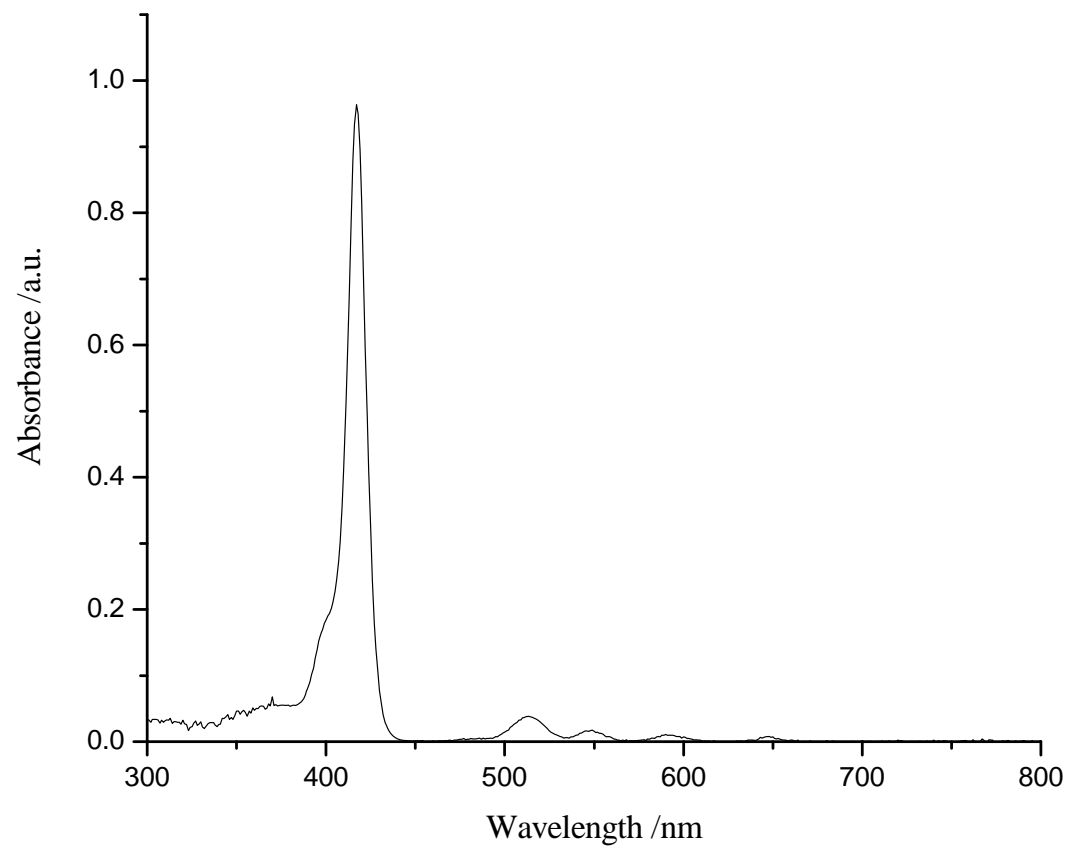


Figure B-3. Absorption spectrum of compound 5.

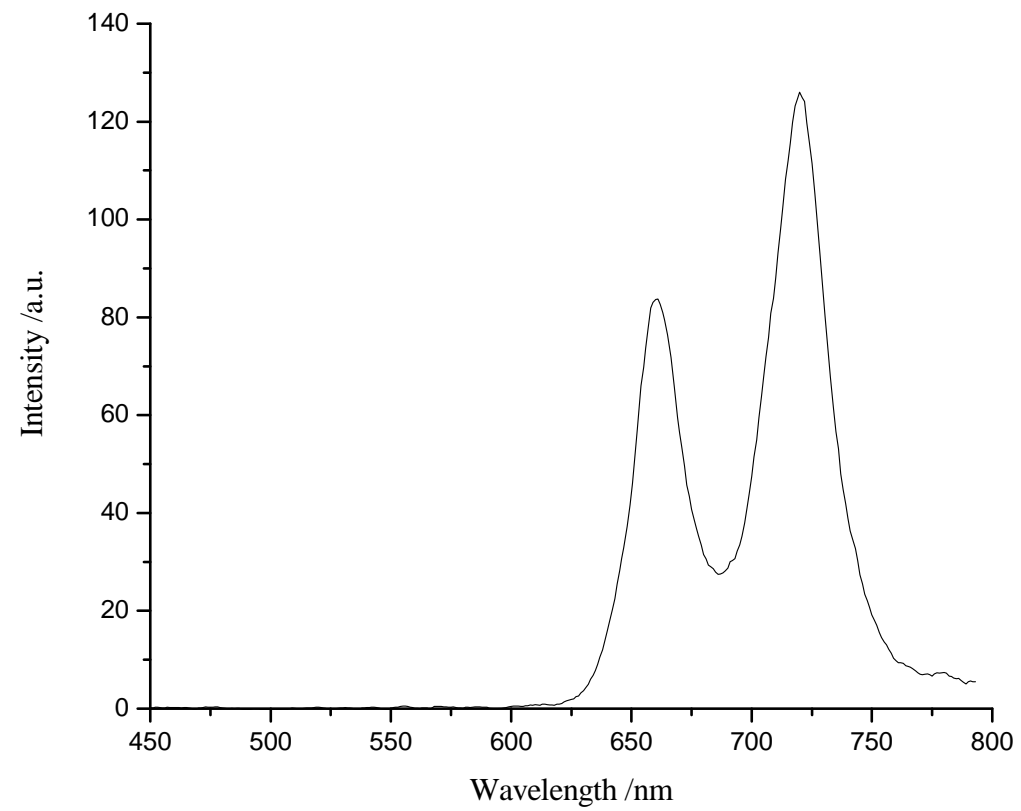


Figure B-4. Emission spectrum of compound 5.

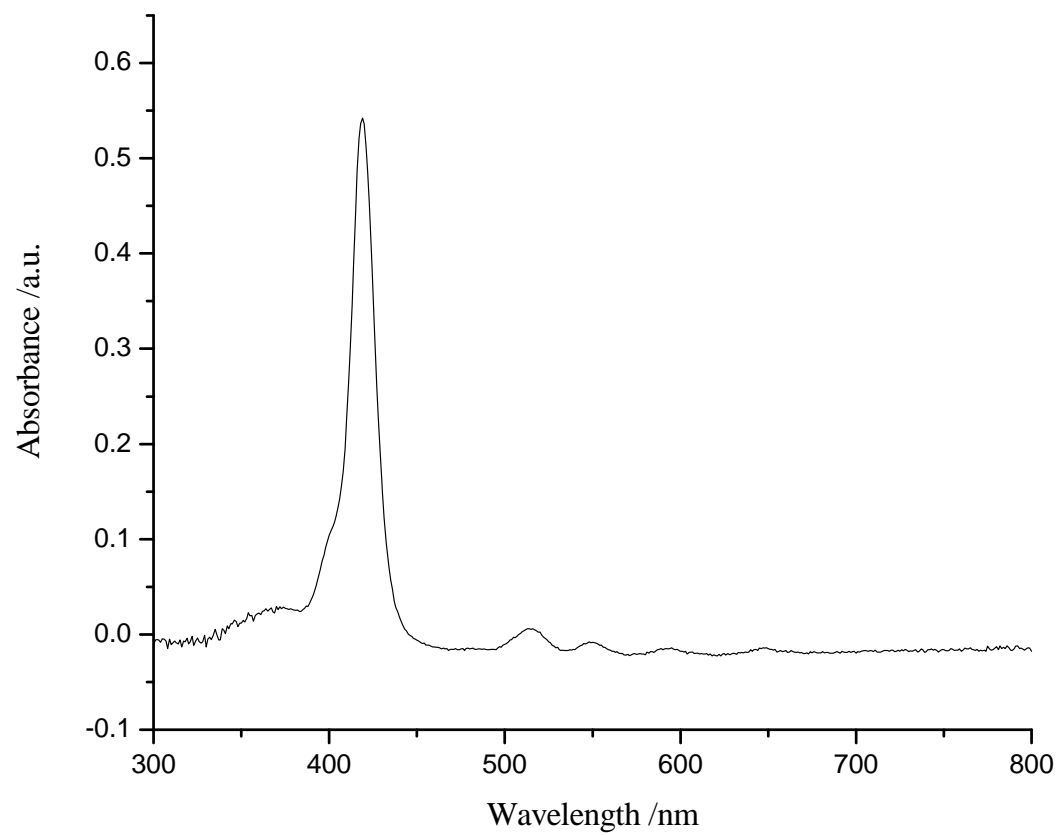


Figure B-5. Absorption spectrum of compound 7.

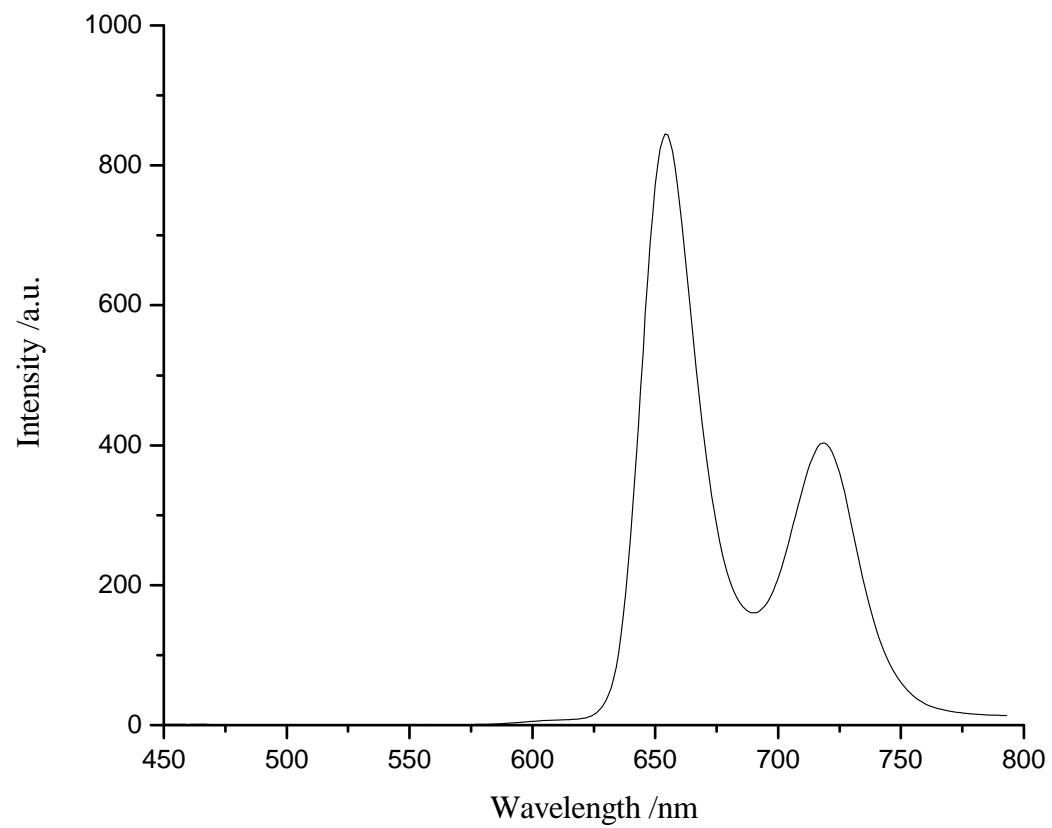


Figure B-6. Emission spectrum of compound 7.

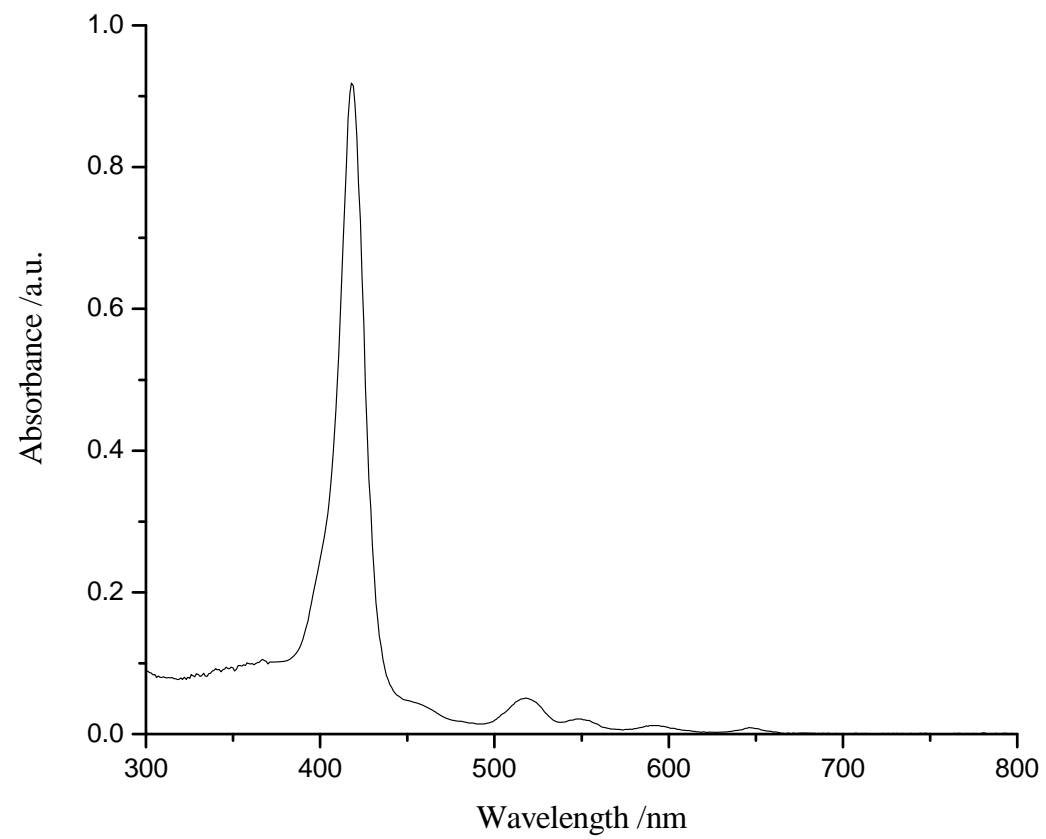


Figure B-7. Absorption spectrum of compound 8.

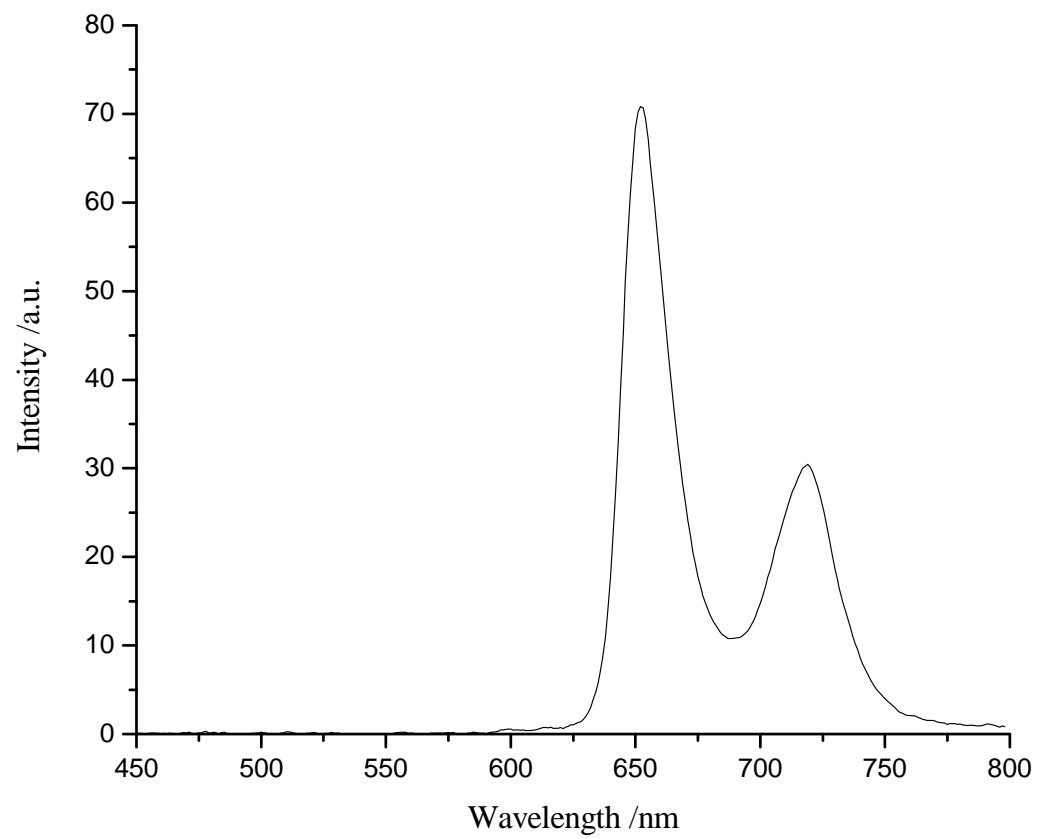


Figure B-8. Emission spectrum of compound **8**.

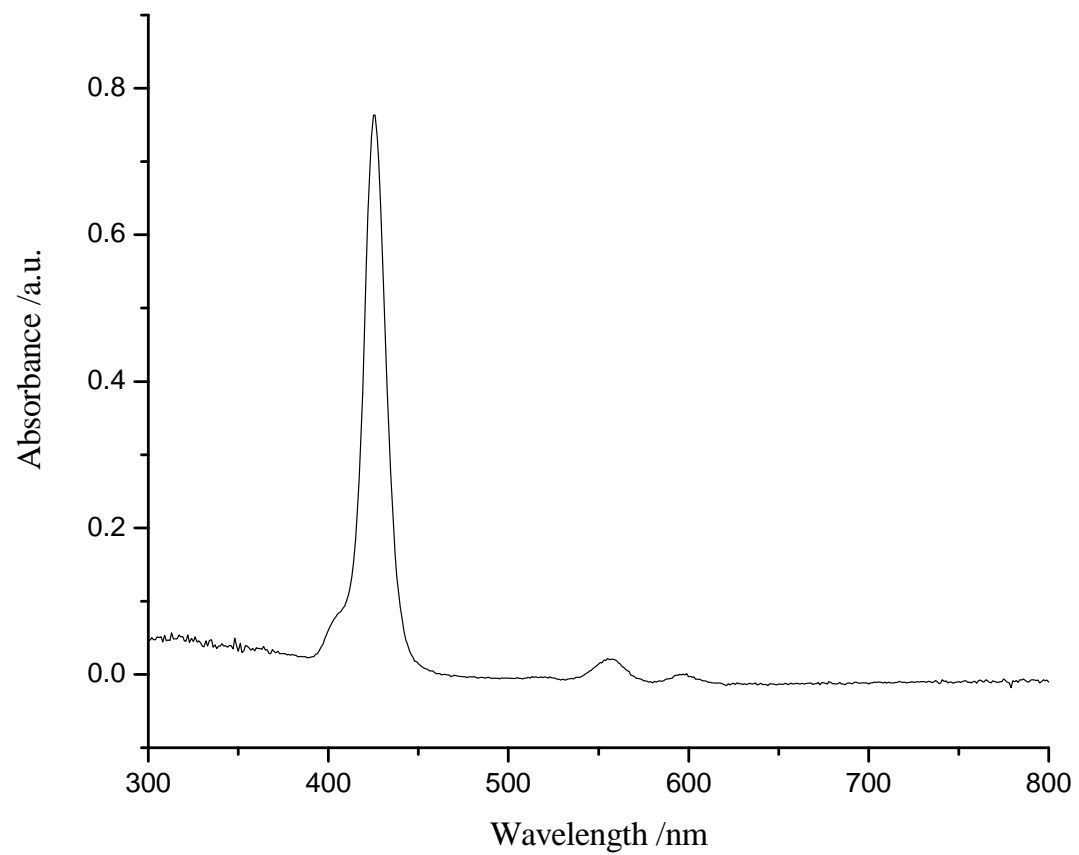


Figure B-9. Absorption spectrum of compound 1.

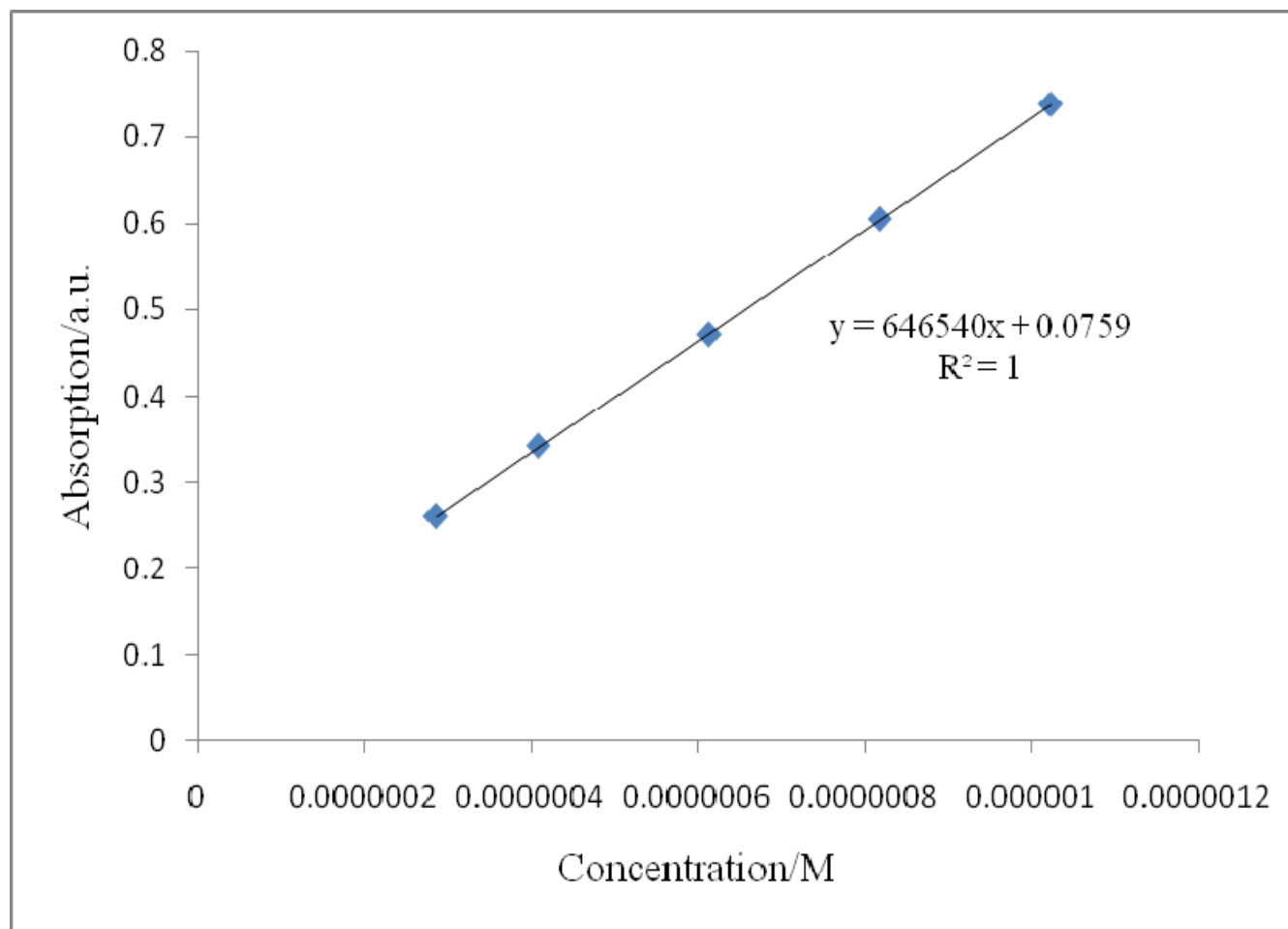


Figure 10. Calibration curve for quantitative determination of compound **1** in THF ($\lambda_{\text{abs}} = 425 \text{ nm}$).

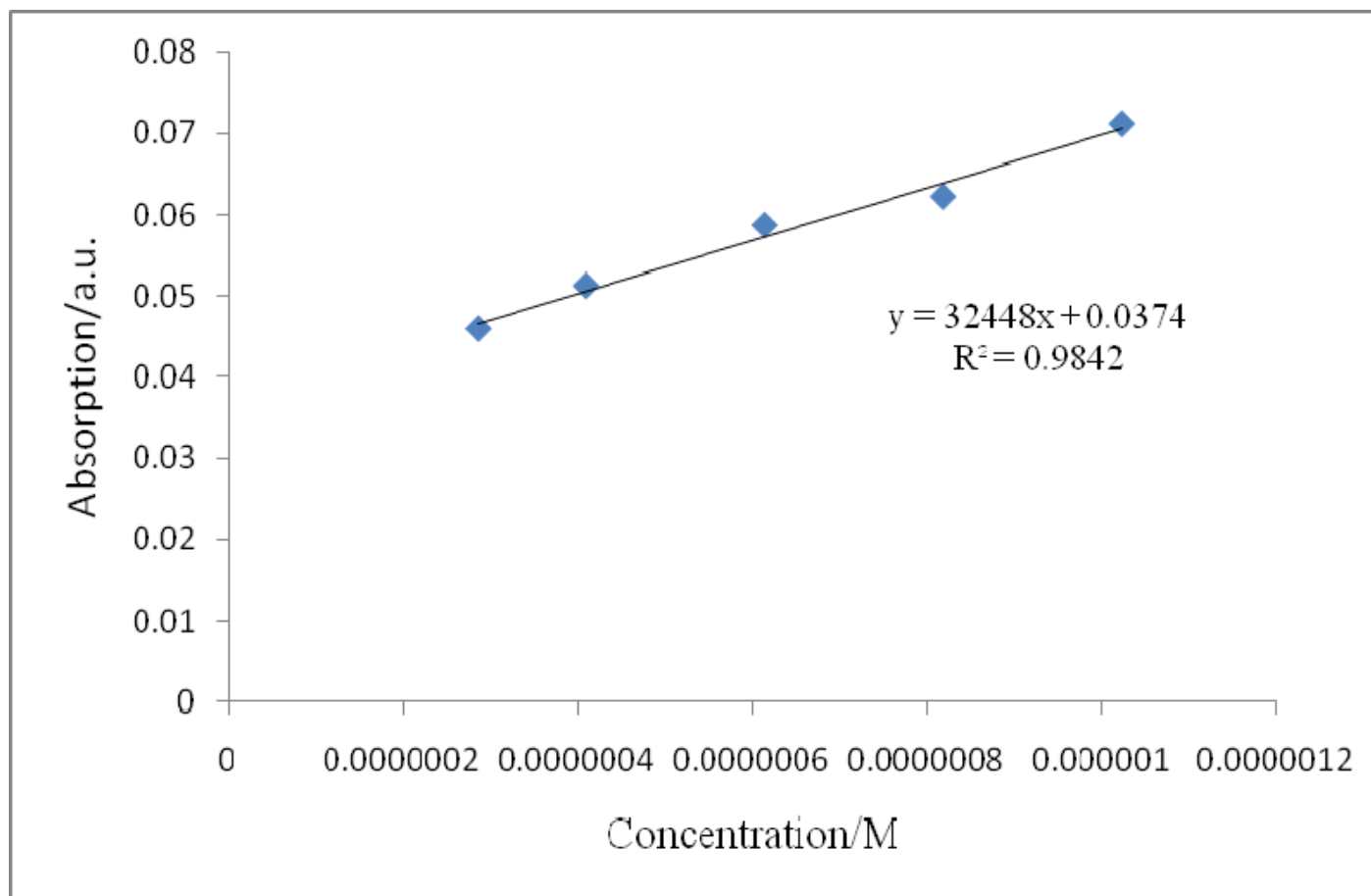


Figure 11. Calibration curve for quantitative determination of compound **1** in THF ($\lambda_{\text{abs}} = 555 \text{ nm}$).

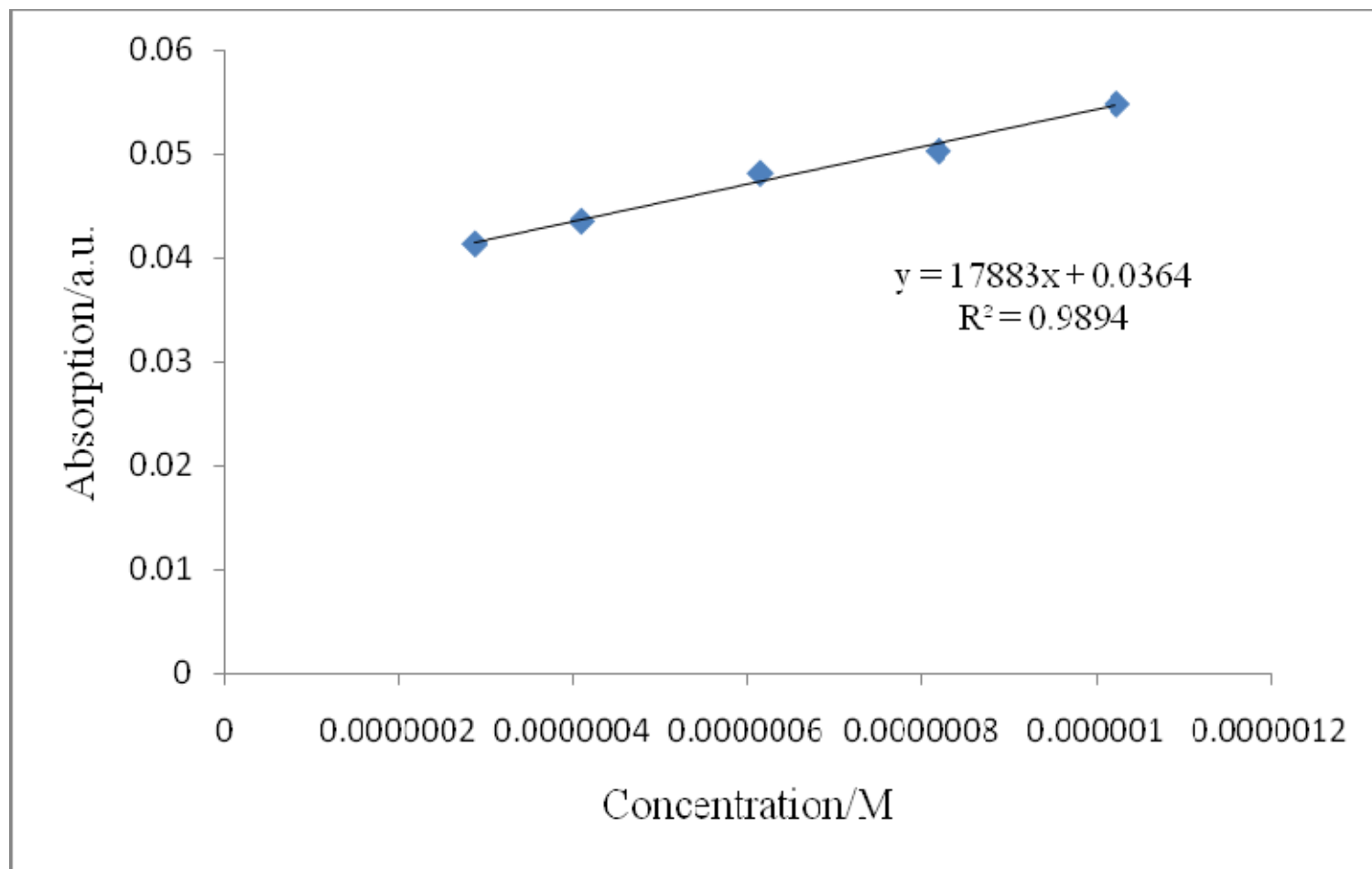


Figure 12. Calibration curve for quantitative determination of compound **1** in THF ($\lambda_{\text{abs}} = 594$ nm).

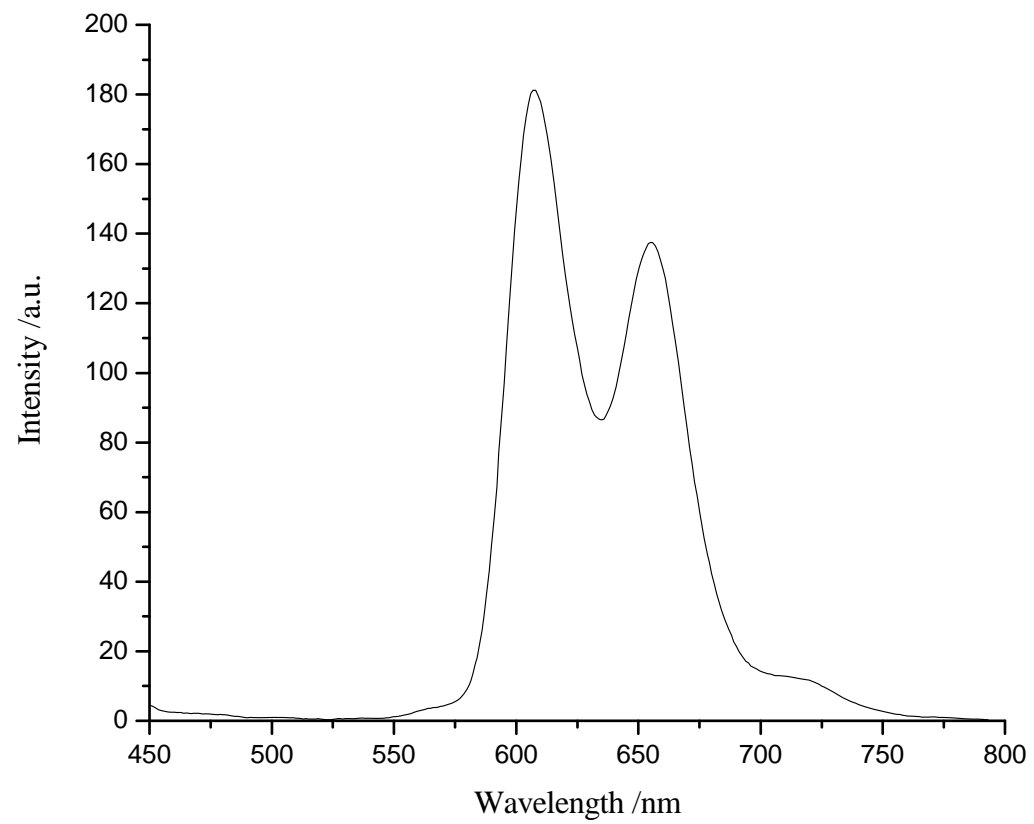


Figure B-13. Emission spectrum of compound 1.

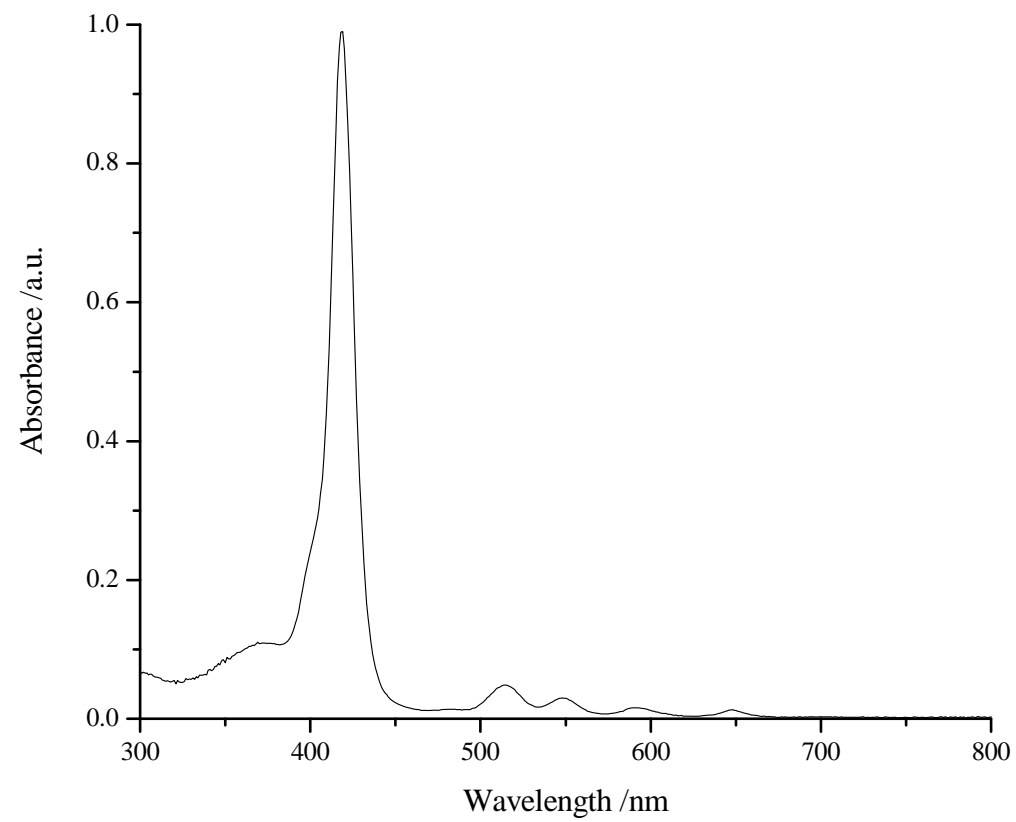


Figure B-14. Absorption spectrum of compound **13**.

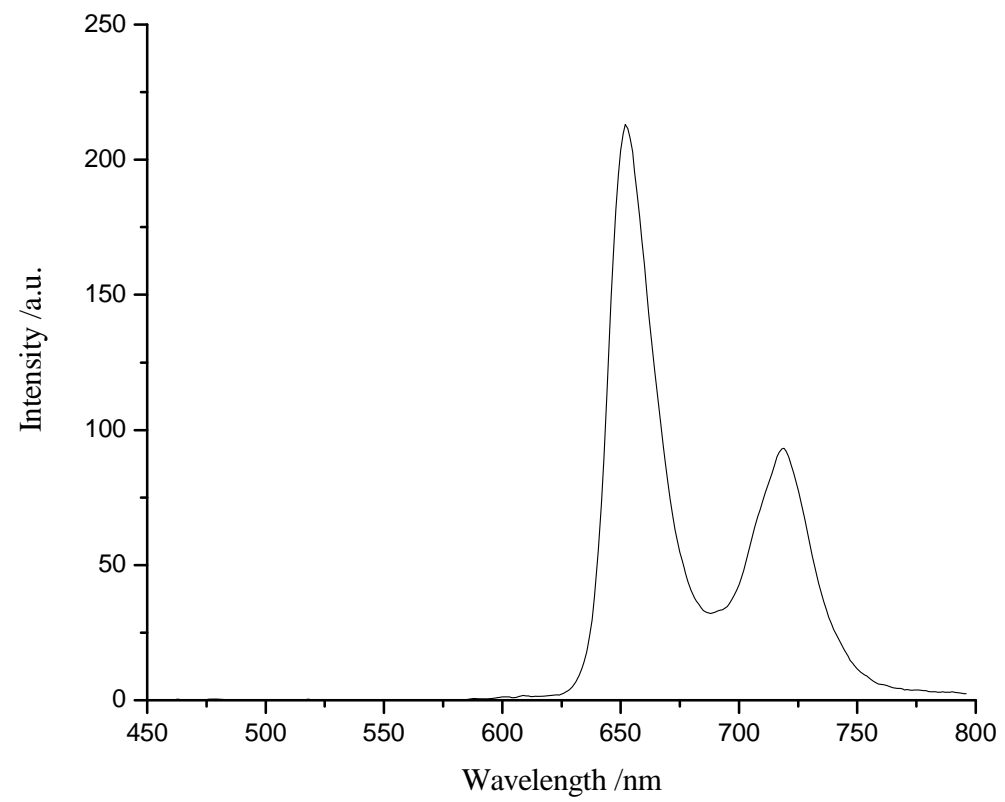


Figure B-15. Emission spectrum of compound **13**.

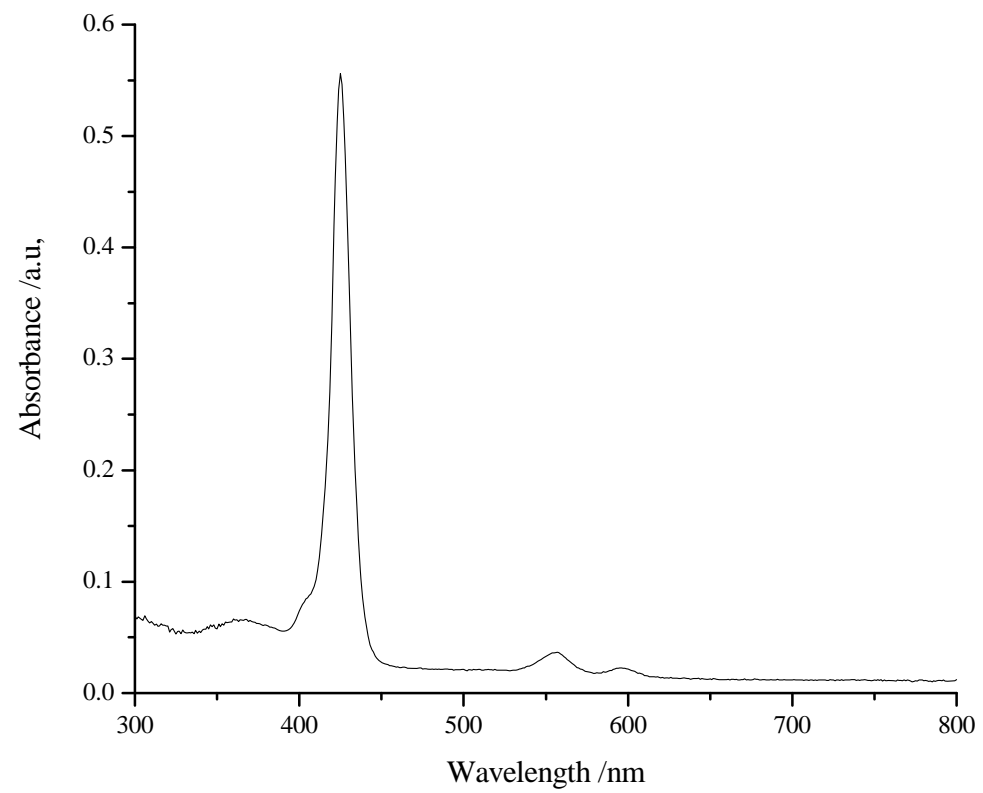


Figure B-16. Absorption spectrum of compound 2.

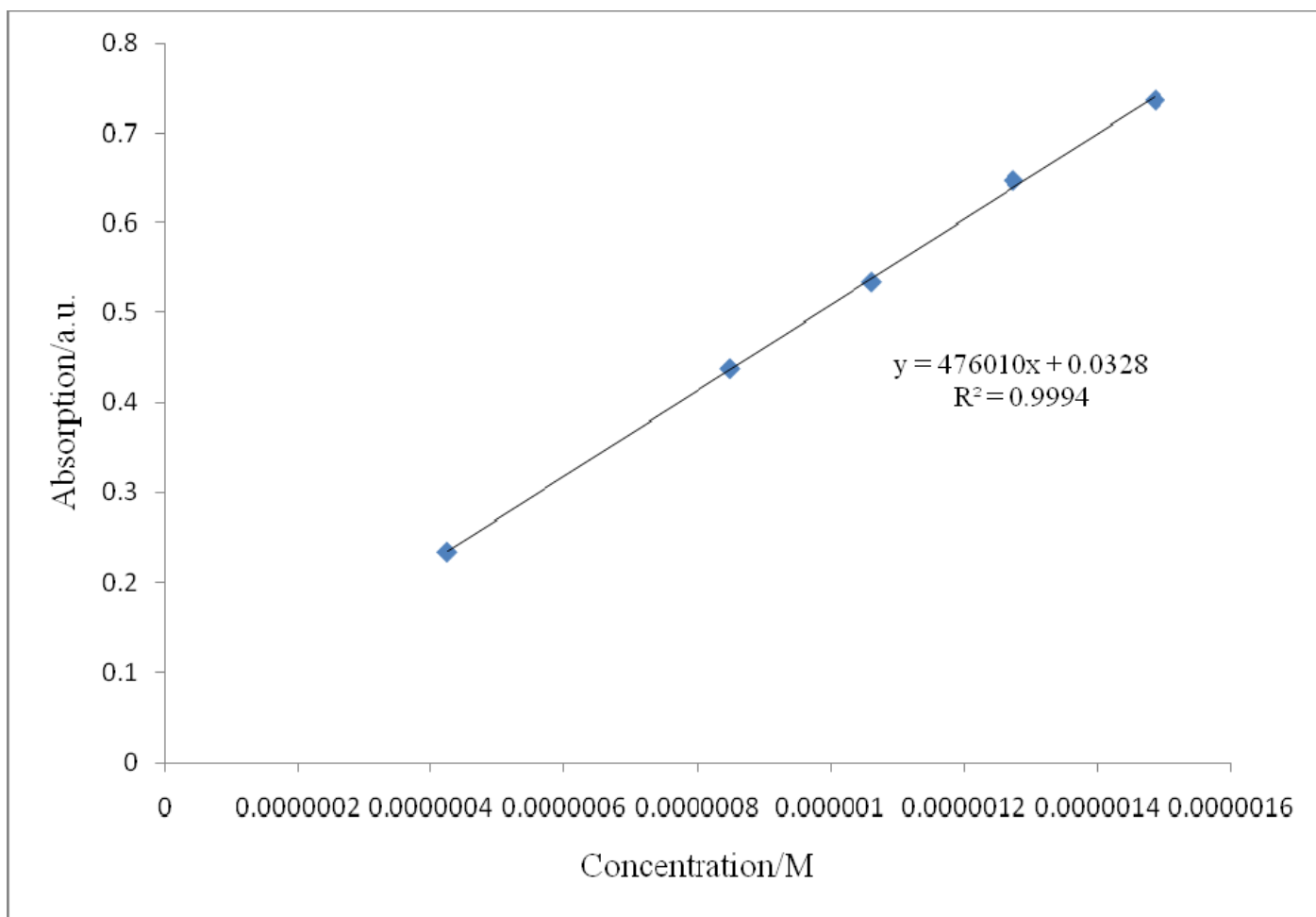


Figure 17. Calibration curve for quantitative determination of compound **2** in THF ($\lambda_{\text{abs}} = 425 \text{ nm}$).

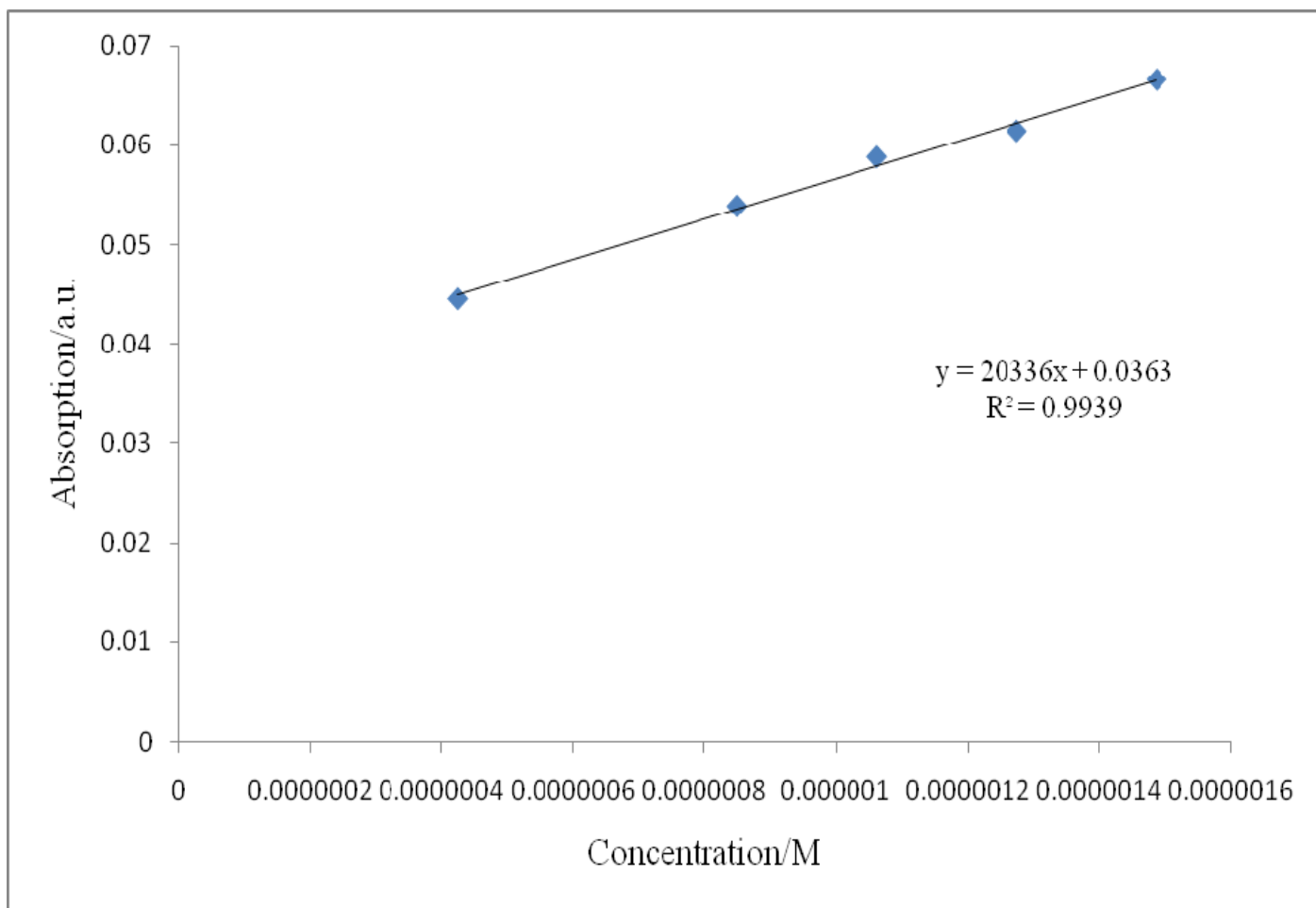


Figure 18. Calibration curve for quantitative determination of compound **2** in THF ($\lambda_{\text{abs}} = 557 \text{ nm}$).

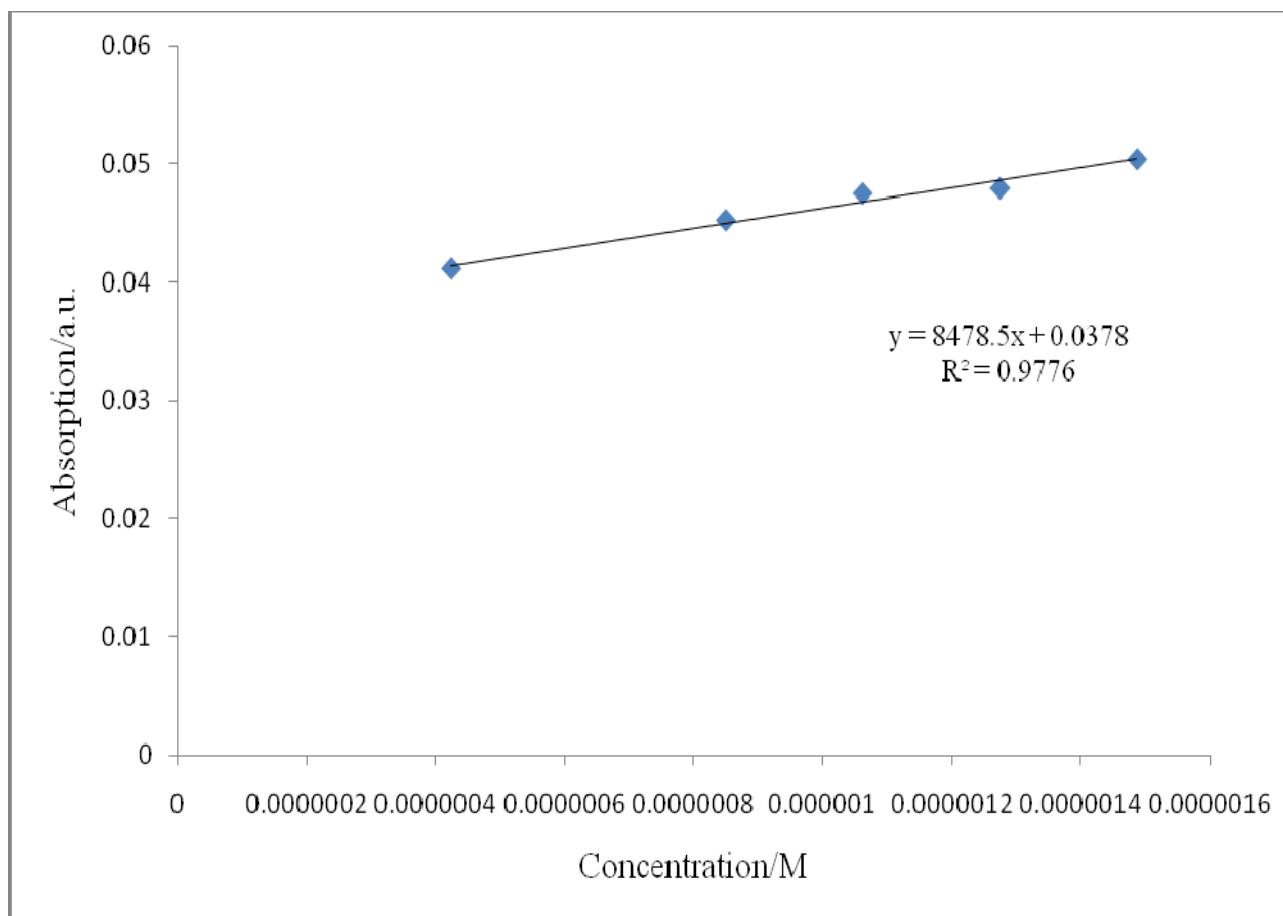


Figure 19. Calibration curve for quantitative determination of compound **2** in THF ($\lambda_{\text{abs}} = 596 \text{ nm}$).

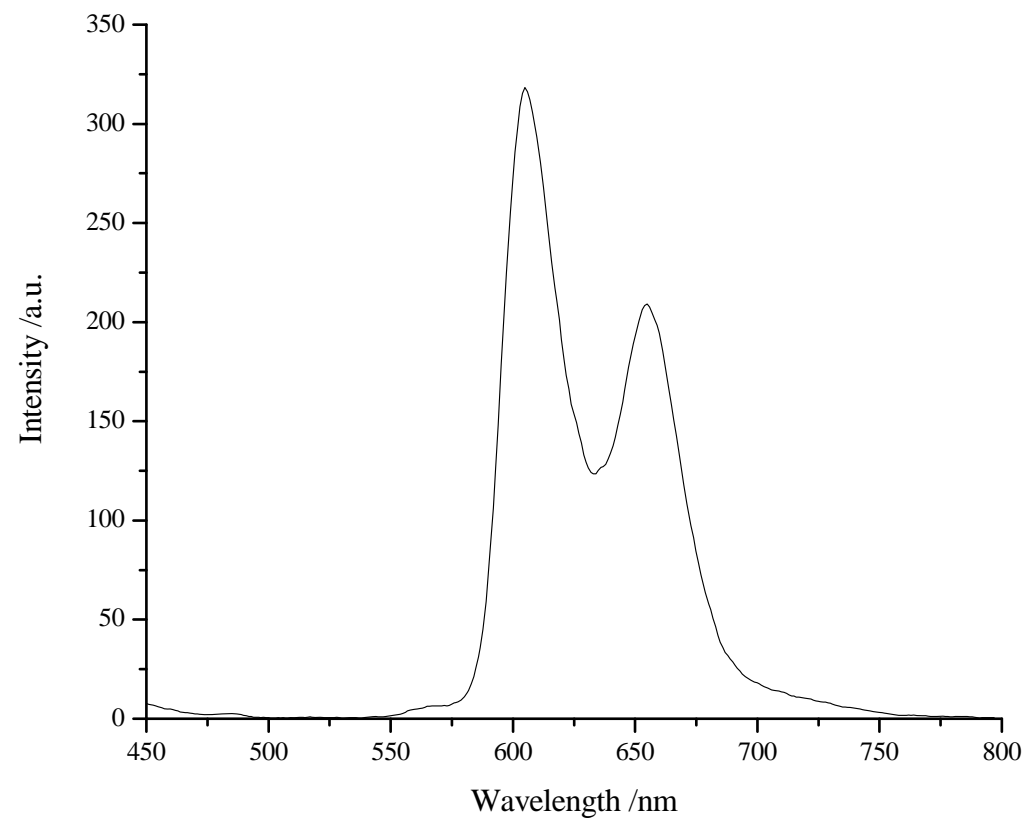


Figure B-20. Emission spectrum of compound 2.

VITA

Miss Thanisa Kengthanomma was born on February 7, 1986 in Bangkok, Thailand. She got a Bachelor Degree of Chemistry from Faculty of Science at Chulalongkorn University, Bangkok in 2008. After that, she was admitted into a Master Degree Program in Petrochemistry and Polymer Science, Faculty of Science, Chulalongkorn University, Bangkok in 2008 and completed the program in 2011.